

DIVISION SNAP-8

TM 4933:65-8-311

DATE 3 August 1965

W.O. 0741-66-2000

CR-72201

TECHNICAL MEMORANDUM

AUTHOR(S): A. J. Sellers, M. K. ...

TITLE: EXPERIMENTAL INVESTIGATION OF FORCED CONVECTION ONCE-THROUGH MERCURY BOILERS PERFORMANCE CHARACTERISTICS

H 07-02063

ABSTRACT

Once-through type mercury boiler performance characteristics were studied experimentally in a single tube New Mercury heat exchanger of concentric counterflow configuration. Heat transfer and two-phase flow pressure drop data were obtained for different mercury flow passage inlet end plug insert geometries. The experimental data were evaluated to determine the validity of proposed single phase flow pressure drop correlations.

a. The initial boiler performance characteristics are dependent on the mercury flow passage internal wall conditioning state and the thermal and dynamic conditions imposed by the flow passage internal geometry.

b. Elevated liquid phase velocity and flow velocity at the preheat section end point combined with similar dynamic conditions in the low vapor quality section demonstrates excellent boiler conditioning effect when the mercury flow passage is cleaned by established methods prior to mercury injection.

c. The boiling heat transfer data obtained from a fully conditioned boiler are in close agreement with the predictions established by the dropwise dry wall boiling heat transfer correlations.

d. The two phase flow pressure drop data are correlated by means of the product (ϕf_v) in terms of a modified Martinelli parameter (λ) as proposed by Reference (1).

e. The introduction of a preheat section plug insert geometry providing elevated liquid velocity significantly improved the boiler performance stability.

DEPARTMENT HEAD

E. Eber

LIBRARY COPY

APR 14 1967

NOTE: This document is considered preliminary and is subject to change as analysis progresses and additional data are acquired. The general reader may encounter internal reference not available to him.



JET-GENERAL CORPORATION

COPY NO.

PAGES:

CONTENTS

	<u>Page</u>
I. <u>INTRODUCTION</u>	1.
II. <u>PURPOSE</u>	2
III. <u>DESCRIPTION OF TEST APPARATUS</u>	2
A. Loop Description	2
B. Boiler Description	3
C. Boiler Test Instrumentation	5
IV. <u>OPERATION</u>	8
A. Boiler Startup	8
B. Test Runs	8
C. Shutdown	9
V. <u>TEST DATA REDUCTION</u>	10
VI. <u>DISCUSSION OF RESULTS</u>	12
VII. <u>CONCLUSIONS</u>	20
VIII. <u>RECOMMENDATIONS</u>	23

APPENDIX A: Results of CL-4 Boiler Test Data Reduction

APPENDIX B: CL-4 Boiler Test Data Reduction Program

APPENDIX C: NaK Temperature Profiles and Associated Test Data

I. INTRODUCTION

Once-through type boiling liquid metal heat transfer rates and associated two-phase flow dynamics have been the subject of a large number of experimental and theoretical studies during the past decade since the initiation of the development of various Rankine cycle SNAP power conversion systems. Difficulties were encountered in achieving rated boiling heat transfer fluxes in NaK heated once-through mercury boilers. These difficulties were encountered to various degrees in mercury flow passages made of 316 SS, Haynes-25 and 9Cr-Mo alloys. Regardless of the material used for the mercury flow passage, some of these boilers demonstrated initial performance characteristics up to design expectations although the length of the required conditioning period varied. Others did not approach the design expectations after hundreds and even thousands of hours of continuous operation. This was believed to be caused by nonwetting, surface contamination, and/or liquid phase slug formation due to absence of early vortex flow establishment in the flow passage next to the liquid-vapor interface.

Several supporting programs were conducted in conjunction with SNAP-8 boiler development activity to investigate these possible causes. The effects of additives on wetting during mercury pool boiling heat transfer were evaluated⁽²⁾. On the basis of the results of this study, rubidium was added to the mercury in amounts up to 860 ppm. The predicted boiling heat transfer rates were achieved after addition of the Rb in a SNAP-8 full-scale boiler initially operating at a highly deconditioned state for several hundreds of hours. To investigate the effect of elevated liquid phase vortex flow velocity on the overall boiler performance, a tight preheat section plug insert geometry, providing a liquid phase velocity of 7.0 ft/sec, was initially tested in an experimental boiler originally performing in a deconditioned state. The results showed immediate improvement in obtained boiling heat transfer rates and the boiler performance stability. The boiling heat transfer rates as represented by the boiler NaK

NOTE: Superscript numbers in parentheses refer to similarly numbered references listed following the text.

temperature profile approaches the design expectations. The boiler exit pressure fluctuations were reduced to a negligible value. This initial qualitative evidence prompted further investigation of the SNAP-8 boiler design concepts.

II. PURPOSE

The object of this experimental study is to investigate the thermal and dynamic performance characteristics of different "once-through" type boiler plug insert geometries.* The availability of design data in this area is very limited, yet these data are very important in controlling the thermodynamic behavior of a boiler such as that used in SNAP-8 and similar Rankine cycle power conversion systems. Since most of these boiler initially exhibit deconditioned boiler characteristics to some extent, it is of particular interest to investigate the effect of different working fluid dynamic aspects in the plug insert section. Initial positive evidence of qualitative value warranted further investigation into this boiler design area.

III. DESCRIPTION OF TEST APPARATUS

A. LOOP DESCRIPTION

CL-4 was designed to simulate the SNAP-8 dynamic cycle conditions for corrosion study. It is a three-loop system, which consists of a heated primary circulation NaK loop, coupled through a boiler simulated mercury Rankine-cycle loop which in turn rejects its heat through the condenser to an air cooled circulating NaK loop. The following operating ranges were used for the boiler plug insert experiment:

NaK Primary Loop

Boiler inlet temperature	1,330°F
NaK flow rate	2,050 lb/hr max.
Heater power input	35 kw max.

Mercury Loop

Mercury flow	500 lb/hr nominal
Boiler inlet temperature	500°F
Boiler inlet pressure	500 psia max.
Boiler outlet pressure	100 psia min.

* Such a geometry consists of a helically wound wire on a solid bar closely fitted and inserted in a mercury tube. The resulting flow passage is of a helical pattern.

Figure 3.1 is the flow diagram of the loop and Figure 3.2 is the schematic arrangement of the loop. The three loop system was constructed to high-vacuum standards.

1. Primary NaK Loop

The NaK primary loop employs a direct resistance heater in which low voltage electrical current is passed through the NaK carrying tube and the NaK. The heater is in a coiled configuration with the two grounded leads on the loop side and an insulated low voltage lead at the mid-point of the coil. Since the resistance of each leg is fixed, the power input is varied by controlling the voltage across the terminals. The voltage is regulated with a saturable core reactor transformer. An electromagnetic pump maintains the NaK flow which is measured by a magnetic flowmeter. A purification system is employed to reduce and maintain the system's oxide level to less than 25 ppm. Other major components in the loop include a level indicator, expansion tank, dump tank, and a cover gas system.

2. NaK Condensing Loop

Major components of the NaK condensing loop consist of a conventional air cooled finned tubes heat exchanger, a magnetic flowmeter, and an electromagnetic pump. A convective type cold trap is employed to maintain a low oxide level in the loop.

3. Mercury Loop

The mercury loop uses two Chempump* Model CFHT-7 1/2-65 (one on a standby basis) for pumping the liquid mercury. A venturi flowmeter is used to measure mercury flow rate. Two semi-standard valves are used for control purposes and for imposing a resistance between the pump and boiler. An adjustable choked nozzle is located downstream of the boiler outlet for the regulation of boiler outlet pressure. The adjustable choked nozzle is a convergent-divergent nozzle in which the throat area may be varied with a moveable pintle. The mercury vapor is then passed through a desuperheater and a turbine blade mockup section before

*Manufactured by Chempump Division of Fostoria Corp., Huntingdon Valley, Penn.

entering the condenser. The desuperheater and the blade mockup are not necessary for the boiler experiment, but were originally designed for corrosion study. The NaK-cooled mercury condenser is a counter-flow heat exchanger consisting of three tapered condensing tubes with a straight length for subcooling.

The rest of the mercury loop consists of semi-conventional liquid metal components such as bellows sealed valves, electrical resistance level probes and a cover gas system.

B. BOILER DESCRIPTION

The mercury boiler is single-pass counter-flow tube-in-shell heat exchanger wound into helix form with a protruding inlet and outlet. Figure 3.3 shows the boiler. The mercury flows in the tube and the NaK through the annulus passage. An inlet plug is inserted into the straight part of the protruding mercury inlet section to increase the liquid mercury and low quality helical velocity. A spiral wire vortex-generator is installed in the coiled mercury tube to promote heat transfer. Spacers are used to center the mercury tube in the annulus. The NaK inlet and outlet are located near the ends of the shell. The boiler configuration and geometry are as follows:

Mean helical coil diameter --- in -----	18
Helical shell pitch --- in -----	1-3/8
Shell size --- in -----	1-1/8 O.D. x 0.083 wall x 9.959 I.D.
Tube size --- in -----	9/16 O.D. x 0.0832 wall x 0.397 I.D.
Vortex wire diameter --- in -----	0.049
Vortex wire pitch --- in -----	1.5
Coil tube length --- ft -----	55
Straight tube length --- ft -----	5
Tube material -----	9 CR-1Mo
Shell material -----	316 SS

The boiler was installed in a metal tank assembly and insulated with about 6-1/2 inches of fused alumina bubbles. Six 1/2 in.-thick layers of fiberflax insulation was affixed to the outside of the boiler supporting tank assembly. The test runs and corresponding plug insert geometries tested are listed in Figure 3.4.

C. BOILER TEST INSTRUMENTATION

1. Temperature Measurement

The NaK boiler inlet, outlet, and the boiler shell temperatures are measured by 1/16" diameter, stainless steel sheathed, MgO insulated thermocouples. These thermocouples have ungrounded junctions, and are attached to the 316 stainless steel tube as shown in Figure 3.5. The NaK boiler inlet temperature is measured by three thermocouples attached circumferentially at the tube 18" from the boiler. The boiler outlet temperature is measured by a thermocouple located at about 9" from the boiler shell. Location of thermocouples along the 60 feet boiler is as follows:

<u>Thermocouple No.</u>	<u>Distance from Boiler Inlet Tube Sheet (in.)</u>	<u>Remarks</u>
1	35.5	Straight section
2	40.5	"
3	45.5	"
4	50.5	"
5	55.5	"
6	60.5	"
7	75.5	"
8	116.5	Coiled section
9	154.5	"
10	201.5	"
11	227.5	"
12	268.5	"
13	306.5	"
14	350.5	"
15	390.5	"
16	427.5	"
17	460.5	"
18	570.5	"
19	592.5	"
20	639.5	"
21	669.5	"

<u>Thermocouple No.</u>	<u>Distance from Boiler Inlet Tube Sheet (in.)</u>	<u>Remarks</u>
22	718.5	Coiled section
23	732.5	"
24	733.5	"

The mercury inlet and outlet temperatures are also measured by Chromel-P-alumel 1/16" diameter, MgO insulated, stainless steel sheathed ungrounded thermocouples. The boiler inlet thermocouple is welded to the tube wall 10" from the boiler inlet. The boiler outlet temperature thermocouple is an immersion type installed 15" downstream of the boiler as shown on Figure 3.6.

Four Pace 150°F reference junctions are utilized to condition the thermocouple signal. The NaK shell temperatures are recorded on a Leeds and Northrup 24 point 0-1500°F. 12" scale strip chart recorder. The NaK boiler inlet temperature is recorded on a Daystrom Weston 24 point, 150°F.-1500°F. 4" scale strip chart recorder. The NaK boiler and the mercury boiler outlet temperature are recorded each on Motorola 2 point, 150°F.-1500°F. 4" scale strip chart recorders.

2. Temperature Measurement Accuracy

The thermocouples carry a manufacturers accuracy guarantee of $\pm 4^{\circ}\text{F}$ from 0°F to 530°F , and $\pm 3/4\%$ above 530°F . The Leeds and Northrup and Daystrom Weston records are periodically calibrated against a Leeds and Northrup portable potentiometer standard to an accuracy of $1/4\%$ of full scale. The Motorola temperature recorders are setup to an accuracy of 1% of full scale, but overall readout accuracy is judged to be approximately 2% .

3. Pressure Measurement

The boiler inlet, outlet, and the two pressure taps in the instrumented plug are measured by 0-500 psia range, unbonded type strain gage transducers. Solid state stable bridge supplies provide 6 v, dc exatation to each transducer. The output signal from each transducer is amplified to the desired level and transmitted to the indicators. These pressure readouts are

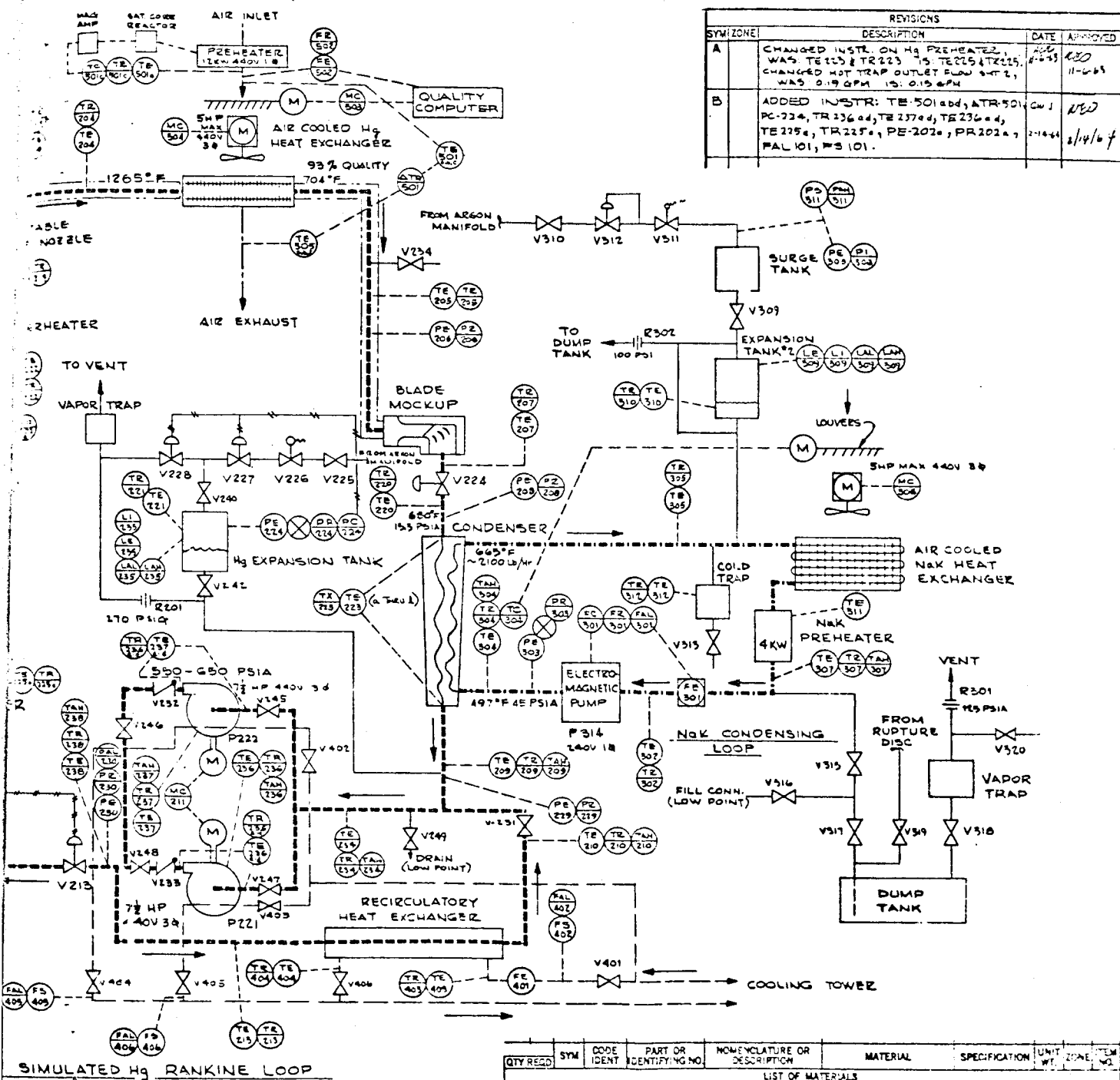
indicated on Motorola 4" scale strip chart recorders that have null balance potentiometer type movements. In addition, these pressures are also transmitted into a "Honeywell Visicorder" which is a mirror galvanometer oscillograph using "Instant Trace" paper. The Visicorder serves to check the small scale Motorola recorder as well as indicating the amplitude and frequency of the recorded pressure. Two 10" diameter 0-400 psig, 1/4% accuracy Heise gauges are also connected in parallel to the pressure taps of the instrumented plug.

The transducers are calibrated when a new plug insert is installed. Calibration of the transducers is accomplished by applying regulated nitrogen gas at the transducer pressure connection, this pressure is simultaneously monitored on a Bordon tube test gauge of traceable accuracy. Several pressure increments throughout the operating range are applied, and the indicator readings recorded. Correction curves are drawn from the results and used to correct subsequent test data. The initial accuracy of each pressure measuring system is found to be the resolution accuracy of the indicator and is within 1% of full scale.

4. Flow Measurement

An ASME standard venturi flow meter with the throat diameter of 0.100" is used for metering mercury flow. The differential pressure across the flowmeter is parallel to an electronic transducer and a pneumatic transmitter. The electrical output signal from the transducer is then amplified and indicated on a Motorola 4" strip chart recorder. The pneumatic transmitter output signal of 3-12 psig is transmitted directly to a 12" circular recorder indicator. Periodically, these recorder readouts are calibrated against known mercury flow rates which are within the test run operating range. The calibration flow rate is established by accumulating a given weight of mercury on a scale over a measured time increment. The maximum overall error in weight flow is $\pm 4\%$.

The NaK flow is measured by a permanent magnet flowmeter manufactured by MSA Research Corporation. The flowmeter dc output is amplified and indicated on a Motorola 4" strip chart recorder indicator. The recorder accuracy is approximately 1% full scale. The overall NaK weight flow accuracy is estimated as $\pm 2\%$.

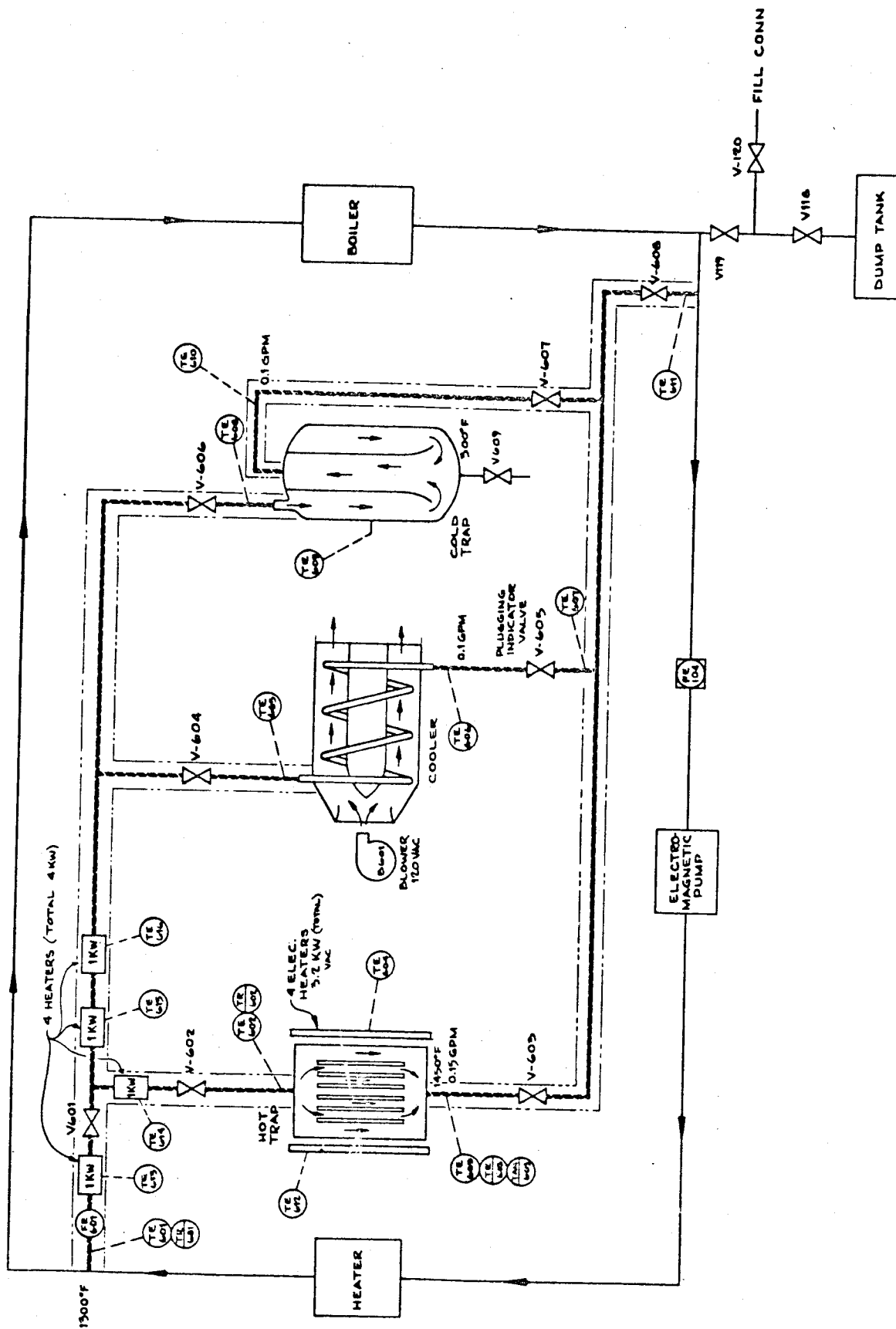


REVISIONS			
SYM/ZONE	DESCRIPTION	DATE	APPROVED
A	CHANGED INSTR. ON Hg PREHEATER, WAS: TE125 & TR223 TO: TE225 & TR225, CHANGED HOT TRAP OUTLET FLOW SHT 2, WAS 0.19 GPM TO: 0.15 GPM	11-6-65	ASD
B	ADDED INSTR: TE 501 add, ATR 501, PC-724, TR 236 add, TE 237 add, TE 236 add, TE 225 add, TR 223 add, PE-202 add, PR 202 add, FAL 101, FAS 101.	2-14-66	ASD

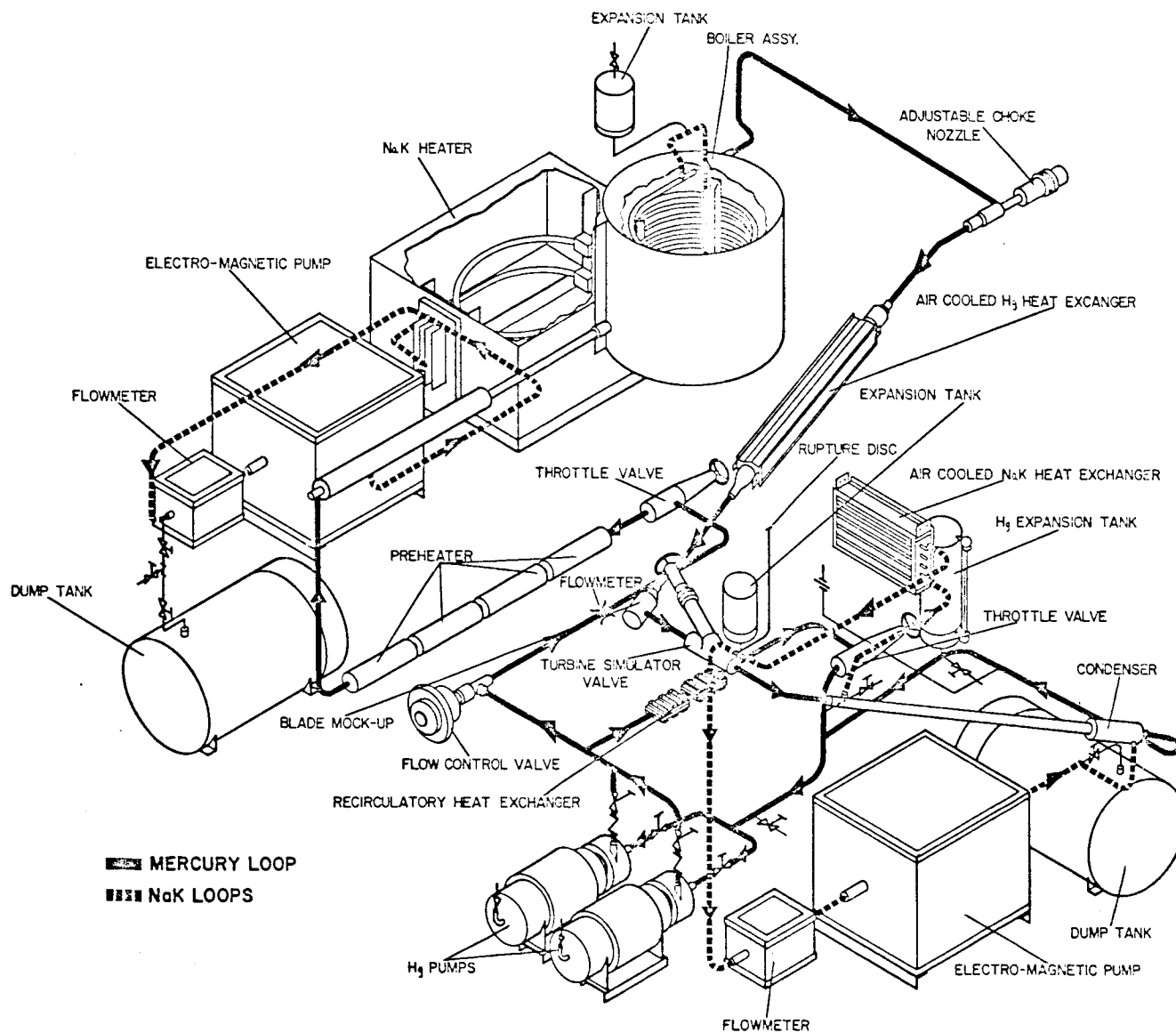
QTY	REQD	SYM	CODE	IDENTIFYING NO.	NOMENCLATURE OR DESCRIPTION	MATERIAL	SPECIFICATION	UNIT	ZONE	TEM
LIST OF MATERIALS										
DRAWN D. TAMURA DATE 10-28-65					SAN RAMON, CALIF.					
CHECKED BY: [Signature] DATE 10-28-65					NUCLEONICS					
DESIGNED BY: [Signature] DATE 10-28-65					P & I DIAGRAM					
STRESS: [Signature] DATE 10-28-65					SNAP-8 CORROSION LOOP					
DESIGN ACTIVITY APPD: [Signature] DATE 10-28-65					CODE IDENT NO. 09336					
PART NEXT FINAL NEXT ASSY USED ON					DWG NO. 409023					
DASH NO. []					RELEASE DATE 10-28-65 SHEET 1 OF 2					
DRAWING LEVEL RAD										

I DIAGRAM, SNAP-8 CORROSION LOOP

40.1-64-1329



P & I DIAGRAM, NaK PURIFICATION SYSTEM FOR SNAP-8 CORROSION LOOP



CORROSION LOOP LAYOUT

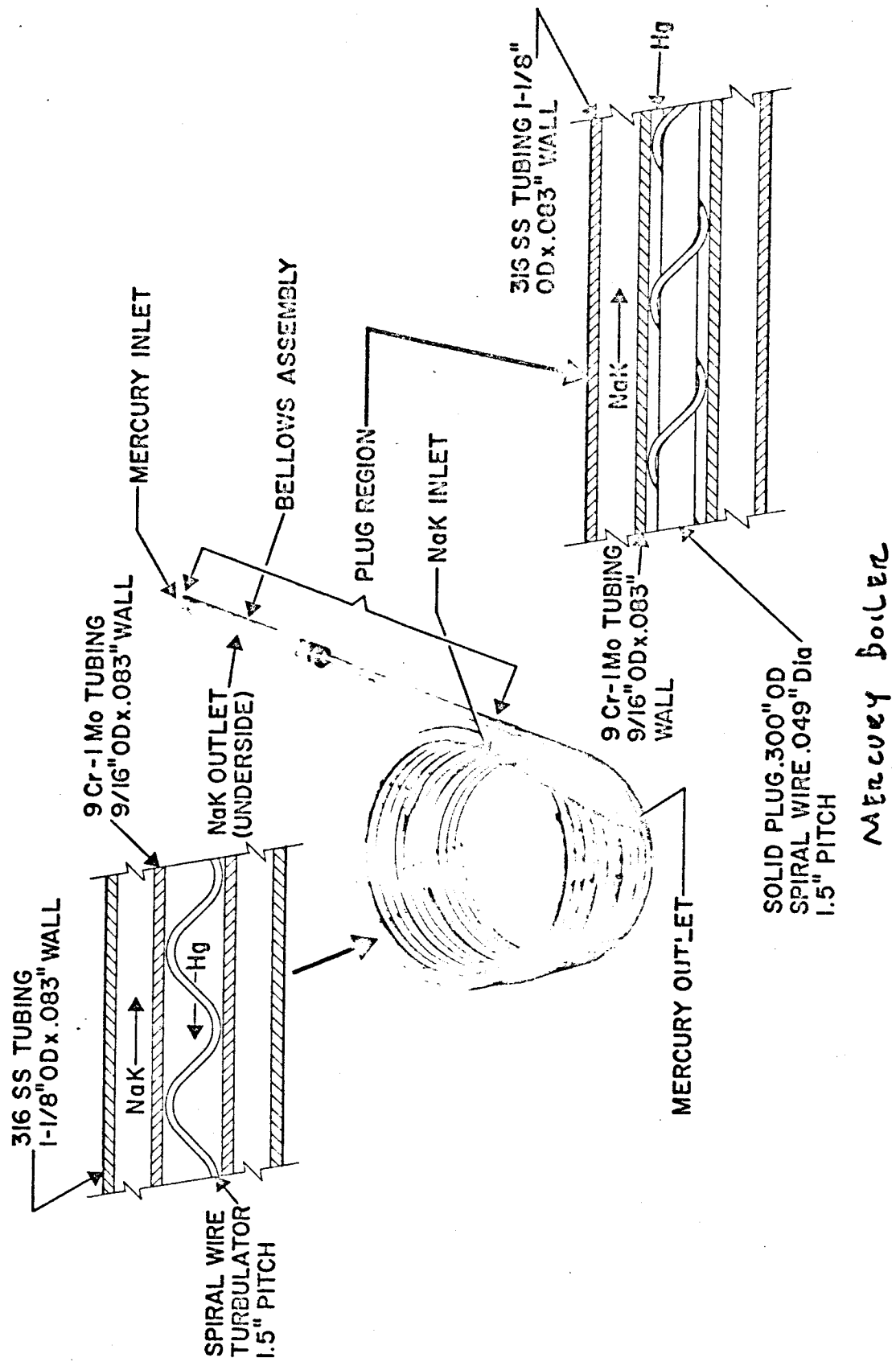


Fig. 3.3

CL-4 BOILER (D X L = 0.400 IN. X 60 FT)

PLUG INSERT GEOMETRIES TESTED

TEST RUN NO.	PLUG INSERT NO.	L	PREHEAT SECTION					VAPOR SECTION				REMARKS
			W		h		P ₁	L ₁	P ₂	INSTRUMENTED		
			IN.	IN.	IN.	IN.				IN.	IN.	
			TYPE ¹					TYPE ¹	IN.	IN.		
1	1	--	W	--	--	.75	21	W	.75	36	NO	POOR PERFORMANCE DURING FIRST 660 HR
2	2	6	W	--	--	.125	15	W	.75	36	NO	GOOD INITIAL PERFORMANCE
3	2	6	W	--	--	.125	15	W	.75	36	NO	GOOD RESTART PERFORMANCE
4	1	--	W	--	--	.75	21	W	.75	36	NO	GOOD RESTART PERFORMANCE
5	3	9	M	.033	.048	.125	15	W	.75	36	YES	GOOD PERFORMANCE D = .397" (ASSUMED)
6	4	9	M	.038	.045	.125	15	W	1.50	36	YES	GOOD PERFORMANCE D = .400" (ASSUMED)
7	4	9	M	.038	.045	.125	15	W	1.50	36	YES	GOOD PERFORMANCE PLUG #4 REINSULTED
8	3a	9	W	--	--	.125	15	W	1.50	36	YES	GOOD PERFORMANCE
9	3a	9	W	--	--	.125	15	W	1.50	36	YES	GOOD PERFORMANCE P _{ex} AND P _{in} OSCILLATION
10	3b	6	W	--	--	.17	15	W	1.50	24	YES	GOOD PERFORMANCE REDUCED P _{PL}

1 M - Machined Thread

W - Wire Wound

NOTES: a. All Wire Uses = 0.049 In. Diameter

b. OD of Plugs = 0.0398 In.

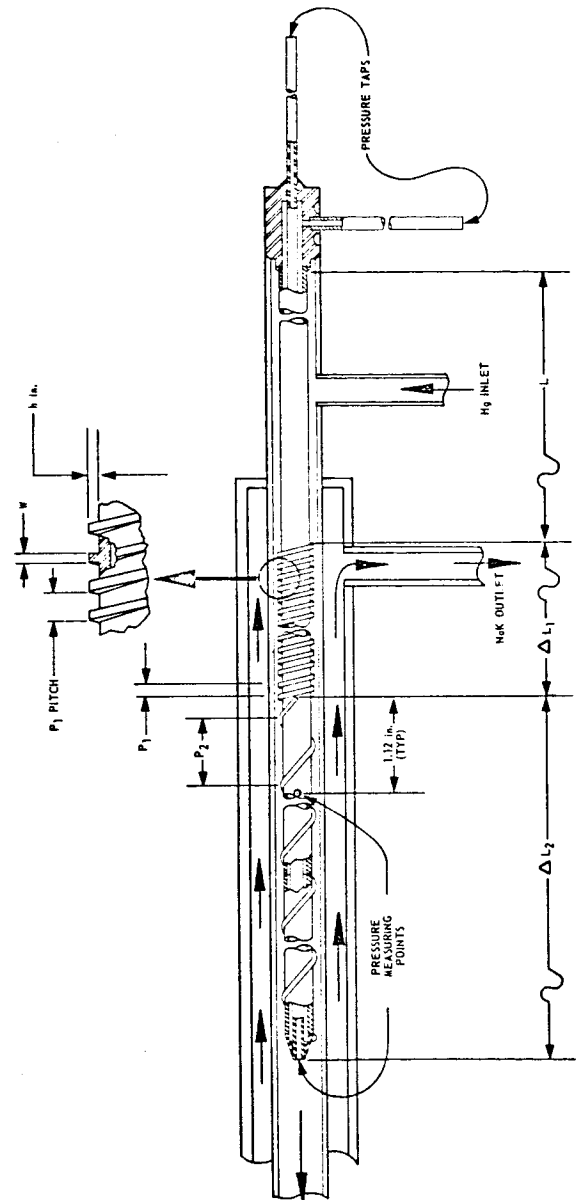
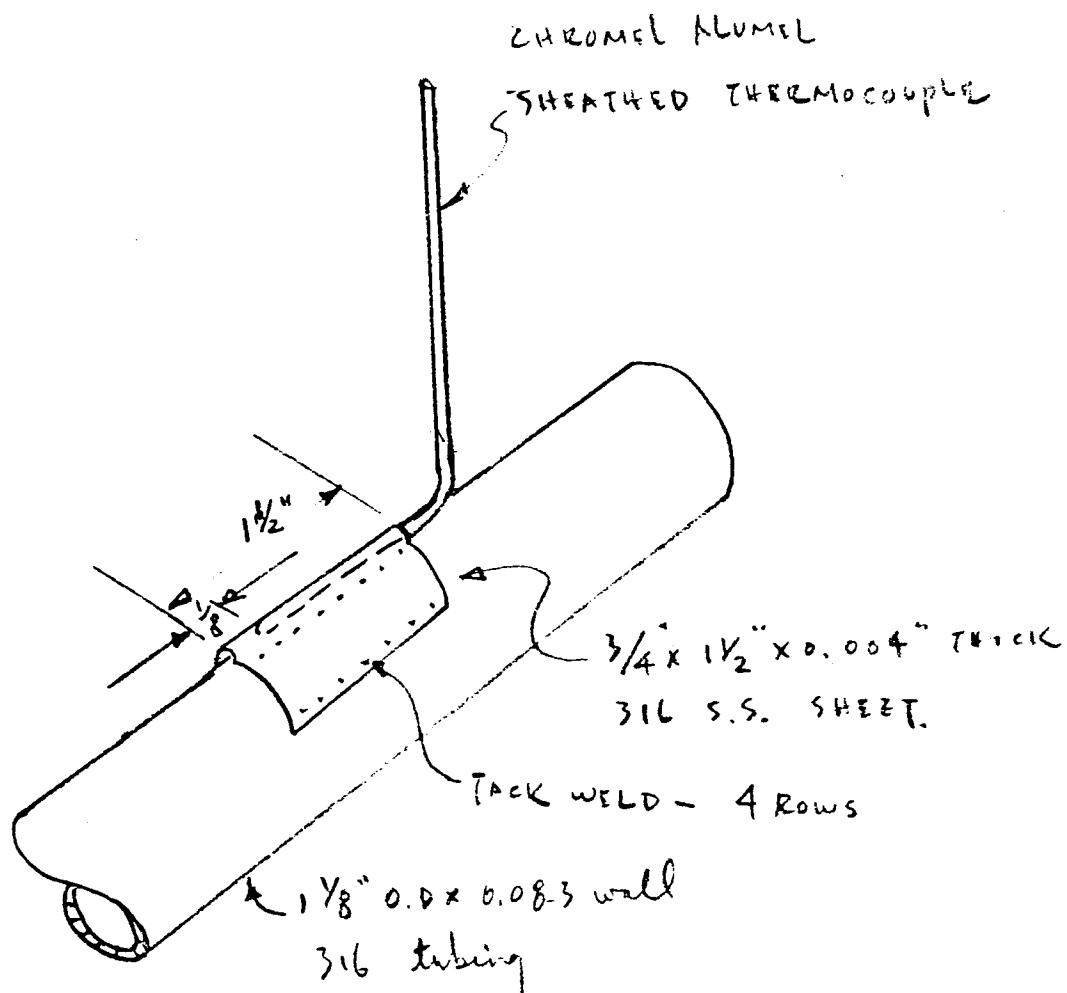


Fig. 3.4



THERMOCOUPLE INSTALLATION ON BOILER

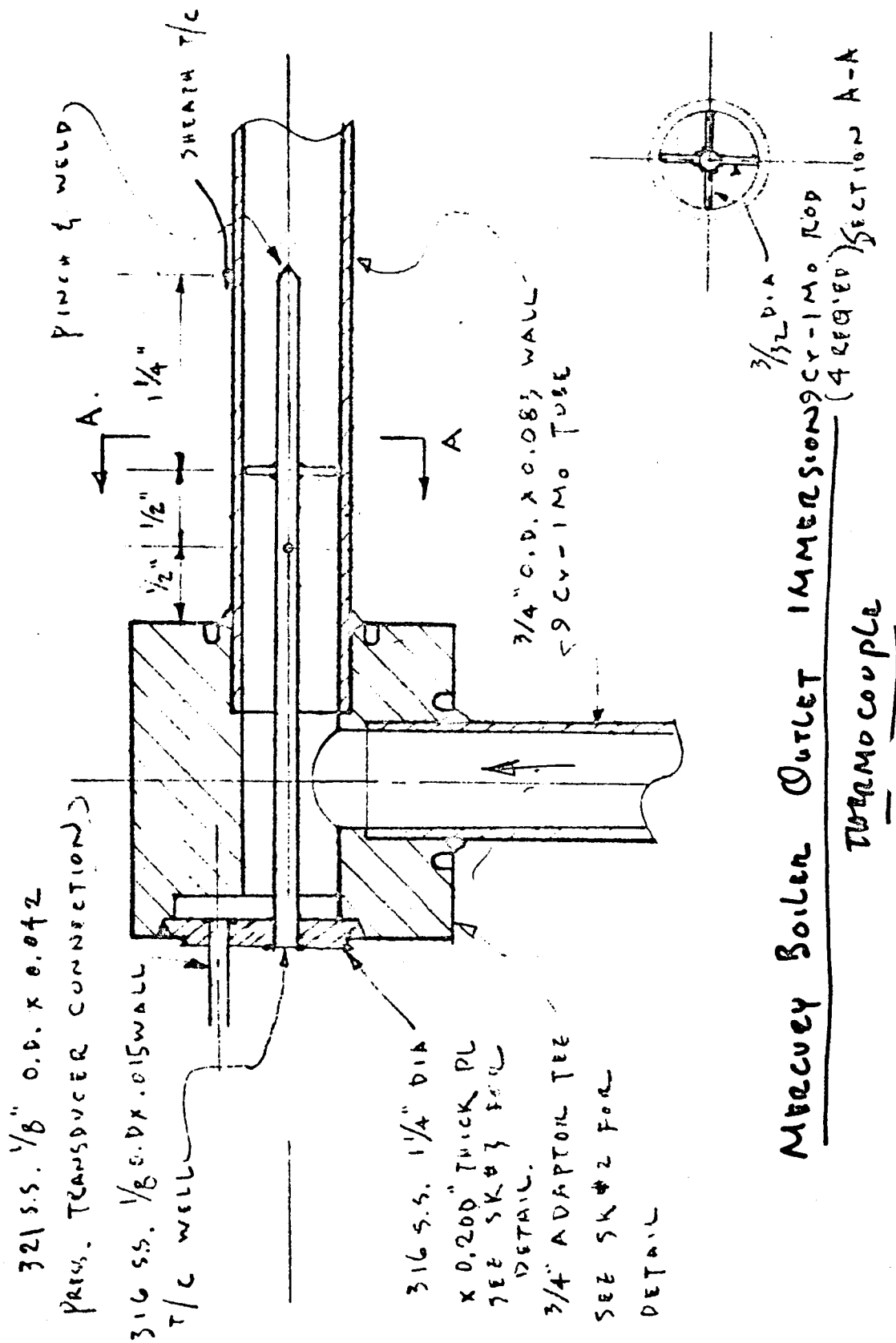


Fig. 3.6

IV. OPERATION*

The pretest preparation includes the instrumentation installation and calibration, mechanical checkout and calibration, and loading of three loops. This preparation is accomplished in accordance with Reference 5.

A. BOILER STARTUP

The temperature of the NaK in the primary loop is slowly raised up to 1150°F measured at the boiler inlet. Four hours is usually required to reach this temperature. During the heating up period, the primary NaK pump is started and flow is slowly increased to a maximum of 2050 lb/hr, and a vacuum of approximately 10-20 torr is maintained in the mercury loop to degas the mercury boiler. A dry ice in acetone trap between the mercury loop and vacuum pump collects any mercury or condensible vapors. Upon reaching the NaK temperature of 1150°F the mercury loop is sealed and the vacuum system is removed. The mercury pump is started initially into a bypass system and then injected into the boiler. The adjustable choke nozzle is in the fully open position during the hot start. An approximate mercury flow rate of 200-350 lb/hr is circulated through the boiler. When the flow is stable the NaK boiler inlet temperature is slowly increased to the test condition. The mercury system is allowed once more to stabilize. To obtain the desired pressure at the mercury boiler outlet, the adjustable choke nozzle is gradually closed. Normally, the time elapsed from mercury injection to the first test point is about two hours and during this period regular observations are made to monitor the boiler NaK shell temperature and other test parameters.

B. TEST RUNS

When a test program is designed, the order in which the test points are run is considered carefully since it is desired to have the least temperature disruption in the boiler. Once the test point conditions are acquired and the boiler temperature appears stable, it is standard practice to allow the NaK shell temperature profile to remain stable for at least thirty minutes before the data is taken. To further substantiate the data validity, several test points are repeated at the end of the test.

* Acknowledgement: The boiler plug insert performance tests were performed by E. McDaniel, B. Farwell, A. Herdt, J. Ralphs, G. Redfern and M. Wong.

C. SHUTDOWN

For a normal shutdown, the mercury flow into the boiler is first valved off and the primary NaK is allowed to circulate. Power to the heater is shutoff as soon as the mercury flow into the boiler is stopped. The NaK flow is continued until the boiler inlet temperature is cooled down to about 600°F by natural convection. After the boiler is cooled to room temperature, the vacuum system and cold trap system are connected to the mercury loop, and a vacuum of 15-20 torr is maintained until the next startup. If a prolonged shutdown or a plug insert change is scheduled, an argon cover gas of a slight positive pressure is applied and maintained on the mercury loop and boiler at all times.

V. TEST DATA REDUCTION

The test data reduction and analysis is based on the obtained NaK and liquid mercury flow measurements, the boiler NaK and mercury flow terminal temperature measurements, and the boiler NaK-shell-tube surface temperature profile in conjunction with mercury flow passage pressure measurements located at the boiler inlet and exit. Two additional pressure measurements in the mercury flow passage are obtained by means of internally located pressure taps in the plug insert section. One is located at the preheat section end point. The other is located at the plug insert vapor section end point. Test data recordings used for test data reduction are contained in Appendix C.

In view of the limited number of mercury flow passage pressure taps, the pressure gradients between $P_{Hbi}-P_1$, P_1-P_2 , and P_2-P_{Hbo} are assumed to be linear. The pressure measurements P_{Hbi} , P_1 , P_2 and P_{Hbo} were taken from the pressure taps located at the boiler inlet, preheat section end point, plug insert end point and the boiler exit, respectively. The NaK shell-tube outer surface temperature profile representation is assumed to be identical to the mercury flow passage internal wall temperature profile. This assumption is based on the obtained overall thermal resistance value across the heat flow pass as determined from the test and the analytically determined total resistance across the NaK film and the tube wall. The comparison of these resistances shows that:

$$\left(\frac{1}{U}\right)_{\text{Test}} < \left(\frac{r_m}{r_o} \frac{1}{h_N} + \frac{t}{k_w}\right)_{\text{design}}$$

which means that (q'') test $>$ (q'') design. Obviously, the available data on tube wall thermal conductivity and the NaK side film heat transfer coefficient determination method is in error. This consideration implies that the NaK side film heat transfer coefficient is infinite, and the mercury tube wall heat transfer resistance is negligible.

Linear correction of the measured NaK temperature profile was introduced in the excess boiler superheat length. This correction was established from the heat balance analysis where the net NaK flow and the NaK temperature drop due to the external boiler heat loss were determined. For the average NaK flow rate used

in these tests the NaK temperature drop due to external heat loss was approximately 30°F. The boiler NaK shell-tube skin thermocouple temperature measurements at their best are estimated to be of $\pm 2.5\%$ accuracy with respect to total full-scale indication.

Test data reduction and analytical computations were conducted on the IBM-7094 Model 2 computer. A detailed analytical program for this purpose is contained in Appendix B. The results are presented in tabulated form in Appendix A.

The main items determined for each test point data set were:

1. Boiler heat balance
2. Plug insert preheat section geometric, dynamic, and thermal parameters
3. Plug insert vapor quality section geometric and dynamic parameters
4. Plug insert section exit vapor quality
5. NaK temperature at liquid-vapor interface
6. NaK temperature in terms of vapor quality
7. Plug insert vapor quality section local boiling thermal and dynamic parameters
8. Unplugged tube vapor quality section local boiling thermal and dynamic parameters
9. Plug insert vapor quality section mean thermal parameters
10. Unplugged tube vapor quality section mean thermal parameters

VI. DISCUSSION OF RESULTS

The results of the test data reduction are evaluated in the light of proposed drop-wise drywall boiling heat transfer and two-phase flow pressure drop correlations. These correlations are based on mercury nonwetting characteristics which are the principal cause for the dropwise two-phase flow regime in the boiling section. To obtain the predicted boiler performance characteristics in accordance with this design approach, the experimental evidence indicates that the initial physical and/or chemical cleanliness of the wall surface in the mercury flow passage prior to mercury injection is of particular importance. Aside from the thermal and dynamic conditions at the liquid-vapor interface and in the vapor flow quality region, which are necessary to promote effective mercury vaporization, the obtained boiling heat transfer characteristics as represented by the NaK temperature profile, can be better or worse than those predicted by the dropwise drywall boiling theory. The boiler performing in accordance to these design expectations is said to be in a conditioned state. The boiler exhibiting better heat transfer characteristics is said to be in a partially-wetted state; the boiler exhibiting poorer heat transfer characteristics is said to be in a deconditioned state. When intermittent physical wetting on the mercury flow passage walls occurs, the boiler is said to be in a partially-wetted state. Partial wetting was observed on the plug insert surface when the plug insert was removed from our test boiler after 96 hours of operation. A typical NaK temperature profile for a deconditioned boiler is depicted in Appendix C, Figure C-1. The same boiler exhibiting fully-conditioned, or partially-wetted boiler heat transfer characteristics is shown in Figure C-4. The reason for obtaining the boiler NaK temperature profile as shown in Figure C-4 can be attributed to significant changes occurring on the mercury flow passage wall surface. The physical and/or chemical changes occurring on the material surface are only poorly understood, and require further investigation.

Initial test results as depicted in Appendix C, Figures C-1 through C-7, are of a qualitative nature. They show the effect of the liquid-phase velocity in the boiler preheat section on the overall boiler performance. Figures C-1 and C-2 depict a typical NaK temperature profile for a deconditioned boiler during the initial test run when the liquid-phase velocity in the helical flow passage was

0.8 ft/sec. Nonmeasurable improvement in the boiler conditioning effect was observed during several hundreds of hours of operation under a nominal SNAP-8 boiler NaK inlet temperature schedule. The same boiler, when restarted with a revised preheat section plug insert geometry providing a liquid-phase velocity of 6 to 7 ft/sec, exhibited effective mercury flow passage conditioning immediately. Also, the projected NaK temperature profile approached the design conditions very rapidly. Figures C-3 and C-4 show the progress in conditioning 4 hours and 20 hours after mercury injection, respectively. The boiler restart, (Figure C-5) with the same plug insert geometry, did not indicate any boiler performance degradation. A subsequent test run (Figure C-6), with the original preheat section plug insert, providing 0.8 ft/sec liquid-mercury velocity, still produced conditioned boiler performance characteristics. This evidence shows that once the tube surface is in a conditioned or wetted state, the liquid-velocity level in the preheat section is not of particular importance. Examination of the NaK temperature profiles (Figures C-6 and C-5) and associated test data reveals that the difference between the two plug insert geometries tested can be detected in the slope of the NaK temperature profile and in the boiling termination point. A tight liquid phase plug insert geometry combined with a similar low vapor quality region seems to be the right design approach for a high performance "once through" type boiler. Once the fully conditioned or even wetted mercury flow passage state is established, the boiler can also be operated without a plug insert. This condition is shown in Figure C-7, where the slope of the NaK temperature profile reflects boiling heat transfer rates comparable to those obtained with plug inserts. However, in the unplugged boiler this heat transfer is accompanied by excessive oscillations in boiler exit pressure and flow. It is postulated that nucleation sites were developed in the mercury flow passage plug insert regions during previous boiler test runs, when the elevated velocity plug insert geometries were tested. Thus, the boiler inlet and tube section, without a plug insert, was operating under a convective nucleate boiling heat transfer regime.

Test data point sets as shown in Appendix C, Figures C-8 through C-36, are representative of the obtained NaK temperature profiles and the associated primary and secondary working fluid operating parameters utilized in the test data reduction program. The results of this reduction are presented in tabulated form in Appendix A.

The calculated heat loss values as obtained from the heat balance closure are in the range from 1 to 16% of the total heat input. This discrepancy can be attributed to inaccuracies in temperature measurements or their corrections; e.g., the boiler NaK temperature drop error of $\pm 10^\circ\text{F}$ results in a heat loss error of ± 1.26 kw. The boiler heat loss was also determined on the basis of boiler operation at zero mercury flow and different NaK flow and temperature levels. The estimated heat loss value is 2 to 2.5 kw or 9 to 10% of the total heat input.

Similar parametric data point scatter resulted from the boiler thermal and dynamic test data analysis, which can also be attributed to the inaccuracy of the boiler instrumentation. The most critical areas in this regard are the establishment of the true mercury temperature and pressure conditions in the boiler plug insert section. The point of particular interest is the determination of the liquid-vapor interface location in the boiler. To perform a detailed test analysis in this area, a much more sophisticated instrumentation technique is necessary. A typical and desirable boiler test data representation in conjunction with such an instrumentation is depicted in Figure 6.0-1. This representation implies that several mercury flow passage temperature measurements in the preheat (T_{PH}) and low quality vapor section (T_{S} , T_{V}) as well as the exact mercury flow pressure (P_{Hg}) and NaK flow temperature (T_{N}) profiles must be experimentally established. In accordance to this diagram, the liquid-vapor interface location (L_{OO}) is determined when T_{SOO} , T_{NOO} and P_{OO} are projected as the point L_{OO} on the abscissa. Our experimental boiler instrumentation is not providing this type of test data representation. Because of these limitations, the test data evaluation was performed on the basis of several assumptions in conjunction with trial and error methods wherever the available test data were not sufficient to support the analysis.

These assumptions are in the form of corrections in the curvature of the NaK temperature profile and the mercury pressure profile. They are further based on plug insert liquid and low vapor quality section calibrations. These calibrations provided pressure drop data, which were utilized to determine the liquid and gas flow frictional pressure drop factors for the different plug insert geometries tested. In making these calibrations, liquid and vapor flow rates were regulated so as to maintain the same Reynold's number range as that existing in the boiler when operating under normal conditions. The results of liquid flow calibrations are shown in Table 6.0-1.

The Darcy type pressure drop correlation for two-phase turbulent flow was used to determine the product ϕf_v , where

$$\phi = \frac{\Delta P_{TP}}{f_v \frac{De}{\Delta L} \frac{(\bar{x} G)^2}{2g_c \rho_v}} = \frac{\Delta P_{TP}}{\Delta P_v}$$

The product ϕf_v is correlated in terms of the Martinelli-type parameter

$$\lambda = \left(\frac{\bar{x} G De}{\mu_v} \right)^{.8} \frac{\mu_v}{\mu_f} \frac{\rho_f}{\rho_v} \frac{\bar{x}}{1-\bar{x}}$$

which is determined from an incremental local boiling heat transfer analysis. ϕf_v versus λ is plotted separately for plug insert section and unplugged tube section geometries. Figure 6.0-2 shows the low vapor quality (up to 15%) pressure drop correlating parameters, when the vapor quality region next to the liquid-vapor interface enters the plug insert preheat section. Figure 6.0-3 shows the same correlating parameters for the plug insert vapor quality range from 0 to 80%. The data in Figure 6.0-3 were fitted by least squares analysis providing the average curve

$$\phi f_v = e^{4.87} \lambda^{-.674}$$

The average two-phase flow pressure drop factor is determined from the above curve using

$$\phi = \frac{\phi f_v}{f_v}$$

where f_v is obtained from N_2 gas flow tests carried out in a Reynold's number range corresponding to 100% vapor flow. Figure 6.0-4 shows a similar plot of data points in the unplugged tube section for the vapor quality range from 20 to 100%. A least squares analysis of the data predicted a curve for best fit given by

$$\ln \phi f_v = 16.06 - 2.224 \ln \lambda + .065 (\ln \lambda)^2$$

The comparison of two plug insert geometries in regard to their pressure drop in terms of plug insert end point vapor quality is illustrated in Figure 6.0-5. Curve 2 as compared to Curve 1 shows that excessive boiler pressure drop may result when the plug insert length is overdesigned. In the case of oversized preheat

section plug insert length and tight pitch helical flow passage geometry, early vapor generation may occur in the preheat section. Under these conditions the total plug insert pressure drop may reach undesirable proportions (Curve 3 and 4).

The magnitude of the obtained initial boiling heat fluxes in terms of the temperature difference at the liquid-vapor interface location is plotted in Figure 6.0-6. In view of the wide scatter of the test data the points can be approximated in the form $q'' = \text{const. } \Delta T_{00}$, which is a linear function with a 45° slope. This interpretation would indicate that convection vortex type boiling was induced from the liquid-vapor interface location by the elevated liquid phase velocity.

The vapor quality section thermal and dynamic operating parameters in dimensional and non-dimensional form were determined on the basis of local boiling heat transfer and two-phase flow pressure drop correlations in 20% vapor quality increments. To check out and compare these results with the dropwise dry wall boiling theory the obtained local boiling mean temperature difference (ΔT_M) of each quality increment was considered in the light of boiling heat transfer design correlations for the purpose of determining whether it was in the contact, intermittent contact, or film boiling regime. These results, as well as the results of the analysis of the overall heat transfer in the plug insert section and the unplugged tube vapor section, are tabulated in Appendix A.

For each vapor quality increment ($\Delta x = .20$) throughout the length of the boiling section the calculated mean heat fluxes are plotted in terms of the mean temperature difference between the NaK temperature and the mercury saturation temperature. The mean NaK temperature of each quality increment is determined from the boiler NaK temperature profile. The mercury saturation temperature is determined from the mercury flow passage pressure representation in the same quality increment. Plots of the obtained local boiling heat fluxes at mean vapor qualities of 10, 30, 50, 70 and 90% in terms of mean temperature differences are shown in Figures 6.0-7 thru 6.0-11, respectively. The data scatter display was analyzed by least squares techniques to obtain curves of best fit. The results of this analysis are shown graphically as well as analytically in the figures indicated above.

The results of local boiling heat transfer representation as discussed above are further differentiated into boiling occurring in the plug insert section

and boiling occurring in the unplugged tube section. The data points of each quality increment of these sections were considered in the light of different boiling regimes as defined by the dry wall dropwise boiling correlations. These correlations are: (1)

Contact boiling:

$$Nu_C = \frac{1}{32} Nu_\delta^2 \left(\frac{k_f}{k_v} \right)^2 \left(\frac{D}{\delta_o} \right)^2 \left(\frac{\rho_v}{\rho_f} \right) \frac{(1-x)^{1/3}}{x}$$

Intermittent contact boiling

$$Nu_{IC} = 234 C^4 \left(\frac{k_v}{k_f} \right)^4 \left(\frac{\delta_o}{D} \right) \left(\tan \alpha \frac{DG}{\mu_v} \frac{h_{fv} \mu_v}{k_v \Delta T_M} \right)^2 (1-x)^{4/3} x$$

Film boiling

$$Nu_F = \frac{6^{1/3}}{4} \left(\frac{D}{\delta_o} \right) \left(\frac{4}{3} \right) \left(\frac{DG}{\mu_v} \tan \alpha \frac{\rho_v h_{fv} \mu_v}{\rho_f k_v \Delta T_M} \right)^{2/3} \frac{(1-x)^{2/3}}{x^{1/3}}$$

The boiling regimes are determined by equating $Nu_C = Nu_{IC}$ and $Nu_{IC} = Nu_F$ and solving then for $\Delta T_M = \Delta T_{cr}$ accordingly. These solutions are:

$$\Delta T_{cr-1} = \frac{h_{fv} \mu_v C^2 (7488)^{1/2} \left(\frac{k_v}{k_f} \right)^3 \left(\frac{DG}{\mu_v} \right) \tan \alpha (1-x)^{1/2} x}{k_v \left(\frac{D}{\delta_o} \right)^{3/2} \left(\frac{\rho_v}{\rho_f} \right)^{1/2}}$$

If $\Delta T_{cr-1} > \Delta T_M \rightarrow$ use contact boiling regime.

If $\Delta T_{cr-1} < \Delta T_M \rightarrow$ calculate ΔT_{cr-2}

$$\Delta T_{cr-2} = C^3 \left(\frac{h_{fv} \mu_v}{k_v} \right) \frac{936^{3/4} \left(\frac{k_v}{k_f} \right)^3 \left(\frac{DG}{\mu_v} \right) (\tan \alpha) (1-x)^{1/2} x}{6^{1/4} \left(\frac{D}{\delta_o} \right)^{3/2} \left(\frac{\rho_v}{\rho_f} \right)^{1/2}}$$

If $\Delta T_{cr-2} > \Delta T_M \rightarrow$ use intermittent contact boiling regime

If $\Delta T_{cr-2} < \Delta T_M \rightarrow$ use film boiling regime.

The empirical constants taken from Reference 1 are:

	ϕ	C	Nu_{δ}
$0 < x < .4$.43	2.3	-
$.4 < x < 1.0$	1.00	3.0	-
$0 < x < 1.0$	-	-	.8

These values were used to plot the design curves (q'' vs. ΔT_M) superimposed on the test data plots. The results of these considerations are depicted in Figures 6.0-12 thru 6.0-19.

Figure 6.0-12 shows the test results in relation to the design expectations. The curves $Nu_{\delta} = .54$ and $C = 2.0$ are derived from the test data and suggest a more conservative design approach in this plug insert mean quality increment.

Figure 6.0-13 shows similar comparison of expected and obtained boiling heat fluxes at $\bar{x} = .30$ in the plug insert section. The design curves $Nu_{\delta} = .8$ and $C = 2.3$ are in good agreement with the test results.

Figure 6.0-14 shows the heat fluxes obtained at $\bar{x} = .30$ in the unplugged tube section. The design curve $C = 2.3$ as well as the curve derived from test data are in close agreement.

Figure 6.0-15 shows the test data at $\bar{x} = .50$ in the plug insert section. The design curve $Nu_{\delta} = 1.26$ derived from the test data is considerably higher than the one used for the design prediction. This may be attributed to the dynamic two-phase flow conditions existing in this mean quality section of the plug insert. The vapor flow helical velocity at $\bar{x} = .50$ is in excess of 100 ft/sec. Considerable radial acceleration g forces could, therefore, be induced on the liquid droplets carried by the vapor. Consequently the contact area of droplets at the tube wall is increased because of droplet deformation or break-up.

Figure 6.0-16 depicts the test results at $\bar{x} = .50$ in the unplugged tube section. The design prediction curve $C = 3.0$ and the average curve $C = 3.1$, as derived from the test data, are, however, in close agreement.

Figure 6.0-17 shows test results at $\bar{x} = .70$ in the plug insert region. It refers to results similar to those shown in Figure 6.0-15. Both cases are accompanied by relatively high pressure drops through the plug insert vapor quality region.

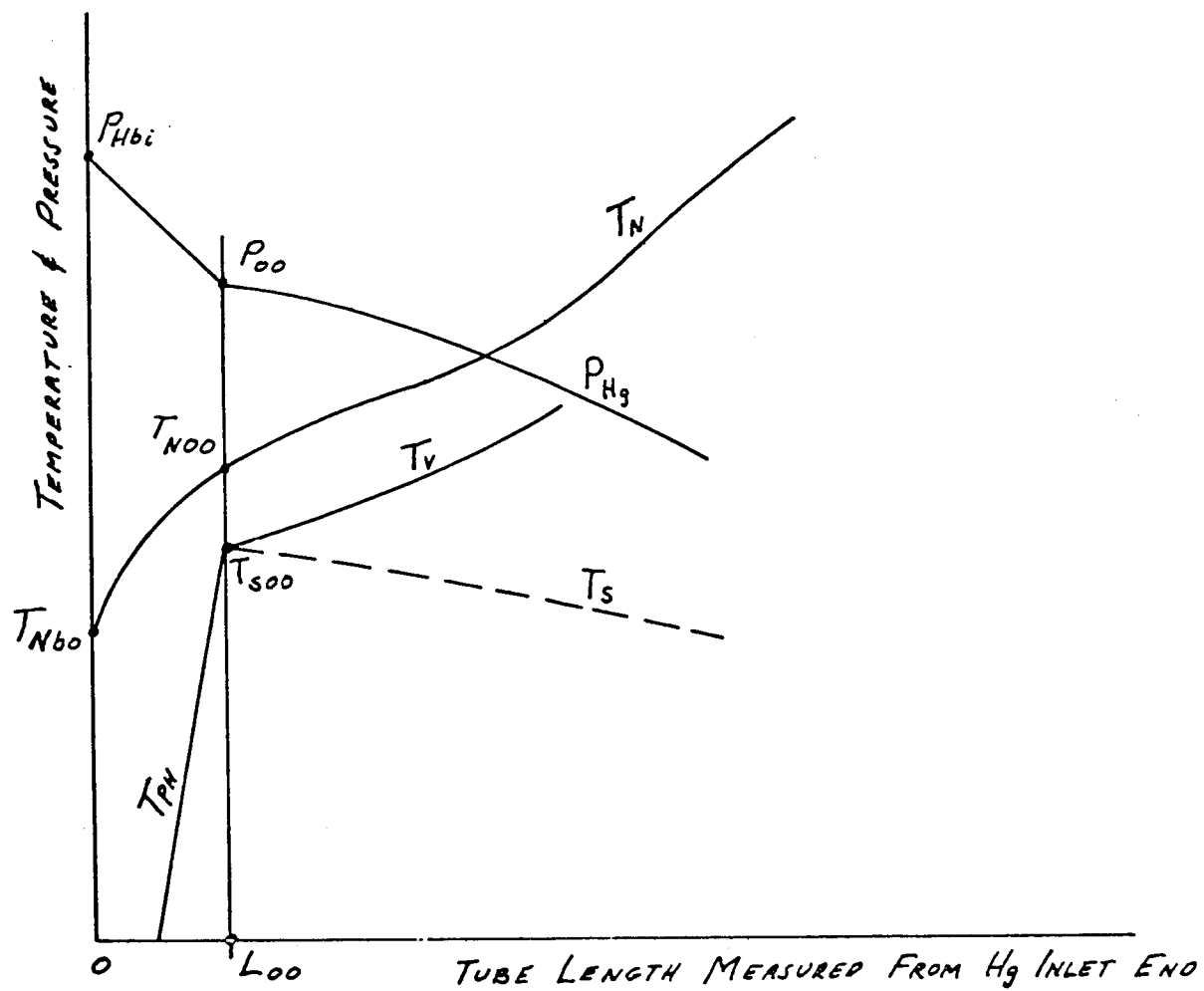
Figure 6.0-18 provides the results at $\bar{x} = .70$ in the unplugged tube section. These heat transfer data can be represented by a local intermittent contact boiling regime at $C = 3.6$. The design prediction using $C = 3.0$ is still a good conservative design approach.

Figure 6.0-19 shows that test data at $\bar{x} = .90$ fall below the expectation of the film boiling regime. This can be explained by test data inaccuracy and error introduced by the estimation of the boiler length at the 100% vapor quality point.

Typical boiling heat flux representations at SNAP-8 operating conditions are shown in Figure 6.0-20. These curves indicate that heat transfer effectiveness and thus the boiler vapor quality section length is dependent on boiler NaK inlet temperature (T_{Nbi}) and the NaK temperature drop (ΔT_N) thru the boiler. The minimum boiling length occurs under a high boiler NaK temperature schedule, which is shown by curve A. The maximum boiling length, as shown by the available heat fluxes of curve B, occurs under a low NaK temperature schedule.

CL-4 BOILER TEST PLUG INSERT FLOW PASS CALIBRATION RESULTS TABLE 6.0-1

PLUG INSERT NUMBER	A _C ft ²	De ft	ΔL' ft	$\frac{\text{lbm}}{\text{sec-ft}^2}$	G lbm/hr-ft ²	μ lbm/hr-ft ²	ρ lbm/ft ³	u ft/sec	W lbm/hr	ΔP psi	T °F	Re	f
3 (Run #5)	3.05x10 ⁻⁵	5.24x10 ⁻³	12.65	3640 4550 5470	1.31 x 10 ⁷ 1.64 x 10 ⁷ 1.98 x 10 ⁷	2.65 " "	824 " "	4.42 5.53 6.63	400 500 600	27 34.8 50.3	300 " "	25,900 32,600 39,000	.00648 .00533 .00531
5 (Run #6)	2.71x10 ⁻⁵	4.95x10 ⁻³	12.81	4110 5130 6150 7200	1.48 x 10 ⁷ 1.85 x 10 ⁷ 2.21 x 10 ⁷ 2.58 x 10 ⁷	2.71 " " "	826 " " "	4.97 6.23 7.45 8.71	400 500 600 700	81 114 156.5 205.5	280 " " "	27,000 33,800 40,400 47,200	.01424 .01281 .01223 .01172
5 (Run #7)	"	"	"	4110 5130 6150	1.48 x 10 ⁷ 1.85 x 10 ⁷ 2.21 x 10 ⁷	2.81 " "	829 " "	4.96 6.21 7.42	400 500 600	71 99 128	250 " "	26,200 32,700 39,200	.0125 .0110 .0100
6 (Run #8)	"	"	"	4360 5450 6530	1.57 x 10 ⁷ 1.96 x 10 ⁷ 2.35 x 10 ⁷	2.64 " "	824 " "	"	400 500 600	62 68 104	300 " "	29,200 36,400 43,700	.0097 .0068 .0073
7 (Run #10)	"	"	"	2950 3430 3780 4120 4470	1.16 x 10 ⁷ 1.24 x 10 ⁷ 1.36 x 10 ⁷ 1.48 x 10 ⁷ 1.61 x 10 ⁷	2.68 " " " "	825 " " " "	"	450 500 550 600 650	30 35.5 41 47 52.5	290 " " " "	24,900 26,500 29,200 31,800 34,400	.0163 .0143 .0136 .0131 .0125
3 (Run #5)	"	"	"	"	"	1.87 " "	783 " "	"	400 500 600	28.4 36.6 52.9	800 " "	36,700 46,200 55,300	"
5 (Run #6)	"	"	"	"	"	"	"	"	400 500 600 700	85.5 120.2 165 217	" " " "	39,100 49,000 58,600 68,300	"
5 (Run #7)	"	"	"	"	"	"	"	"	400 500 600	75.2 105 135.4	" " "	39,400 49,200 58,900	"
6 (Run #8)	"	"	"	"	"	"	"	"	400 500 600	65.3 71.5 109.4	" " "	41,500 51,600 61,900	"
7 (Run #10)	"	"	"	"	"	"	"	"	450 500 550 600 650	31.6 37.4 43.2 49.5 55.3	" " " " "	35,700 38,000 41,800 45,600 49,300	"



TYPICAL BOILER TEMPERATURE AND PRESSURE PROFILES
AT MERCURY INLET END

FIG. 6.Q-1

CL-4 BOILER TEST
TWO PHASE FLOW PRESSURE DROP CORRELATING PARAMETERS
IN PLUG INSERT PREHEAT SECTION

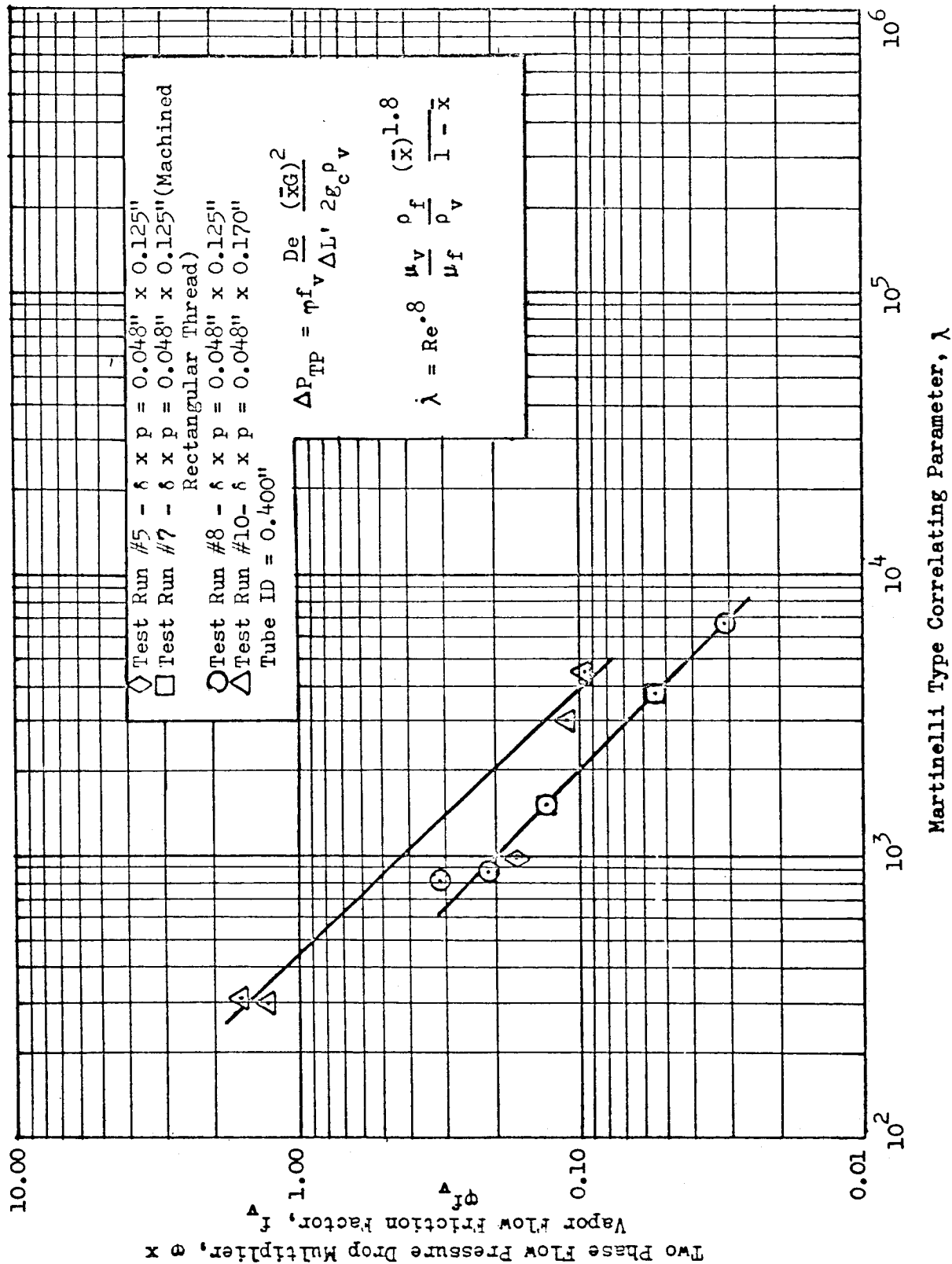


Figure 6.0-2

CL-4 BOILER TEST
PLUG INSERT TWO PHASE FLOW PRESSURE DROP
CORRELATING PARAMETERS

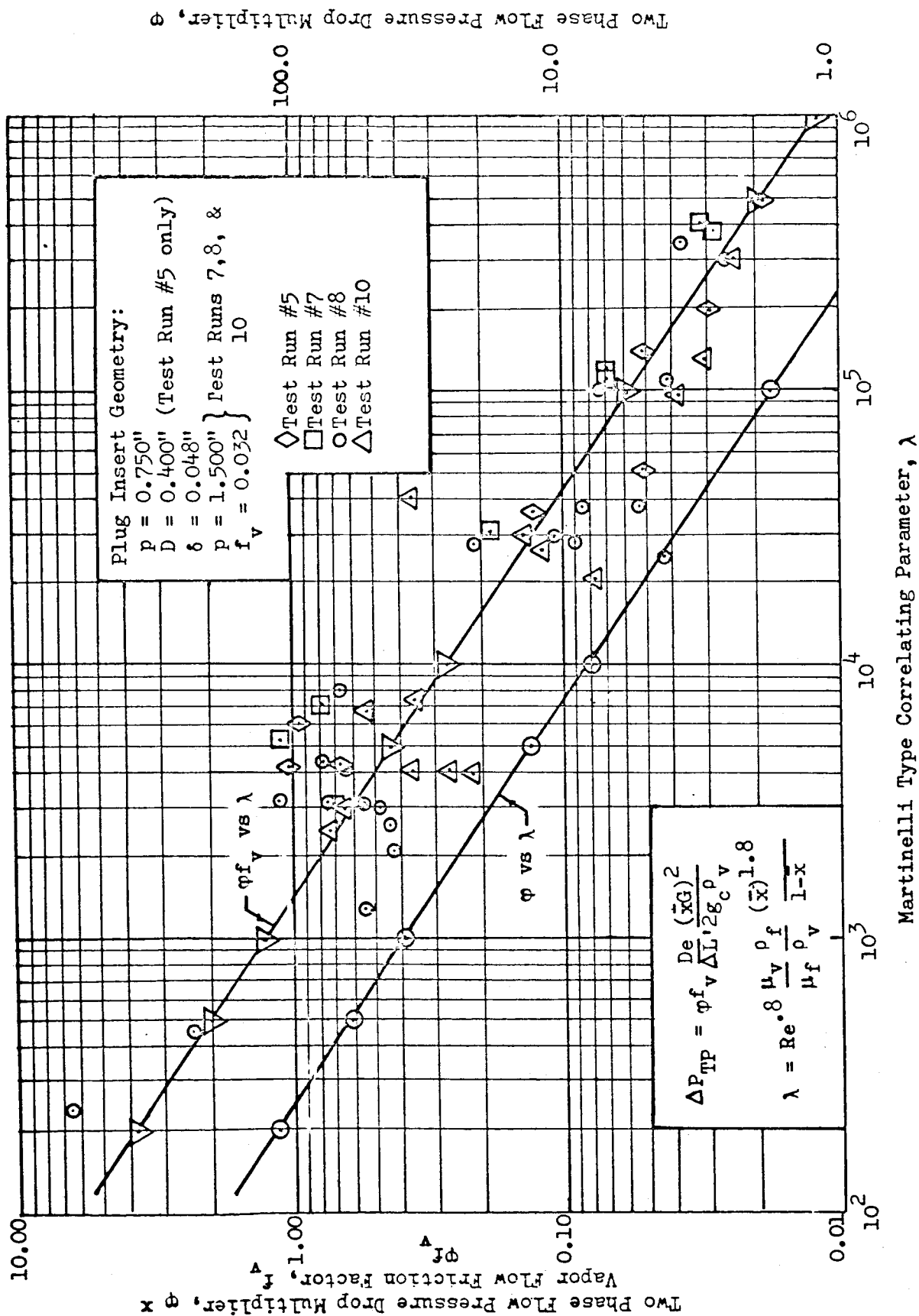


Figure 6.0-3

CL-4 BOILER TEST
UNPLUGGED TUBE TWO PHASE FLOW PRESSURE DROP
CORRELATING PARAMETERS

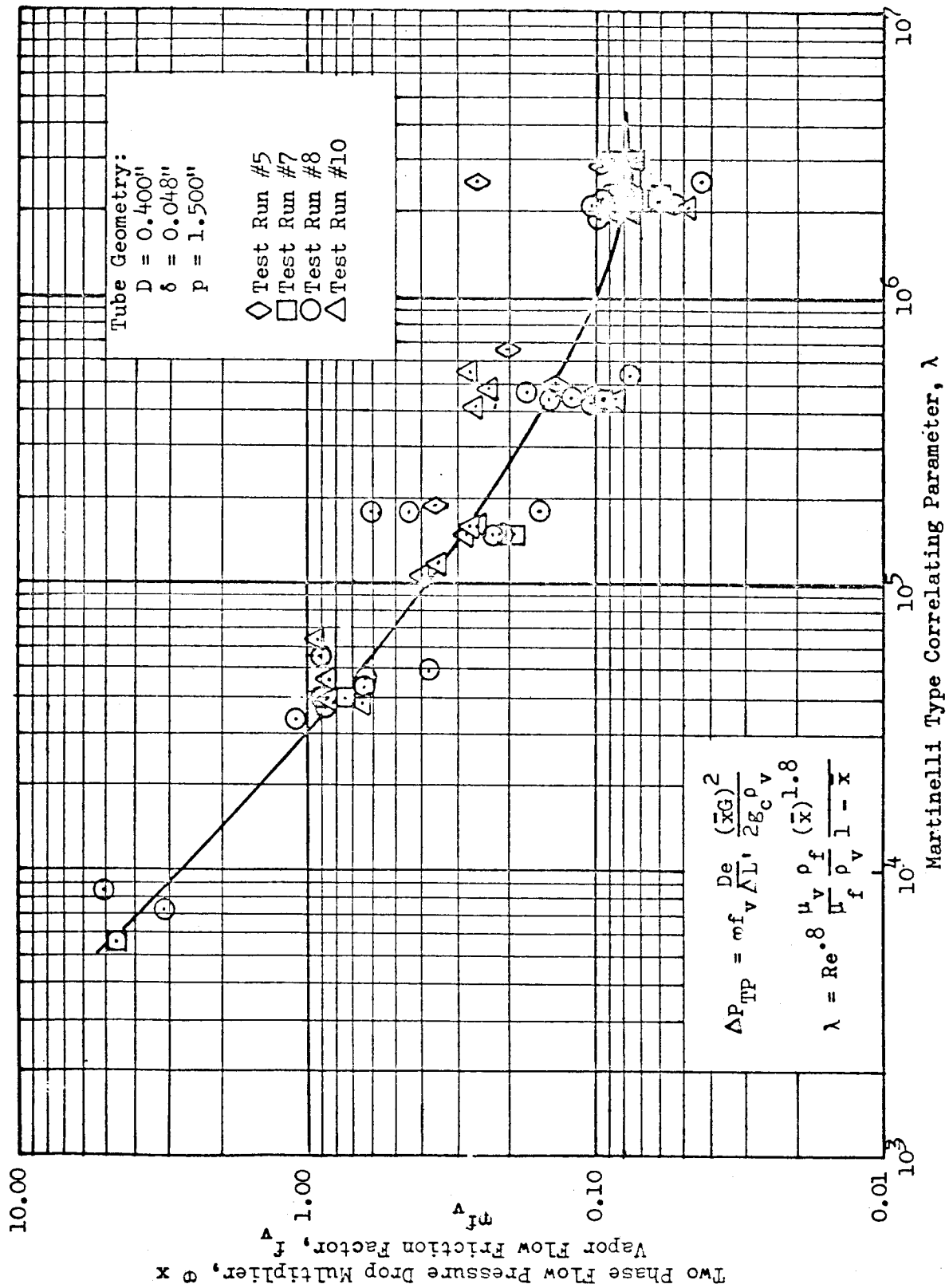


Figure 6.0-4

CL-4 BOILER TEST
 PLUG INSERT VAPOR SECTION PRESSURE DROP
 VS PLUG INSERT VAPOR EXIT QUALITY

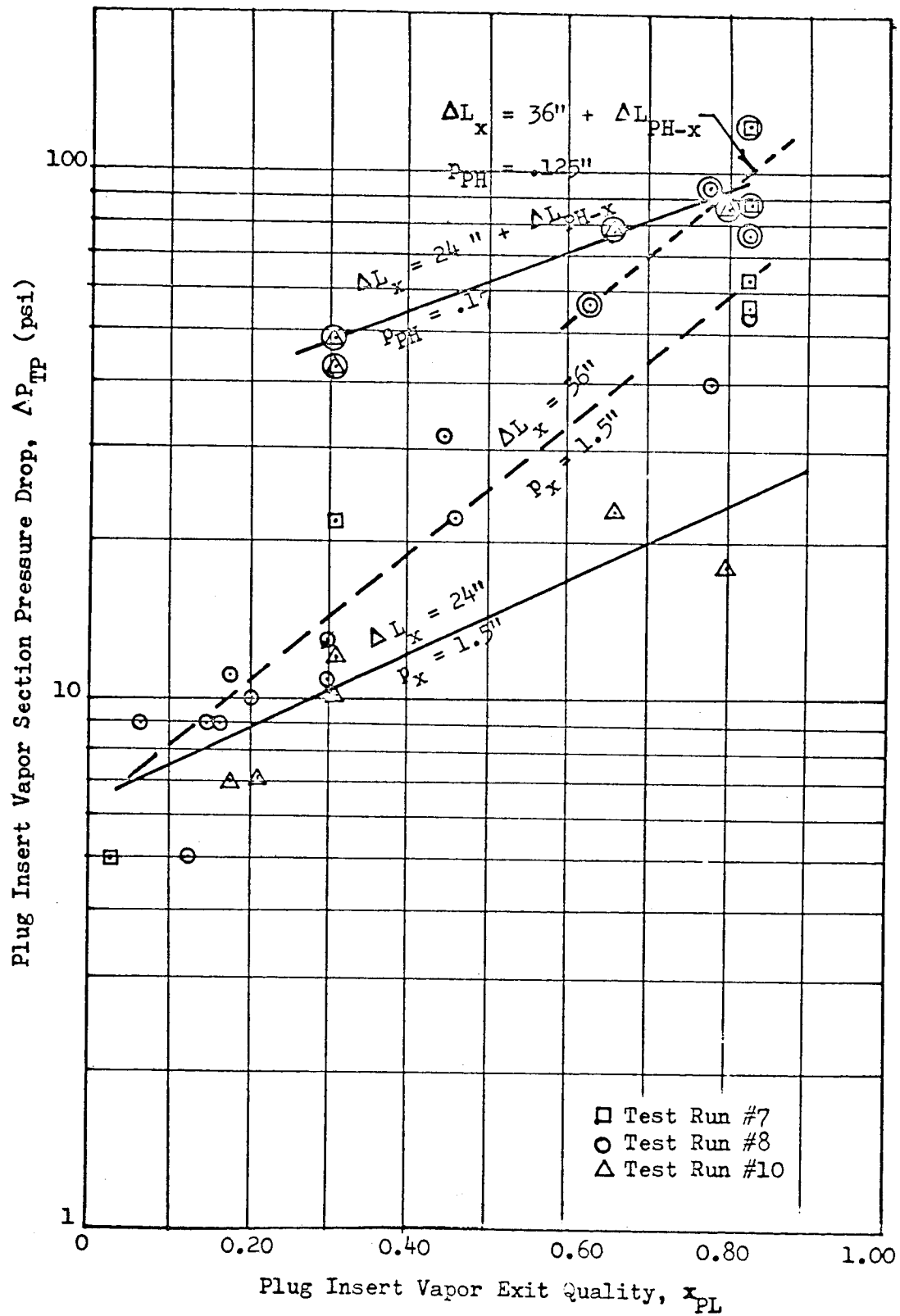


Figure 6.0-5

CL-4 BOILER TEST
INITIAL BOILING HEAT FLUX VS
PINCH POINT TEMPERATURE DIFFERENCE

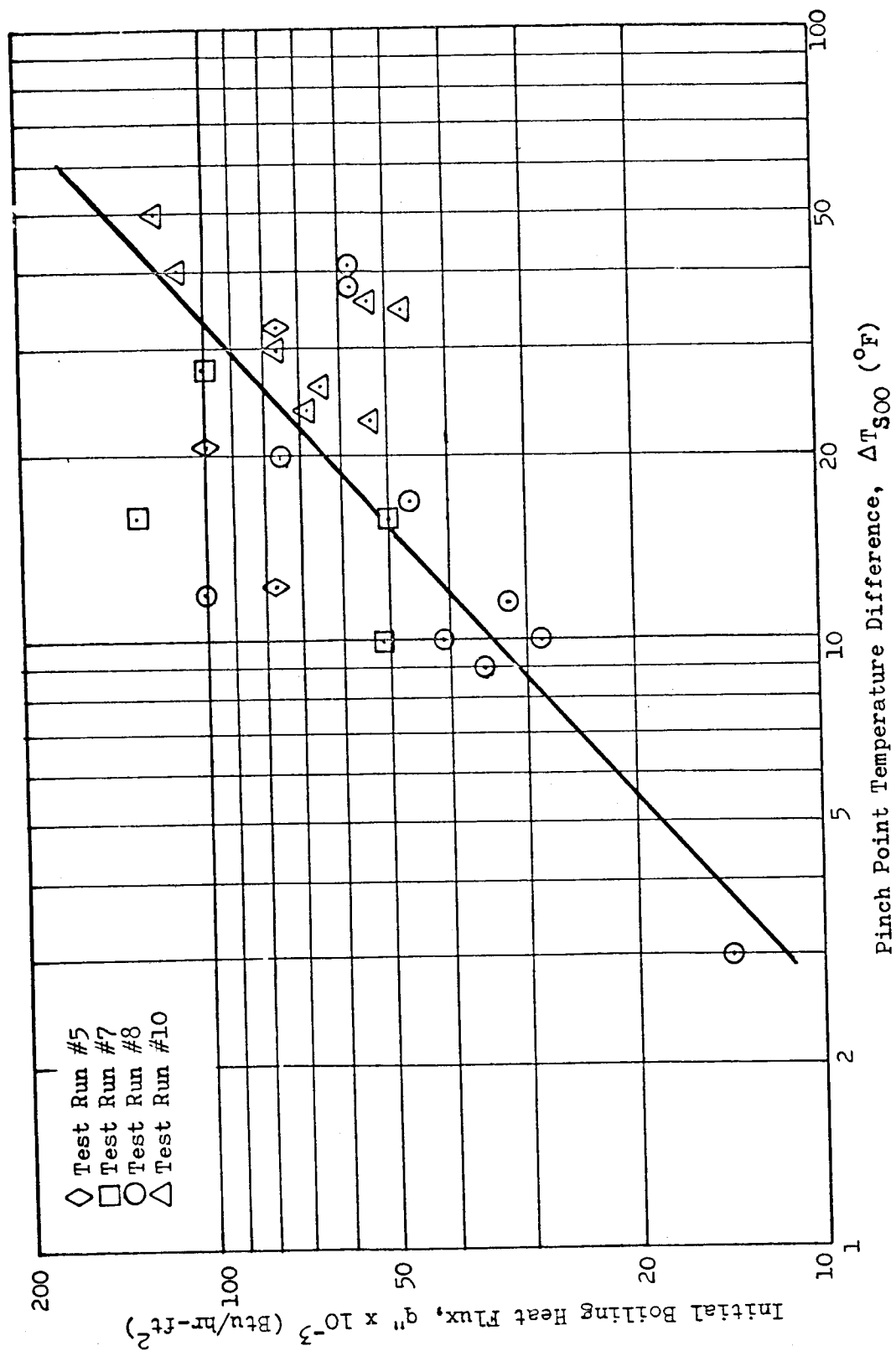


Figure 6.0-6

CL-4 BOILER TEST
 LOCAL BOILING - q'' vs ΔT_M @ $\bar{x} = .10$

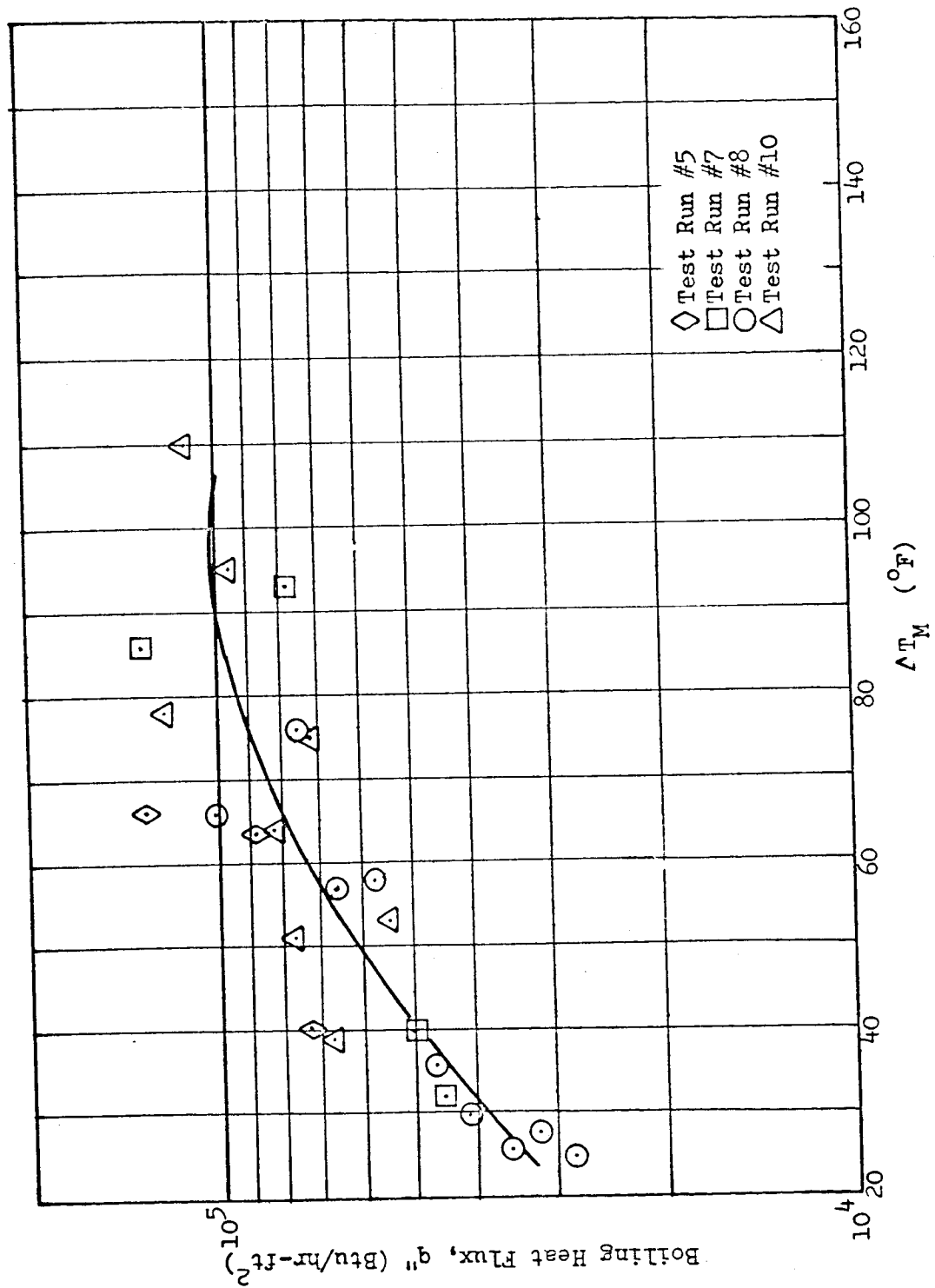


Figure 6.0-7

CL-4 BOILER TEST
 LOCAL BOILING - q'' vs ΔT_M @ $\bar{x} = .30$

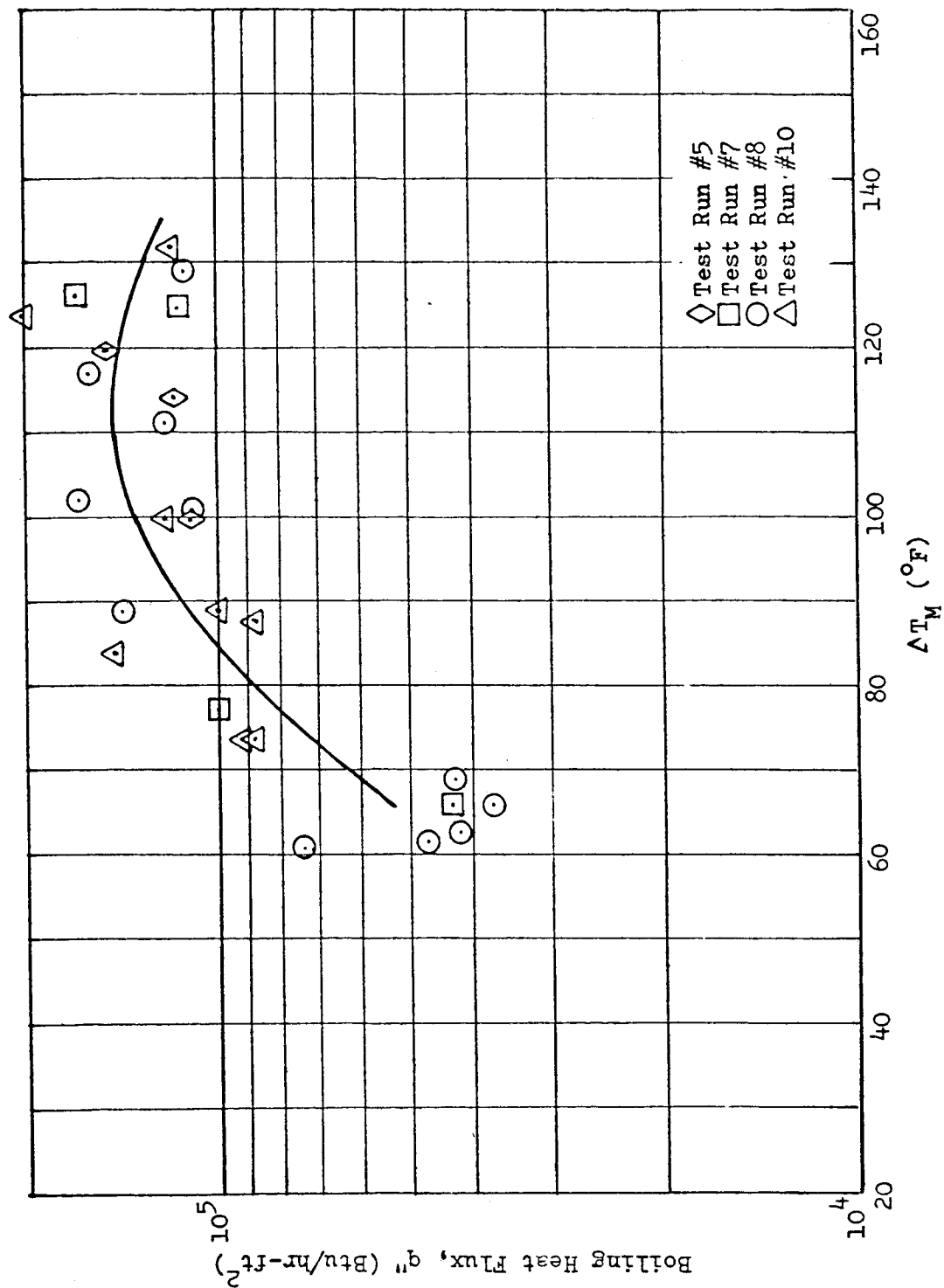


Figure 6.0-8

CL-4 BOILER TEST
LOCAL BOILING - q'' vs ΔT_M @ $\bar{x} = .50$

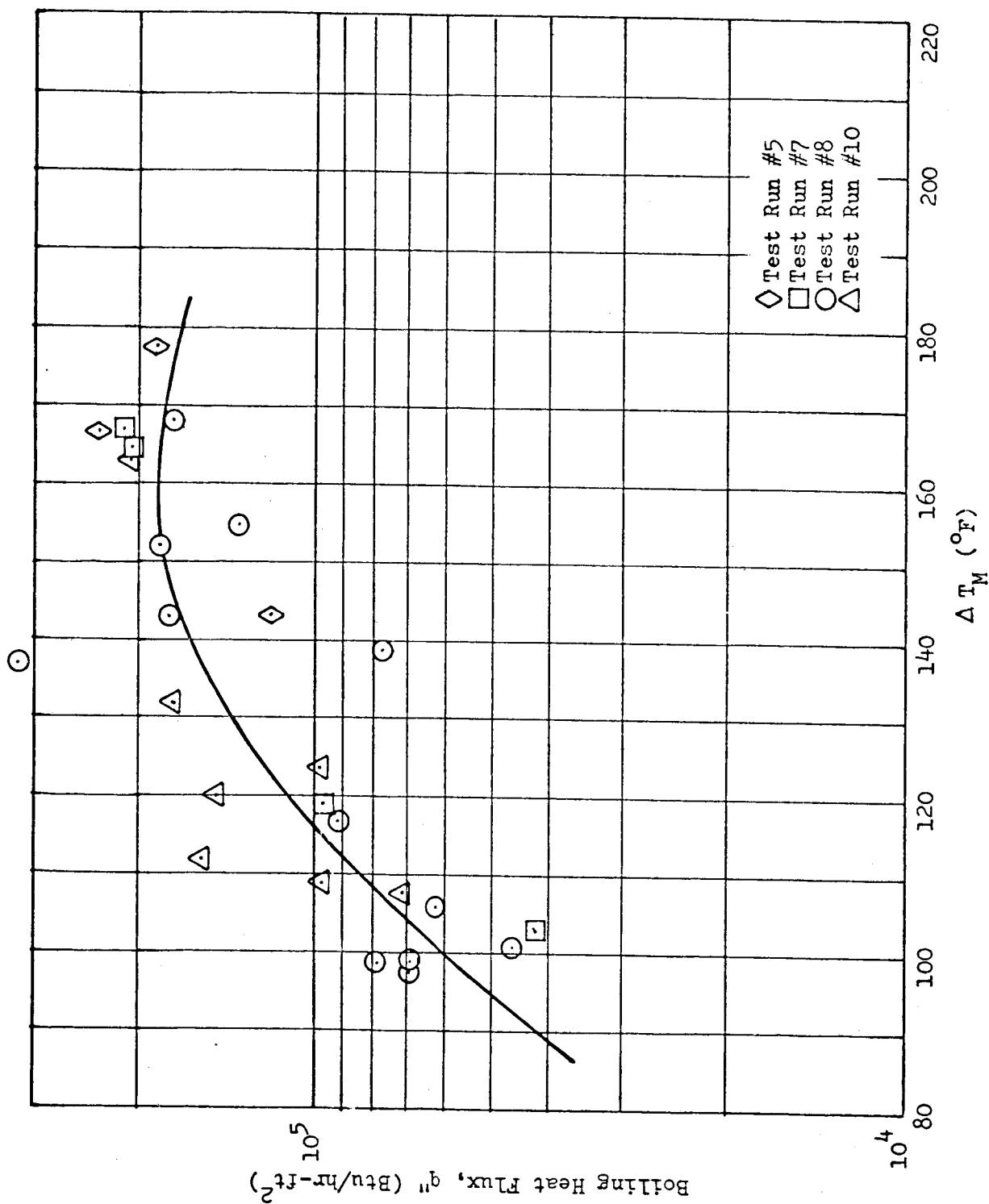


Figure 6.0-9

CL-4 BOILER TEST
LOCAL BOILING - q'' vs ΔT_M @ $\bar{x} = .70$

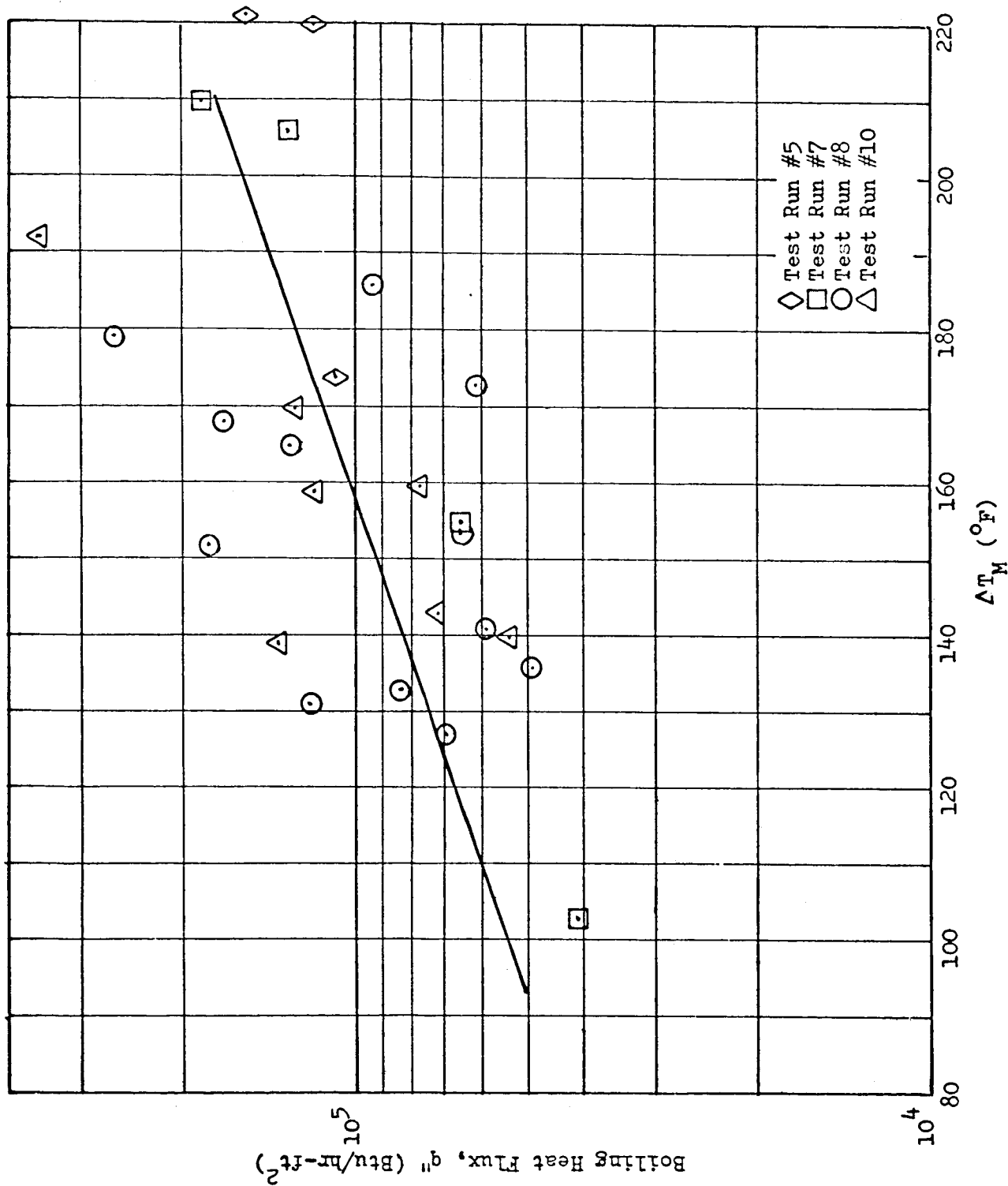


Figure 6.0-10

CL-4 BOILER TEST
LOCAL BOILING - q'' vs ΔT_M @ $\bar{x} = .90$

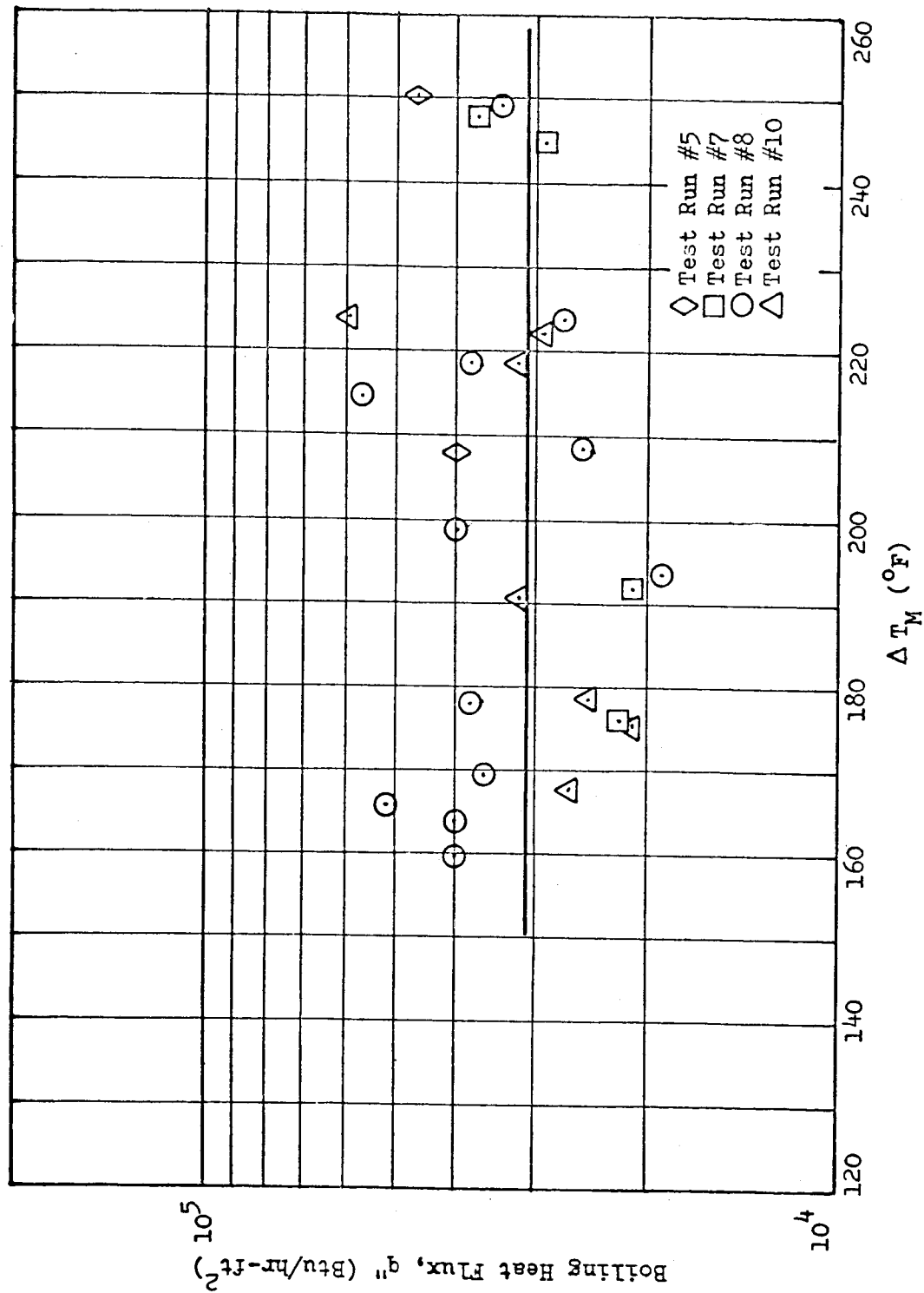


Figure 6.0-11

CL-4 BOILER TEST
LOCAL BOILING IN PLUG INSERT REGION
 q'' vs ΔT_M @ $\bar{x} = .10$

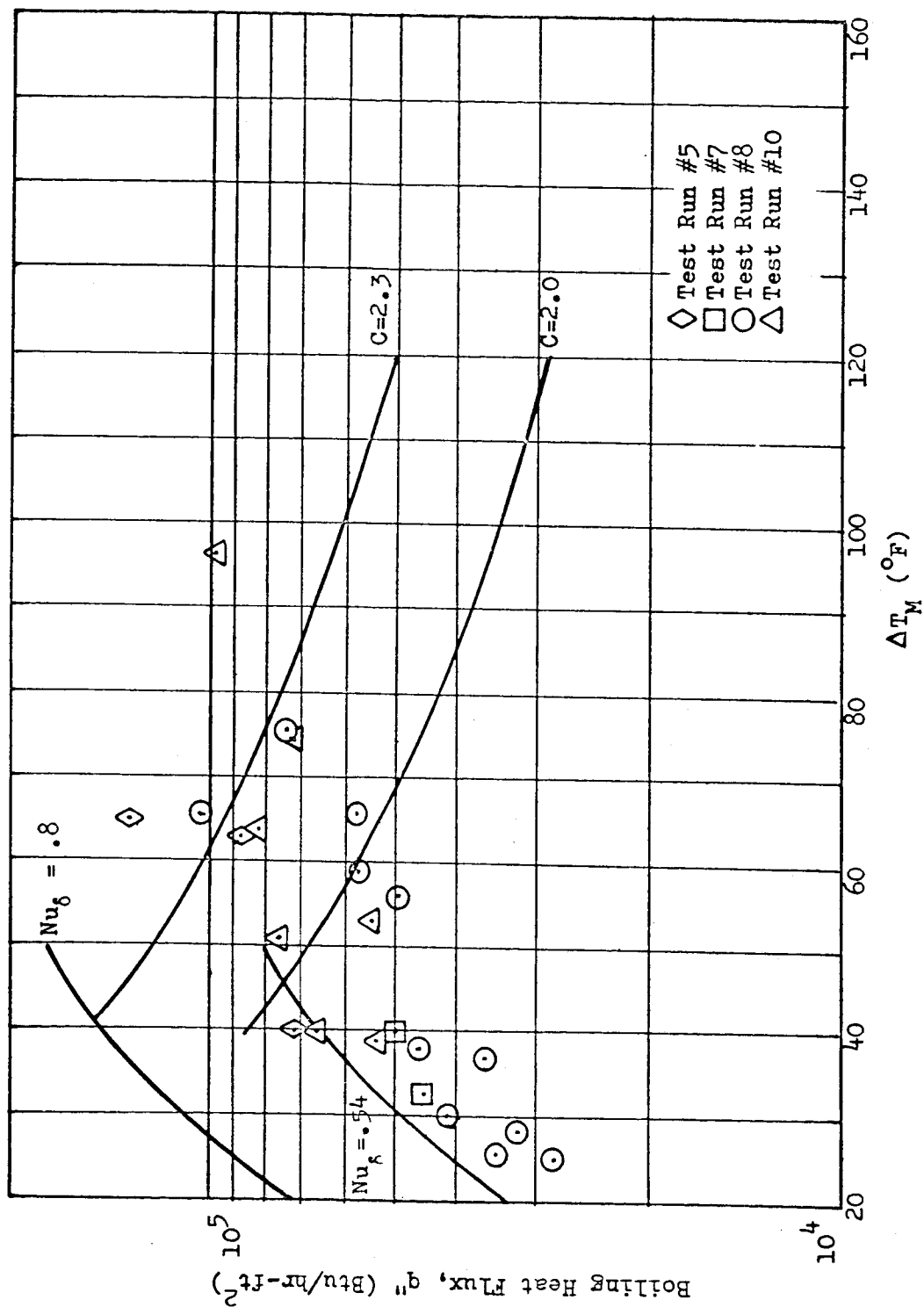


Figure 6.0-12

CL-4 BOILER TEST
LOCAL BOILING IN PLUG INSERT REGION
 q'' vs ΔT_M @ $\bar{x} = .30$

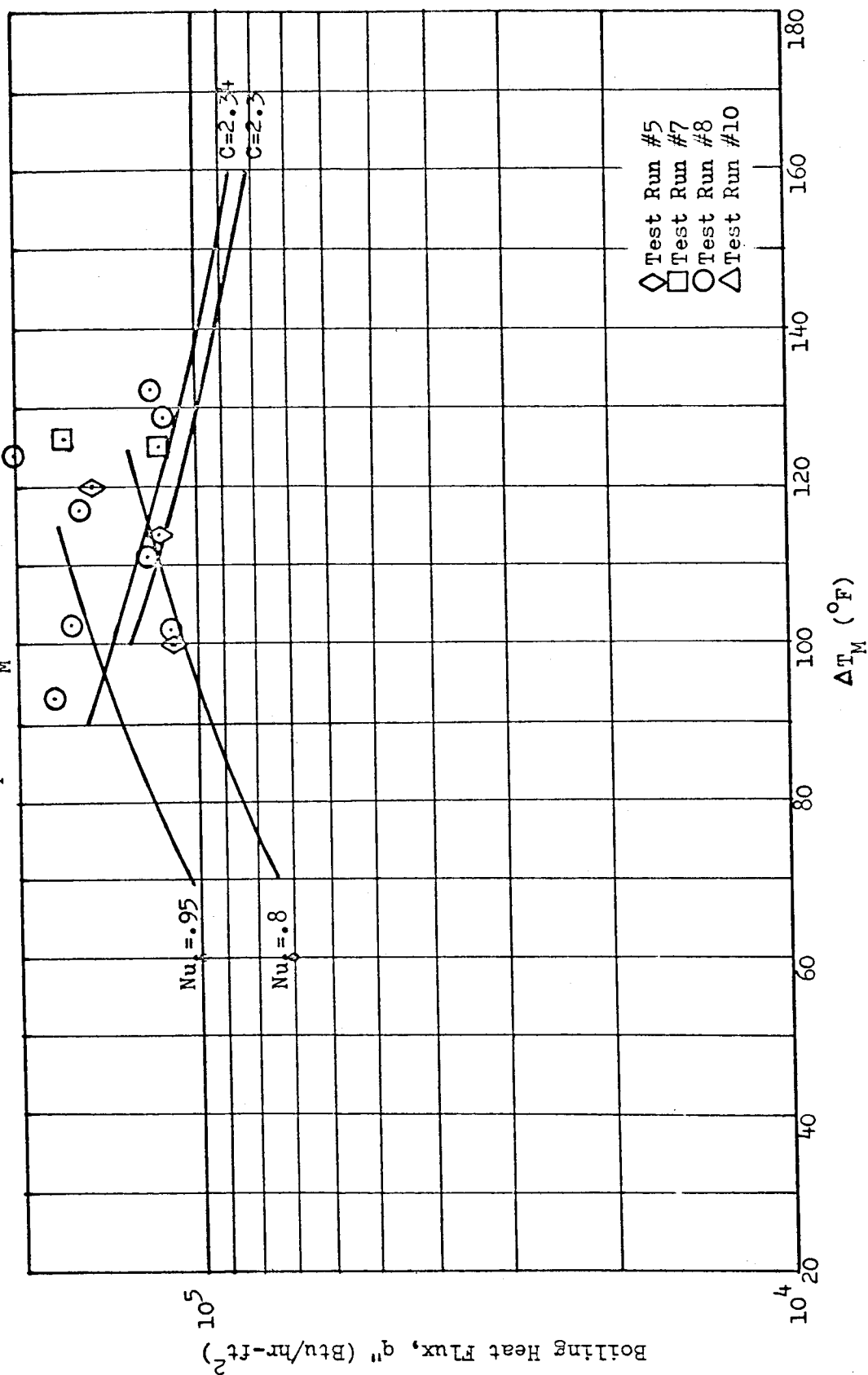


Figure 6.0-13

CL-4 BOILER TEST
 LOCAL INTERMITTENT CONTACT BOILING IN UNPLUGGED TUBE REGION
 q'' vs ΔT_M @ $\bar{x} = .30$

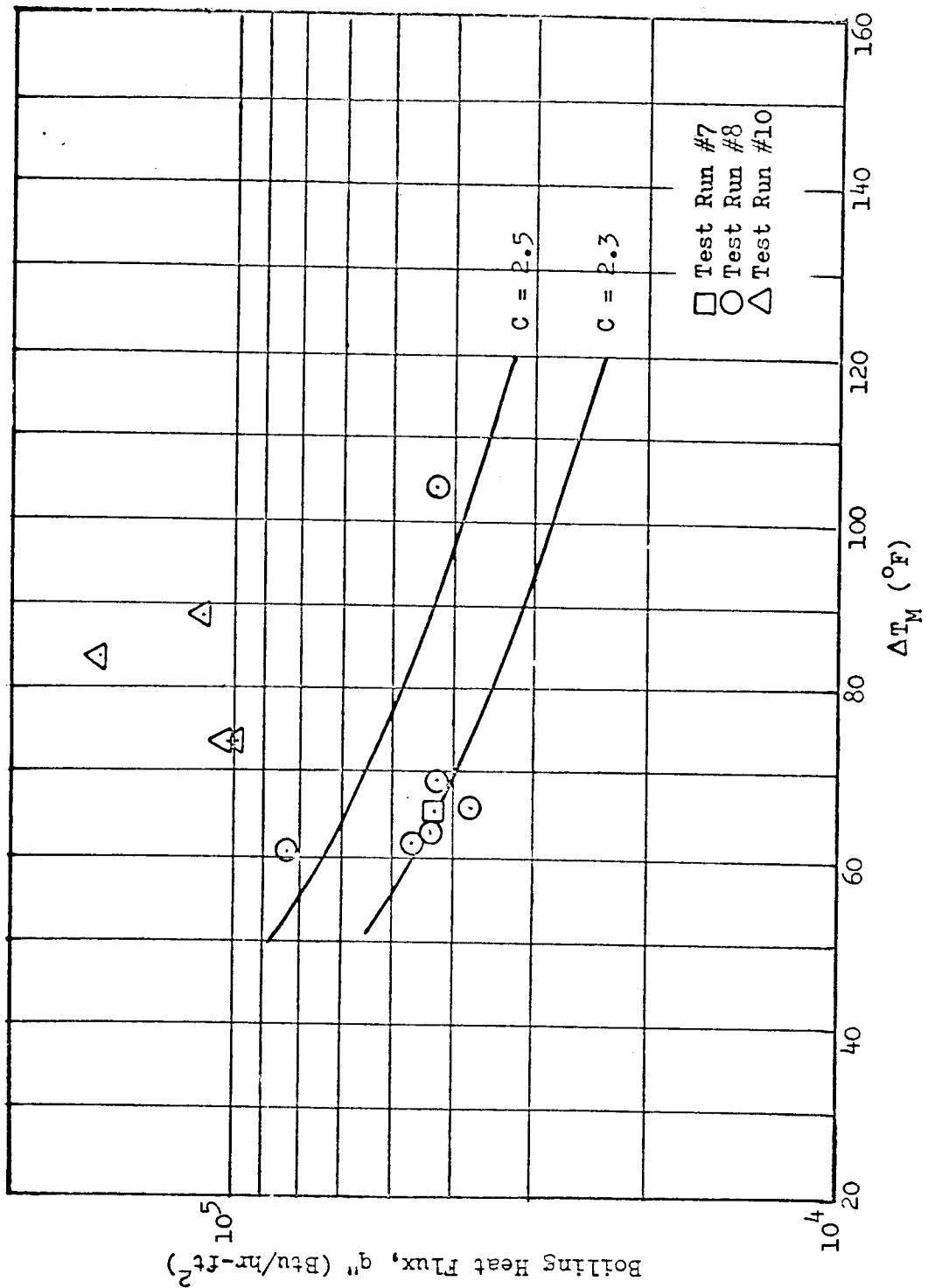


Figure 6.0-14

CL-4 BOILER TEST
 LOCAL CONTACT BOILING IN PLUG INSERT REGION
 q'' vs ΔT_M @ $\bar{x} = .50$

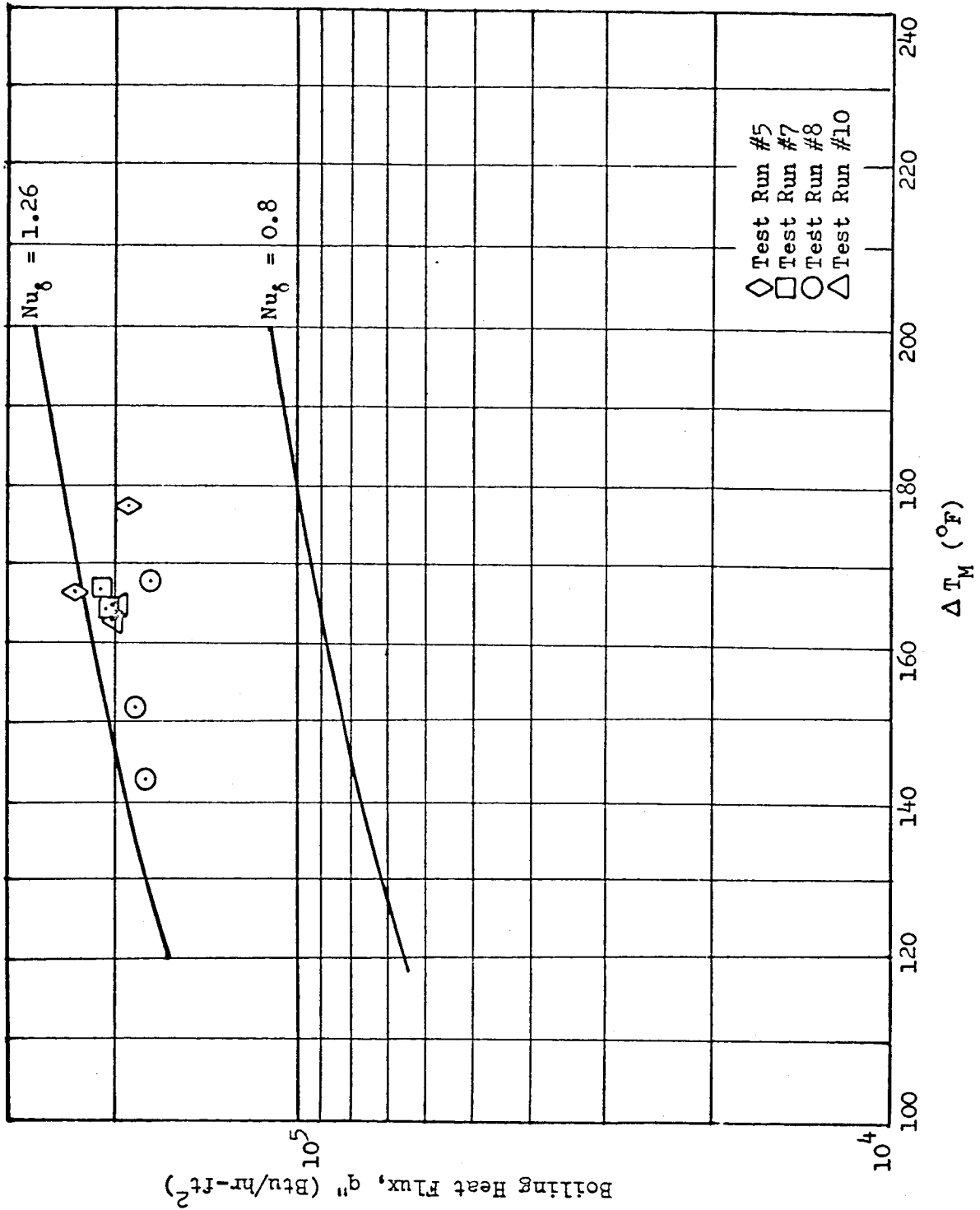


Figure 6.0-15

CL-4 BOILER TEST
 LOCAL INTERMITTENT CONTACT BOILING IN UNPLUGGED TUBE REGION
 q'' vs ΔT_M @ $\bar{x} = .50$

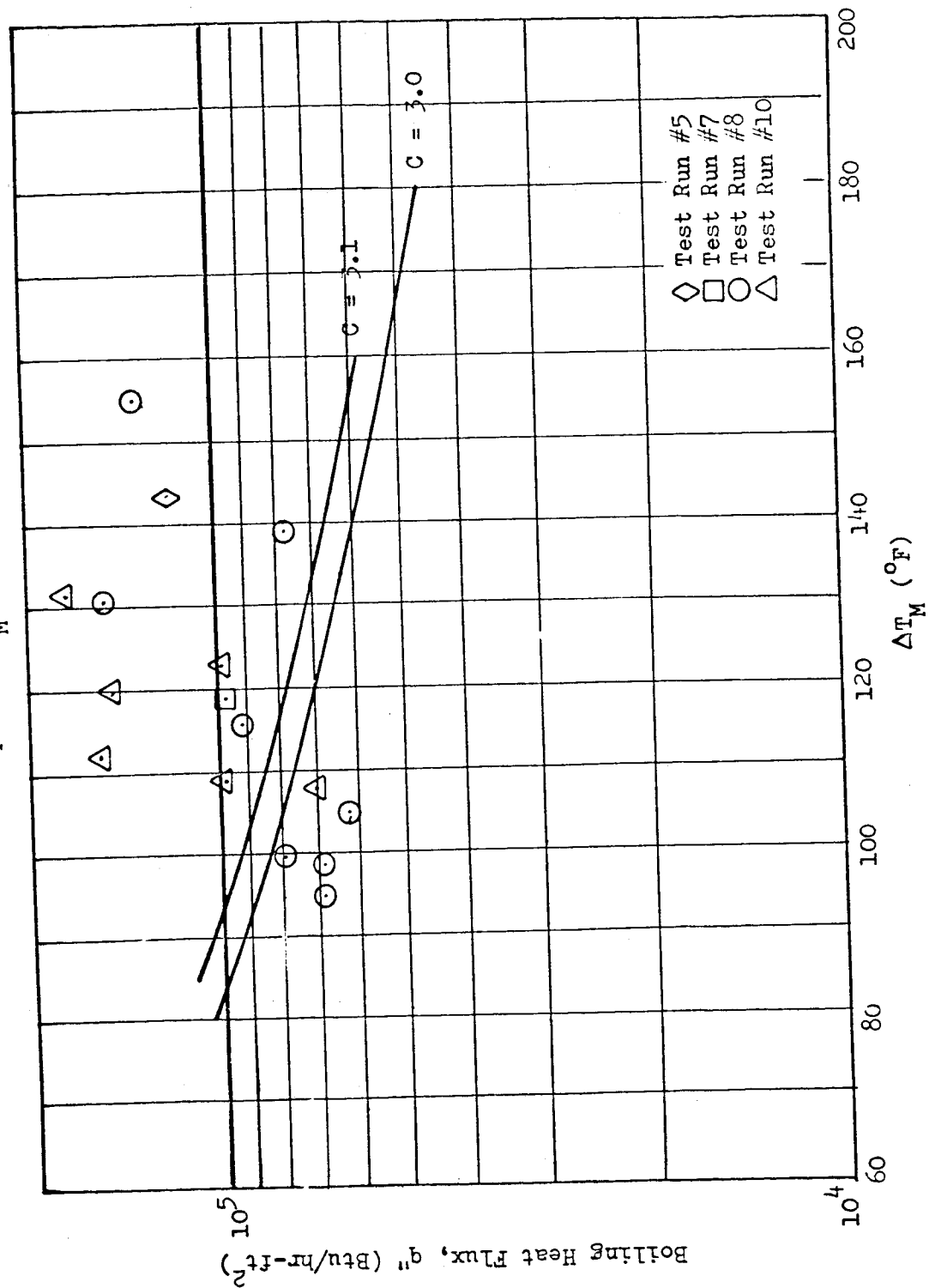


Figure 6.0-16

CL-4 BOILER TEST
 LOCAL CONTACT BOILING IN PLUG INSERT REGION
 q'' vs ΔT_M @ $\bar{x} = .70$

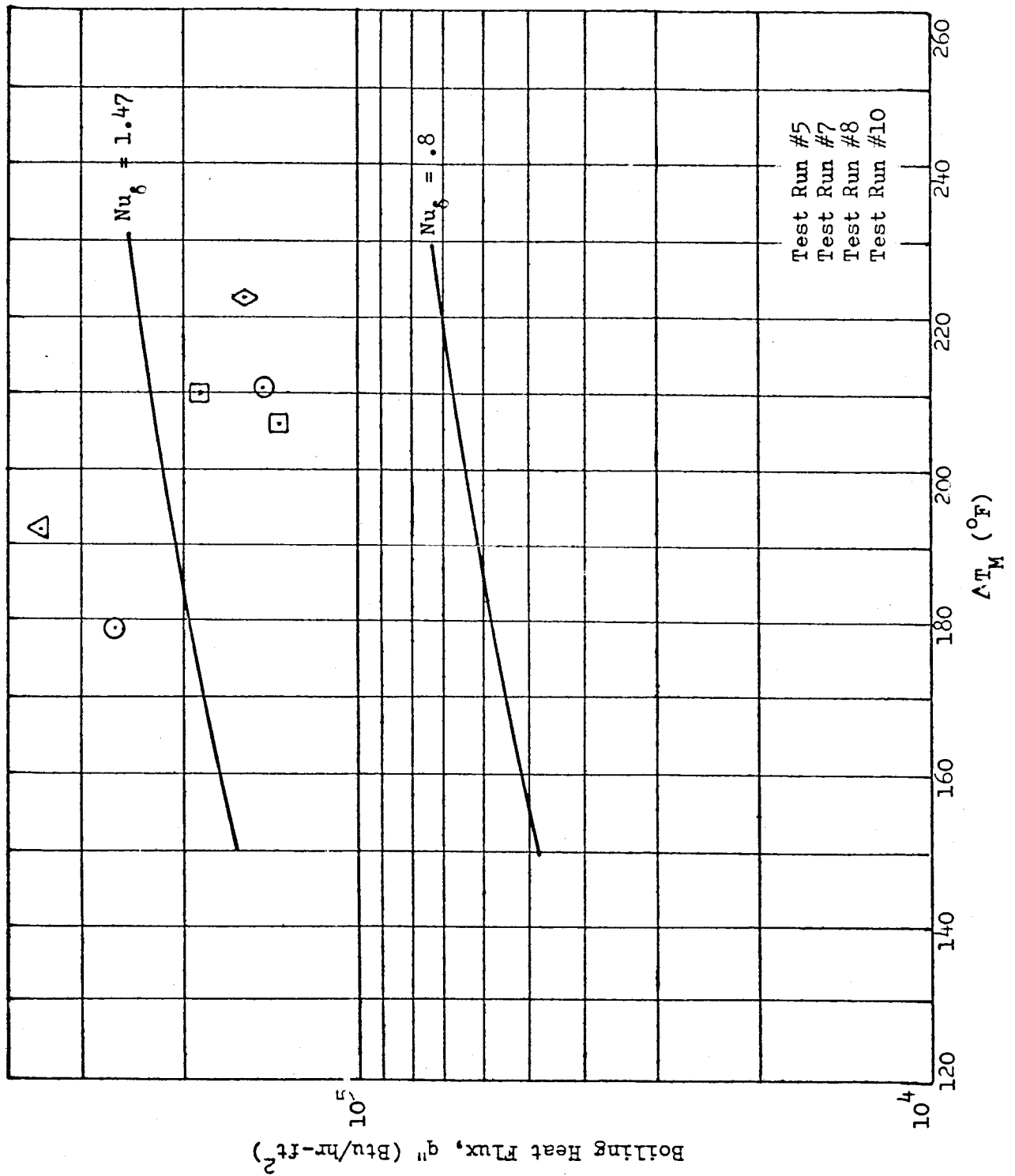


Figure 6.0-17

CL-4 BOILER TEST
 LOCAL INTERMITTENT CONTACT BOILING IN UNPLUGGED TUBE REGION
 q'' vs ΔT_M @ $\bar{x} = .70$

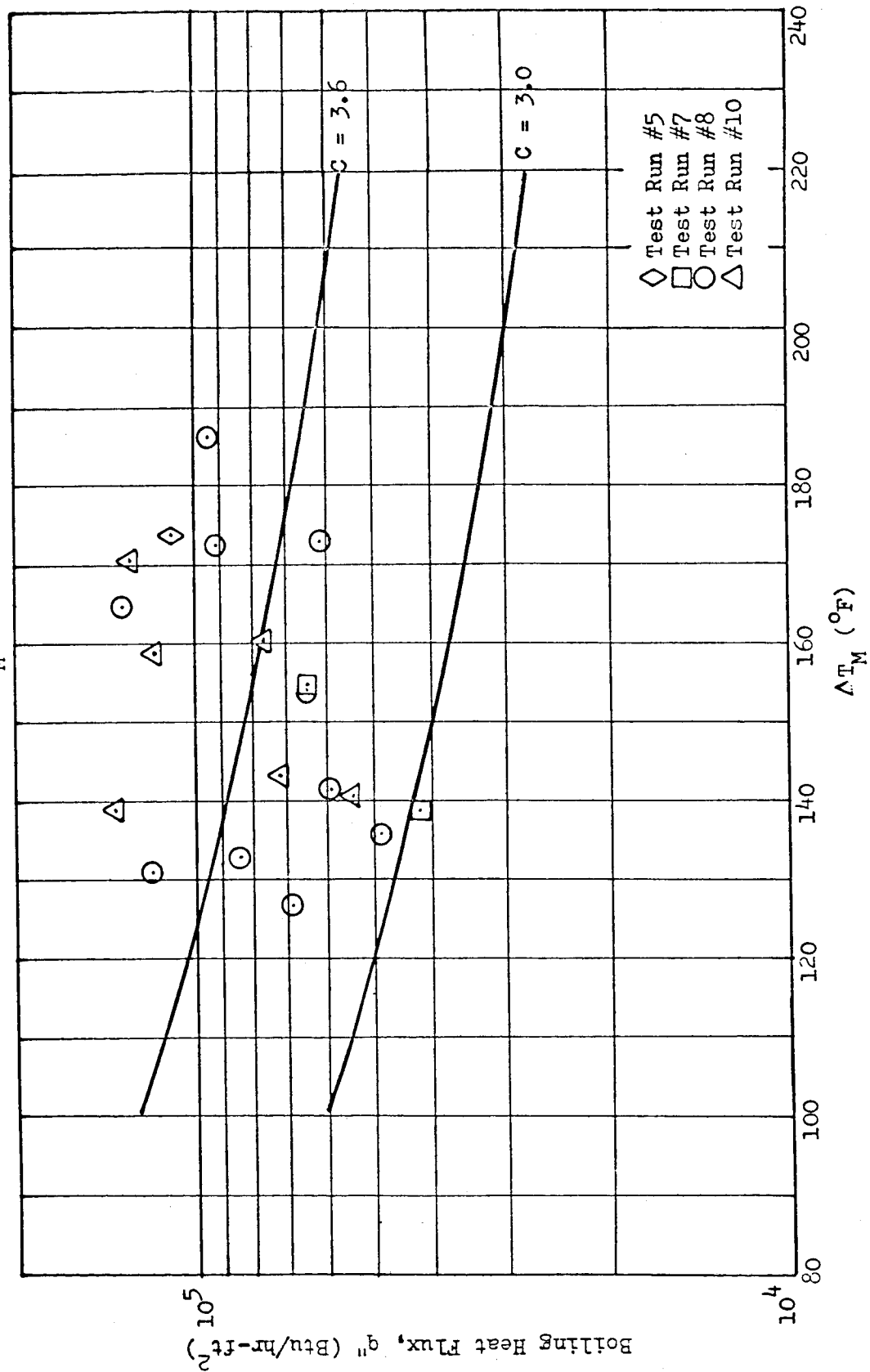


Figure 6.0-18

CL-4 BOILER TEST
LOCAL FILM BOILING IN UNPLUGGED TUBE REGION
 q'' vs ΔT_M @ $\bar{x} = .90$

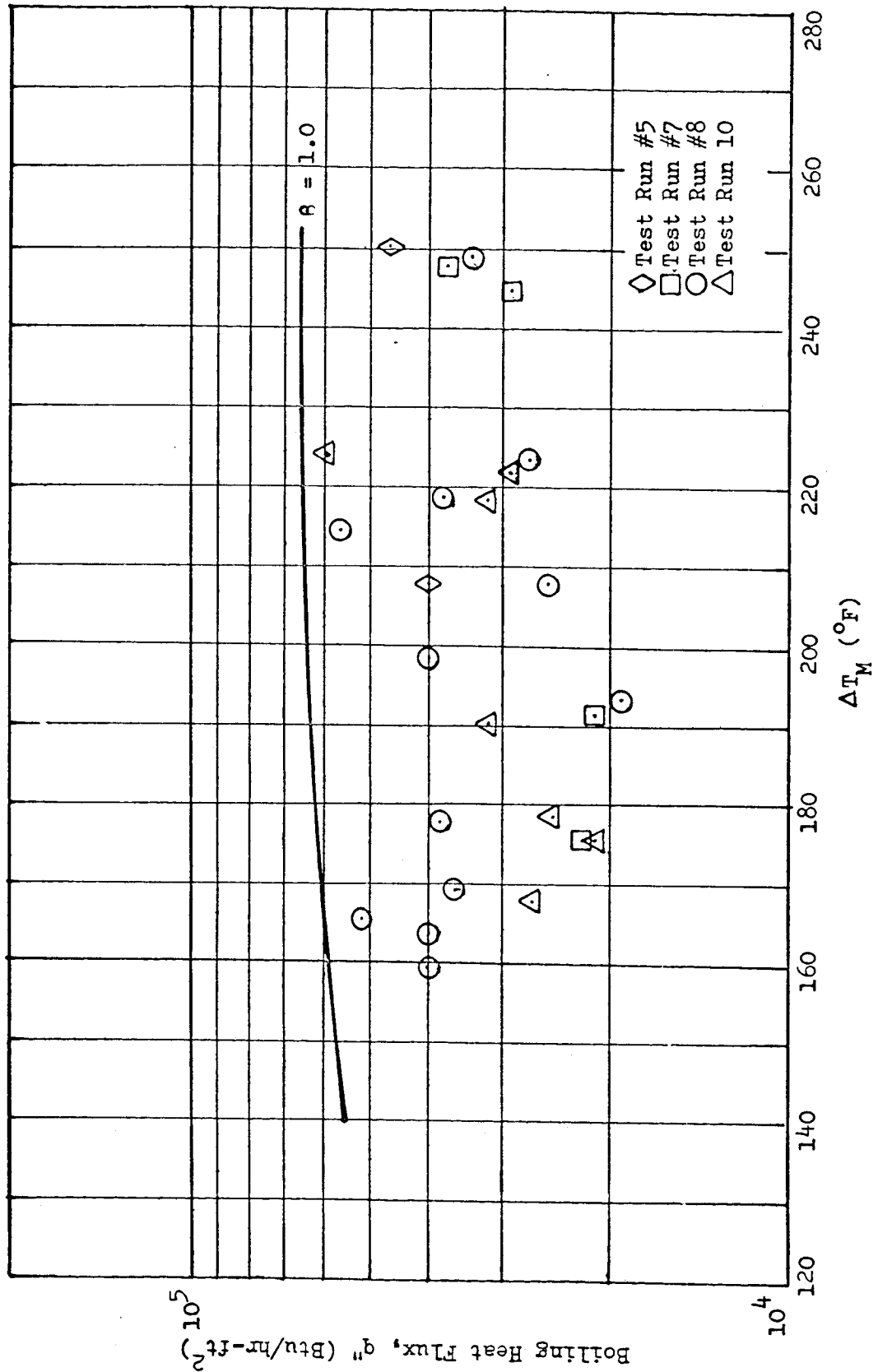


Figure 6.0-19

CL-4 BOILER TEST
TYPICAL BOILING HEAT FLUX REPRESENTATION
THROUGHOUT THE BOILER VAPOR QUALITY SECTION

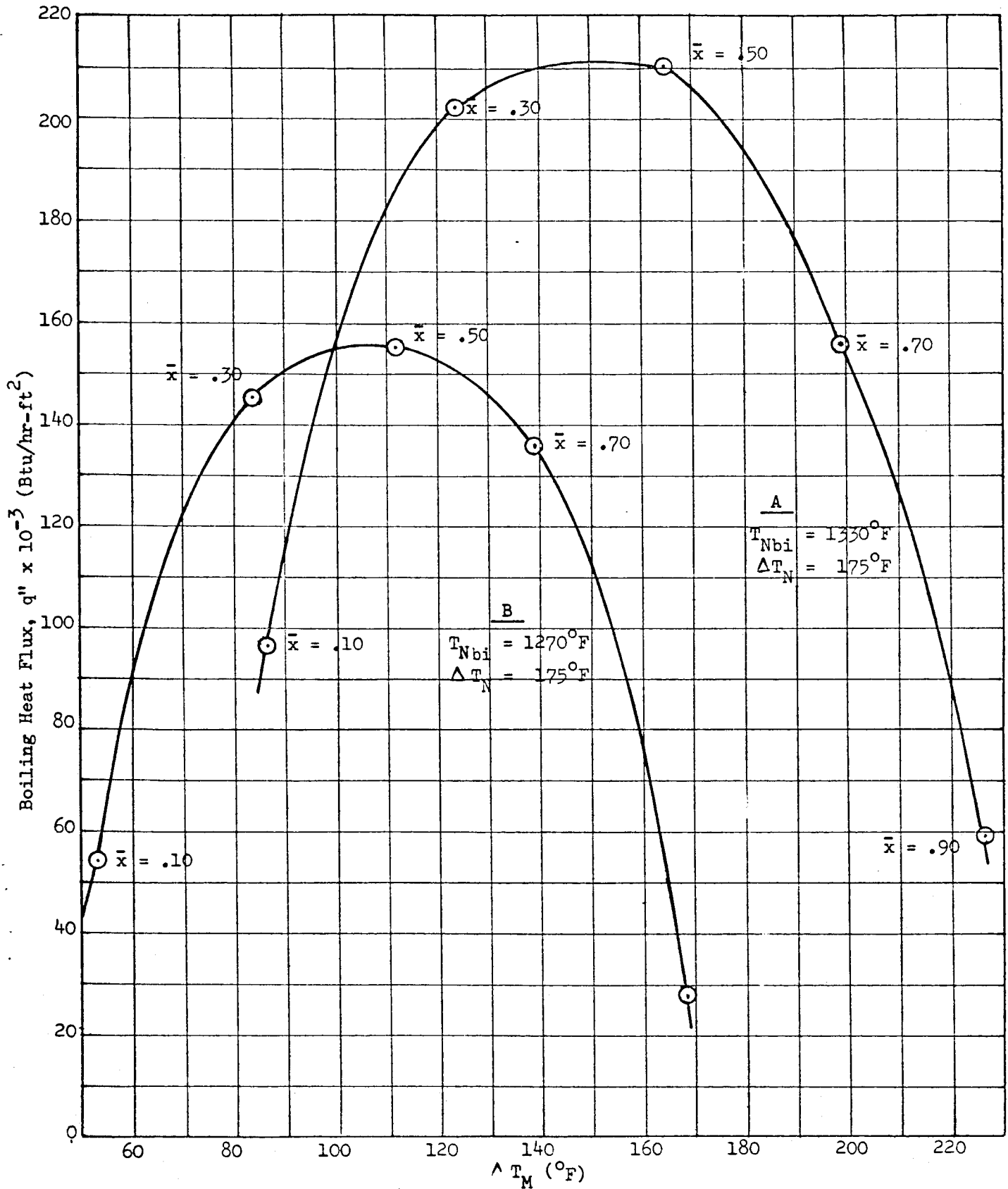


Figure 6.0-20

VII. CONCLUSIONS

The introduction of a preheat section plug insert providing elevated liquid phase velocity at the liquid-vapor interface location demonstrates significant improvement in the boiler conditioning effect. As shown in Appendix C, Figures C-3 thru C-5, the obtained boiler NaK temperature profiles are approaching the design prediction indicated in Figure C-3. It is postulated that elevated liquid phase velocities at the liquid-vapor interface significantly reduce or even completely eliminate the convective mercury boiling transition regime between the liquid-vapor interface and the fully established two-phase vortex flow pattern.

The boiler conditioning time is apparently dependent upon the cleanliness of the internal wall surface of the mercury flow passage. To define the surface cleanliness in conjunction with boiler conditioning effect, a better understanding of surface physics and chemistry is needed. Up-to-date experience suggests that tight plug insert geometries provided in the boiler preheat section, as well as in the low vapor quality section are capable of accelerating the boiler conditioning effect by several orders of magnitude when the boiler mercury flow passage is cleaned by established⁽⁴⁾ methods prior to mercury injection. This method involves flushing with strong caustic solution, followed by flushing with Alionox detergent solution.

The test of two tight preheat section plug insert geometries providing liquid phase velocity of 4.5 and 6.5 ft/sec at the liquid-vapor interface accordingly resulted in very stable boiler performance characteristics. As compared to a loose preheat section plug insert geometry ($u_L = .8$ ft/sec), the tight plug inserts demonstrate reduction in boiler exit pressure fluctuations by an order of magnitude; e.g., the comparative boiler exit pressure fluctuations are ± 10 and $\pm \frac{1}{2}$ psia.

Most effective boiling heat transfer was obtained from extended length plug insert geometries (Test runs No. 5, 7 and 8) where the plug insert end point vapor quality and vapor phase velocity were up to 80% and 180 ft/sec, respectively, at high NaK temperature schedules. At low NaK temperature schedules the same parameters were found to be 45% and 100 ft/sec, respectively. Aside from the high pressure drop penalty, it is felt that under these dynamic conditions most effective mist or even fog flow can be expected at the plug insert end point and thus the droplet carry-over thru the excess superheat length is minimized. It is obvious that high vapor flow velocity; e.g., 180 ft/sec, at the plug insert end point provides elevated vapor flow velocity; e.g. 40 ft/sec in the unplugged tube next to the

plug insert end point. Thus effective vortex flow takes place in the unplugged tube. As a result of droplet radial acceleration in this flow regime the droplets are forced against the tube wall and effectively vaporized.

In accordance with the early vortex two-phase flow establishment definition by means of Weber number ($We = \frac{\delta_o \rho_v u_v^2}{\sigma}$) as proposed by Reference 1; e.g. $\rho_v u_v^2 \geq 142$, a certain vapor phase velocity (u_v) must be obtained in order to carry droplets of diameter δ_o in the vapor stream. In the case of low liquid phase velocities ($u_L = .8$ ft/sec) the initial boiling is under the influence of the 1 g gravity field because of the absence of sufficient liquid and vapor phase velocity effects. Considerable transition length accompanied by liquid slugging is needed until a fully developed vortex two-phase flow regime ($u_v \geq \sqrt{\frac{142}{\rho_v}}$) is established. In the case of elevated liquid phase velocities ($u_L \cong u_v = 6.2$ ft/sec) the liquid-vapor interface disintegration and initial boiling may take place in a vortex type flow pattern, where the liquid spheroids are forced against the tube wall thus producing effective initial vapor generation. This design approach suggests that elevated liquid phase velocities (u_L) at the liquid-vapor interface location initially accelerate the highly deficient vapor phase ($\bar{x} \rightarrow 0$), simultaneously promoting effective boiling heat transfer rates. The latter in turn do elevate the vapor phase velocity ($u_v \rightarrow u_L \rightarrow u_{v-cr} = \sqrt{\frac{142}{\rho_v}}$) causing finally the entrainment of liquid drops into the vapor stream. It is postulated that this early vortex two-phase flow boiling regime is desirable for boiler operation in zero or adverse gravity environments.

The two-phase flow pressure data, as shown in Figures 6.0-2 thru 6.0-4, are in non-dimensional form, and compare reasonably well with similar data scatter in Reference (1). It is therefore felt that these results can be used to evaluate the pressure drop conditions of other tube sizes and plug insert geometries considered for SNAP-8 and similar Rankine cycle power conversion systems. Empirically determined gas flow frictional pressure drop coefficients are permitting the analysis of two-phase flow pressure drop using the Martinelli parameter for relatively complex flow passage geometries.

The results derived from an analysis of the local boiling heat transfer test data reveal reasonable agreement with the dropwise dry wall boiling formulation as proposed by Reference (1). The boiling heat transfer rates can be adequately predicted from proposed semi-empirical correlation. The test data comparison with the reference information is shown in Figures 6.0-12 thru 6.0-19. The discrepancies are primarily in the test data areas referring to the plug insert vapor quality section. These discrepancies are caused by the introduction of the helical flow passage geometric values into the referenced boiling heat transfer correlations. These correlations were established for round tubular flow passages with swirl wire in them. The plug insert section flow passage can be analytically treated on the basis of its equivalent or hydraulic diameter only.

The inaccuracies in NaK temperature profile interpretation and in analytical estimates in lieu of missing test information are the primary reasons for the test data point scatter. The instrumentation deficiencies were particularly felt in the boiler mercury inlet end region. The plot of mercury temperature rise in the preheat section in terms of mercury tube length was not available. Consequently, the true position of the liquid-vapor interface could not be established.

The existing NaK loop flow and heat input capacity placed serious limitations upon the scope of the test objectives. The boiler operation, therefore, was limited to 80% of its design capacity. The test results also show that the length of this boiler has been overdesigned by at least a factor of two.

VIII. RECOMMENDATIONS

To eliminate boiler deconditioning, means must be provided to prevent oxidation of the tube wall or the entrance of oil or other substances into the mercury tubes during the system's assembly, operation or shutdown.

Clarification is needed in regard to mercury liquid and vapor phase thermal conductivities to be used for the SNAP-8 operating conditions. As can be seen from proposed semi-empirical correlations⁽¹⁾ the Husselt's number for intermittent contact boiling regime is proportional to $(\frac{k_v}{k_f})^4$. Comparison of Reference (3)

data with WADD data indicates significant differences in their numerical values;

$$\text{e.g., } \left(\frac{k_v}{k_f}\right)_{\text{Ref. (3)}}^4 = 1.9 \times 10^{-12}; \left(\frac{k_v}{k_f}\right)_{\text{WADD}}^4 = 6.0 \times 10^{-12}.$$

To investigate the boiler's off design operating characteristics, the nominal NaK loop flow rate and heat input capacity have to be oversized by a factor of 2 and 1.25, respectively.

Long duration continuous tests up to several thousands of hours are required on SNAP-8 boilers to establish the time effects on boiler performance and their structural reliability.

More sophisticated instrumentation is required to investigate and define the thermal and dynamic design aspects in the boiler plug insert section. These requirements can be detected from the curves shown in Figure 6.0-1.

In order to verify the derived non-dimensional boiler design formulations additional experimental boilers of different mercury flow passage sizes and internal geometries should be built and tested under SNAP-8 operating conditions. The evaluation of these results shows uncertainties arising from limited instrumentation, in regard to true liquid-vapor interface location. True temperature and pressure profile representations must be obtained throughout the length of the boiler plug insert section.

REFERENCES

1. The SNAP-2 Power Conversion System Topical Report No. 17, Mercury Boiling Research, TRW Report No. ER-4833, Oct. 1964.
2. L. T. Clark and M. F. Parkman, Effects of Additives on Wetting During Mercury Pool Boiling Heat Transfer, ASME, 64-WA/HT-22.
3. Properties of SNAP-8 Fluids, NaK and Mercury, ET-378, Aerojet-General Corp., March 1964.
4. Cleaning of SNAP-8 Power Conversion System Components Prior to Final Assembly - Method II, AGC-10319/6
5. M. K. Wong, Corrosion Test Loop Operation Manual, Aerojet-General Nucleonics Report No. AN-SNAP-64-177, 16 February 1964

NOMENCLATURE

C	-	Constant
D	-	Mercury tube diameter
D_e	-	Equivalent tube diameter
f	-	Flow friction factor
G	-	Specific mass flow
g_c	-	Standard acceleration at sea level
h	-	Heat transfer coefficient
h_{fv}	-	Latent heat
h_N	-	NaK side film coefficient
k	-	Thermal conductivity
k_w	-	Tube material thermal conductivity
L'	-	Axial tube length
Nu	-	Nusselt number
Nu_δ	-	Droplet Nusselt number
P_{Hbi}	-	Mercury inlet pressure
P_{Hbo}	-	Mercury unit pressure
P_{POO}	-	Pressure at liquid vapor interface
P_1	-	Preheat section end point pressure
P_2	-	Plug insert end point pressure
q''	-	Heat flux
Re	-	Reynolds number
r_m	-	Log mean radius
r_o	-	Tube outside radius
t	-	Tube wall thickness
ΔT_{OO}	-	Temperature difference at liquid-vapor interface
ΔT_{NOO}	-	NaK temperature at $x = 0$
ΔT_{SOO}	-	Saturation temperature at liquid-vapor interface

NOMENCLATURE (Cont.)

- U - Overall heat transfer coefficient
- x - Vapor quality, vapor weight/total weight
- \bar{x} - Mean vapor quality

GREEK SYMBOLS

- α - Swirl wire angle
- β - Nu (actual)/ Nu_{δ} (film-sphere)
- δ_o - Initial droplet diameter, swirl wire diameter
- λ - Martinelli correlating parameter
- ρ - Density
- ϕ - Two-phase flow pressure drop factor, $\Delta P_{TP}/\Delta P_v$
- μ - Viscosity

SUBSCRIPTS

- C - Contact boiling
- F - Film boiling
- IC - Intermittent contact boiling
- M - Mean
- TP - Two-phase
- cr - Critical
- f - Liquid at saturation temperature
- v - Vapor

APPENDIX A

RESULTS OF CL-4 BOILER TEST DATA REDUCTION

TEST RUN NO. PLUG INSERT NO.		5-161C 3	5-17C1 3	5-19C1 3	7-1C2 5	7-2C2 5	7-3C2 5	7-4C2 5	8-1C2 6	8-2C2 6	8-3C2 6
PLUG INSERT QUALITY SEC											
XPL		0.419	0.448	0.670	0.830	0.826	0.318	0.027	0.452	0.054	0.457
DLP	FT	3.250	3.000	3.000	3.350	3.450	3.000	3.000	3.000	3.000	3.000
OPPL	PSI	133.000	70.000	110.000	123.000	145.000	22.000	4.000	34.000	13.000	22.000
OX-FLUX	3/HK-FT2	145533.	88402.	131311.	149938.	140149.	62021.	5214.	88632.	10621.	80443.
UWPL	4/HK-FT2-F	1278.408	1273.293	1114.640	1164.231	1183.891	1197.314	380.589	970.775	729.474	1125.057
UWPL	DEG-F	112.540	69.540	117.700	126.080	118.380	51.800	13.700	91.300	14.540	60.940
U2VPL	FT/SEC	131.316	150.216	160.395	132.067	124.810	43.100	3.324	62.794	5.949	59.215
U2VT	FT/SEC	41.279	22.770	36.516	40.172	43.635	15.068	1.162	21.993	2.444	20.702
WPL		72760.	75423.	75632.	51595.	49525.	50490.	49790.	50185.	50588.	50204.
PHI-F		0.0310	0.1157	0.0426	0.1493	0.2448	0.2642	7.1962	0.2000	5.5334	0.1330
LWPL		7.563E 04	2.207E 04	5.297E 04	6.426E 04	5.936E 04	9.021E 04	7.545E 01	1.647E 04	2.745E 02	1.514E 04
UNPLUGGED TIME QUAL. SEC											
OX		0.181	0.552	0.330	0.170	0.174	0.632	0.973	0.548	0.946	0.543
XWPL	FT	0.909	0.724	0.935	0.915	0.913	0.659	0.513	0.725	0.527	0.728
OLUPL	PSI	4.450	4.850	3.250	2.760	3.450	9.950	15.750	6.250	12.250	4.250
OPPL	3/HK-FT2	10.000	9.000	13.000	9.000	7.000	14.000	19.000	12.000	16.000	8.000
OPPL	4/HK-FT2-F	21037.964	67907.751	59897.947	37439.409	29466.195	44550.735	36097.937	51597.765	45675.599	75169.142
OMUPL	DEG-F	75.935	379.914	267.737	150.868	120.133	297.431	330.875	267.543	415.158	439.340
OTWUPL		271.660	173.480	241.780	243.160	245.240	149.760	100.180	192.850	110.020	171.080
RF		74139.996	80555.817	81331.498	43119.287	80125.004	72426.910	76911.308	79194.765	78382.834	77801.042
PHI-F		0.0396	0.132	0.273	0.073	0.097	0.145	0.201	0.143	0.106	0.150
LWPL		2.507E 00	5.835E 05	1.365E 06	3.100E 06	2.913E 06	3.777E 05	1.571E 05	5.703E 05	1.753E 05	5.410E 05

TEST RUN NO. PLUG INSERT NO.		5-161C	5-17C1	5-18C1	7-1C2	7-2C2	7-3C2	7-4C2	8-1C2	8-2C2	8-3C2
		3	3	3	5	5	5	5	6	6	6
MEAN QUALITY INCREMENT											
DX		0.0265	0.1000	0.1000	0.0290	0.0500	0.1000	0.0135	0.1000	0.0250	0.1000
DE		0.053	0.200	0.200	0.058	0.100	0.200	0.027	0.200	0.050	0.200
DLX		0.005	0.007	0.007	0.005	0.005	0.008	0.008	0.008	0.008	0.008
DPX		0.250	1.650	1.350	0.350	0.450	2.350	3.000	2.000	3.000	2.000
PMX		27.000	40.000	51.000	60.000	89.000	17.000	4.000	24.000	13.000	16.000
OX-FLUX		391.500	308.000	319.500	330.000	342.500	287.500	305.000	290.000	299.500	304.000
UX		1.226E 05	7.219E 04	9.742E 04	1.003E 05	1.300E 05	4.977E 04	5.255E 03	5.740E 04	9.857E 03	5.735E 04
DTM		3800.564	1803.780	1342.374	2018.085	2643.054	1244.239	383.657	867.116	790.036	979.940
DTCPX		32.260	40.020	63.080	49.700	49.200	40.000	13.700	65.200	14.080	58.760
DTCP2		150.517	79.871	78.551	163.645	267.064	37.963	5.333	38.155	9.956	37.973
DTCP2		1066.113	533.810	524.930	1089.690	1784.884	253.722	35.645	255.002	65.540	253.786
NUDX		0.477	0.593	0.517	0.402	0.597	0.502	0.099	0.414	0.183	0.416
CX2		0.714	1.259	1.483	0.805	0.763	1.673	1.159	1.959	1.171	1.989
RETAX.		0.426	0.943	0.959	0.405	0.570	1.051	0.143	1.024	0.268	1.031
REX		3.248E 05	7.569E 04	7.432E 04	3.723E 05	3.575E 05	5.039E 04	4.979E 04	5.060E 04	5.059E 04	5.012E 04
NUX		1739.341	1212.241	923.901	893.840	1163.697	868.614	265.112	604.392	435.348	674.696
KX		36.492	69.519	44.124	56.025	56.619	69.488	203.053	41.992	197.520	47.340
LAMX		1.005E 03	4.348E 03	4.194E 03	1.486E 03	3.819E 03	3.262E 03	7.753E 01	3.256E 03	2.435E 02	3.145E 03
PHIFG		0.168	0.622	1.222	0.128	0.055	0.658	6.993	1.060	6.366	0.735
FG		0.	0.022	0.022	0.	0.	0.032	0.032	0.032	0.032	0.032
PHI		0.	28.254	40.467	0.	0.	20.552	218.525	33.120	198.937	22.981
MEAN QUALITY INCREMENT											
DX		0.1265	0.3250	0.3000	0.1290	0.1500	0.2550	0.1135	0.3250	0.1250	0.3320
DE		0.147	0.250	0.200	0.142	0.100	0.110	0.173	0.252	0.150	0.264
DLX		0.007	0.007	0.007	0.008	0.008	0.008	0.033	0.003	0.033	0.009
DPX		0.650	1.350	0.800	0.650	0.750	0.650	2.250	0.950	2.450	0.950
PMX		30.000	30.000	28.000	14.000	14.000	5.000	3.000	10.000	3.000	6.000
OX-FLUX		363.000	273.000	230.000	293.000	291.000	276.500	301.500	273.000	290.500	293.000
UX		1.308E 05	1.103E 05	1.472E 05	1.322E 05	7.802E 04	9.896E 04	4.491E 04	1.561E 05	3.621E 04	1.633E 05
DTM		2005.395	1103.523	1227.274	1527.897	830.203	1320.940	1374.929	1334.666	942.834	1593.000
DTCPX		65.220	99.940	119.900	86.540	93.980	74.920	32.660	116.940	36.840	102.540
DTCP2		94.172	227.760	210.897	49.718	55.264	48.488	9.266	108.422	10.302	109.006
DTCP2		629.388	1522.204	1409.505	332.287	369.352	591.398	61.931	724.628	58.849	728.530
NUDX		0.669	0.924	0.922	0.631	0.505	0.865	0.265	1.004	0.238	1.080
CX2		1.565	1.464	1.665	2.410	2.131	1.968	2.221	2.394	2.124	2.319
RETAX		1.309	1.692	1.919	1.902	1.346	2.129	0.735	3.007	0.634	3.132
REX		7.139E 04	7.755E 04	7.624E 04	5.190E 04	5.026E 04	5.030E 04	7.648E 04	5.124E 04	7.831E 04	5.049E 04
NUX		1312.868	757.249	838.448	1062.666	578.304	928.576	4173.290	940.308	3093.122	1108.258
KX		42.742	27.791	23.173	32.127	29.581	37.078	95.154	23.751	75.460	27.114
LAMX		5.847E 03	5.292E 04	4.290E 04	5.396E 03	7.099E 03	2.191E 04	5.647E 03	3.825E 04	7.068E 03	3.773E 04
PHIFG		0.911	0.049	0.094	1.119	0.763	0.104	4.593	0.085	3.286	0.052
FG		0.022	0.022	0.022	0.032	0.032	0.032	0.	0.032	0.	0.
PHI		41.389	2.211	4.281	34.972	23.829	3.245	0.	2.654	0.	1.636

TEST RUN NO.
PLUG INSERT NO.

MEAN QUALITY INCREMENT	5-161C	5-17C1	5-18C1	7-1C2	7-2C2	7-3C2	7-4C2	8-1C2	8-2C2	8-3C2
DX	0.3000	0.5250	0.5350	0.3000	0.3000	0.3550	0.3000	0.5260	0.3000	0.5320
DE	0.200	0.150	0.270	0.200	0.200	0.090	0.200	0.148	0.200	0.136
DLX	0.007	0.033	0.007	0.008	0.008	0.033	0.033	0.033	0.033	0.033
DPX	1.000	0.750	0.850	1.050	0.700	0.350	2.700	0.650	2.800	0.250
PMX	40.000	2.000	31.000	21.000	13.000	1.000	4.000	2.000	4.000	1.000
QX-FLUX	328.000	257.000	250.500	275.500	277.500	273.500	298.000	267.000	287.000	289.500
UX	1.157E 05	1.191E 05	1.870E 05	1.153E 05	1.672E 05	1.504E 05	4.326E 04	1.340E 05	4.224E 04	3.198E 05
DTM	1011.776	830.259	1050.507	921.256	1330.088	1598.375	651.133	862.875	609.024	2331.011
DTGRX	114.320	143.460	177.640	125.140	125.700	94.080	66.440	155.260	69.360	137.060
DTGR2	273.491	55.409	529.287	104.409	100.866	24.999	21.789	54.516	22.144	54.248
DTGR2	1360.009	207.700	1994.031	697.904	674.122	167.075	145.622	204.354	147.993	203.348
NUDX	0.791	0.520	1.272	0.793	0.950	0.551	0.309	0.524	0.303	0.842
CX2	1.533	3.483	1.960	2.242	2.503	3.313	2.233	3.664	2.241	4.377
BFTAX	1.516	2.266	3.117	2.223	2.973	2.285	0.863	2.400	0.850	4.609
REX	7.278E 04	8.045E 04	7.793E 04	5.257E 04	5.076E 04	7.805E 04	7.666E 04	7.890E 04	7.821E 04	7.760E 04
NUX	573.406	2591.350	732.692	648.022	934.416	4936.575	1990.274	2676.008	1865.025	7133.165
KX	24.355	19.343	15.615	22.197	22.101	29.522	41.357	17.883	40.073	20.282
LAMX	3.761E 04	1.906E 05	1.996E 05	3.219E 04	3.116E 04	6.517E 04	4.147E 04	1.843E 05	4.312E 04	1.788E 05
PHIFG	0.127	0.359	0.028	0.182	0.182	0.922	0.723	0.437	0.658	0.598
FG	0.022	0.	0.022	0.032	0.032	0.	0.	0.	0.	0.
PHI	5.789	0.	1.270	5.681	5.679	0.	0.	0.	0.	0.

MEAN QUALITY INCREMENT	5-161C	5-17C1	5-18C1	7-1C2	7-2C2	7-3C2	7-4C2	8-1C2	8-2C2	8-3C2
DX	0.5000	0.7000	0.7350	0.5000	0.5000	0.5000	0.5000	0.7000	0.5000	0.7000
DE	0.200	0.200	0.130	0.200	0.200	0.200	0.200	0.200	0.200	0.200
DLX	0.007	0.033	0.033	0.008	0.008	0.033	0.033	0.033	0.033	0.033
DPX	0.500	1.100	0.650	0.550	0.550	1.200	2.800	1.250	1.900	0.900
PMX	24.000	2.000	2.000	12.000	11.000	2.000	3.000	2.000	2.500	1.000
QX-FLUX	296.000	255.000	234.000	259.000	265.500	272.000	294.500	265.000	283.750	288.500
UX	2.313E 05	1.083E 05	1.177E 05	2.201E 05	2.128E 05	9.747E 04	4.172E 04	9.414E 04	6.225E 04	1.306E 05
DTM	1386.221	622.662	533.830	1313.822	1294.815	817.937	405.169	505.591	588.947	792.705
DTGRX	166.880	173.900	220.520	167.520	164.340	119.160	102.960	186.200	105.700	164.700
DTGR2	494.160	58.777	57.944	252.247	243.090	52.778	52.283	57.775	53.138	57.171
DTGR2	1852.358	220.325	217.204	945.549	911.221	197.837	195.982	216.570	199.189	214.305
NUDX	1.310	0.563	0.562	1.323	1.201	0.489	0.334	0.501	0.409	0.607
CX2	1.996	3.874	4.390	2.812	2.814	3.154	2.435	3.811	2.705	3.969
BFTAX	3.269	2.729	3.087	4.651	4.578	1.930	1.018	2.385	1.383	3.014
REX	7.415E 04	8.057E 04	8.089E 04	5.322E 04	5.121E 04	7.814E 04	7.686E 04	7.902E 04	7.840E 04	7.766E 04
NUX	937.568	1945.904	1691.065	933.911	916.589	2528.599	1234.928	1569.973	1807.219	2425.212
KX	16.663	15.955	12.567	16.567	16.893	23.307	27.006	14.910	26.291	16.869
LAMX	1.424E 05	5.098E 05	6.650E 05	1.186E 05	1.133E 05	1.564E 05	1.470E 05	4.899E 05	1.525E 05	4.584E 05
PHIFG	0.050	0.137	0.200	0.068	0.068	0.270	0.186	0.128	0.216	0.096
FG	0.022	0.	0.	0.032	0.032	0.	0.	0.	0.	0.
PHI	2.295	0.	0.	2.111	2.116	0.	0.	0.	0.	0.

TEST RUN NO.
PLUG INSERT NO.

5-161C 3 5-17C1 3 5-18C1 3 7-1C2 5 7-2C2 5 7-3C2 5 7-4C2 5 8-1C2 6 8-2C2 6 8-3C2 6

MEAN QUALITY INCREMENT

DX	0.7150	0.9000	0.9000	0.7150	0.7150	0.7000	0.7000	0.9000	0.7000	0.9000
DE	0.230	0.200	0.200	0.230	0.230	0.200	0.200	0.200	0.200	0.200
DLX	0.007	0.033	0.033	0.007	0.007	0.033	0.033	0.033	0.033	0.033
DPX	0.850	3.000	2.600	0.750	0.750	1.800	2.800	4.350	2.000	3.100
PMX	32.000	5.000	16.000	16.000	16.000	3.000	3.000	8.000	2.500	6.000
QX-FLUX	268.000	251.500	225.000	245.000	245.000	251.000	291.000	260.000	281.250	255.000
UX	1.505E C5	3.971E C4	4.508E C4	1.455E C5	1.340E C5	6.498E C4	4.172E C4	2.705E C4	5.914E C4	3.792E C4
DTM	733.198	190.495	179.315	853.439	652.451	419.314	299.858	120.875	417.944	190.757
DTCR-F	222.540	208.420	252.500	210.100	205.280	154.960	139.120	223.300	141.500	193.800
DTCR-X	530.888	43.716	43.757	274.503	264.491	57.302	56.762	42.947	141.500	42.499
DTCR-Z	2023.769	163.871	164.022	1023.942	991.444	214.700	212.771	161.175	214.236	159.306
NUDX	1.271	0.427	0.429	1.454	1.238	0.453	0.372	0.335	0.445	0.417
CX2	2.172	4.279	4.724	3.155	2.949	3.321	2.805	3.955	3.135	4.142
ACTAX	3.453	2.292	2.537	5.755	4.546	1.881	1.333	1.654	1.745	2.110
REX	7.569E C4	8.073E C4	8.144E C4	5.379E C4	5.177E C4	7.828E C4	7.702E C4	7.931E C4	7.554E C4	7.786E C4
NUX	494.076	595.663	571.376	633.554	466.178	1298.341	915.654	376.546	1234.509	584.890
KX	12.477	13.310	10.969	13.199	13.448	17.920	19.943	12.401	19.637	13.980
LAMX	5.140E C5	2.430E C6	2.604E C5	4.134E C5	3.953E C5	4.812E C5	4.525E C5	2.345E C6	4.674E C5	2.132E C6
PHIFG	0.018	0.075	0.259	0.031	0.028	0.137	0.034	0.087	0.104	0.100
FG	0.022	0.000	0.000	0.032	0.032	0.000	0.000	0.000	0.000	0.000
PHI	0.305	0.000	0.000	0.941	0.936	0.000	0.000	0.000	0.000	0.000

MEAN QUALITY INCREMENT

DX	0.9150	0.9150	0.9150	0.9150	0.9150	0.9000	0.9000	0.9000	0.9000	0.9000
DE	0.170	0.170	0.170	0.170	0.170	0.200	0.200	0.200	0.200	0.200
DLX	0.033	0.033	0.033	0.033	0.033	0.033	0.033	0.033	0.033	0.033
DPX	4.850	2.750	3.450	2.750	3.450	5.600	5.200	3.100	3.100	3.100
PMX	10.000	5.000	7.000	5.000	7.000	8.000	6.000	4.000	4.000	4.000
QX-FLUX	247.000	234.500	238.500	234.500	238.500	264.000	287.000	276.000	276.000	276.000
UX	2.027E C4	3.742E C4	2.883E C4	2.883E C4	2.883E C4	2.089E C4	2.246E C4	3.815E C4	3.815E C4	3.815E C4
DTM	74.621	150.772	117.558	104.260	104.260	127.368	127.368	214.543	214.543	214.543
DTCR-X	271.660	248.160	245.280	245.280	245.280	192.920	176.360	177.840	177.840	177.840
DTCR-Z	39.947	41.989	40.535	40.535	40.535	42.651	42.209	42.831	42.831	42.831
NUDX	149.742	157.395	151.944	151.944	151.944	159.878	158.221	160.740	160.740	160.740
CX2	0.278	0.403	0.354	0.354	0.354	0.316	0.332	0.436	0.436	0.436
PHIFG	4.129	4.629	4.390	4.390	4.390	3.586	3.534	4.035	4.035	4.035
REX	1.438	2.332	1.942	1.942	1.942	1.416	1.468	2.200	2.200	2.200
NUX	7.981E C4	8.312E C4	8.013E C4	8.013E C4	8.013E C4	7.860E C4	7.728E C4	7.873E C4	7.873E C4	7.873E C4
KX	234.402	477.460	371.313	371.313	371.313	336.384	390.938	660.729	660.729	660.729
LAMX	10.209	11.168	11.301	11.301	11.301	14.390	15.760	15.622	15.622	15.622
PHIFG	2.921E C6	3.140E C6	3.022E C6	3.022E C6	3.022E C6	2.306E C6	2.160E C6	2.236E C6	2.236E C6	2.236E C6
FG	0.093	0.072	0.047	0.047	0.047	0.070	0.051	0.064	0.064	0.064
PHI	0.000	0.000	0.000	0.000	0.000	0.000	0.000	0.000	0.000	0.000

TEST RUN NO.
PLUG INSERT NO.

8-4C2 6 8-5C2 6 8-7C2 6 8-11C2 6 8-12C2 6 8-13C2 6 8-14C2 6 8-15C2 6 8-16C2 6 8-17C2 6

TEST DATA

WN	LB/HR	1770.00	1770.00	1950.00	2070.00	2055.00	2055.00	2055.00	2055.00	2070.00
INRI	DEG-F	1295.00	1328.00	1280.00	1275.00	1265.00	1265.00	1328.00	1260.00	1325.00
INRI	DEG-F	1085.00	1112.00	1085.00	1080.00	1075.00	1075.00	1135.00	1080.00	1126.00
DELIN	DEG-F	210.00	216.00	185.00	195.00	190.00	180.00	193.00	180.00	199.00
WH	LB/HR	483.00	507.00	499.00	522.00	492.00	480.00	512.00	496.00	493.00
THAT	DEG-F	520.00	520.00	516.00	435.00	435.00	435.00	438.00	435.00	435.00
THAO	DEG-F	1225.00	1250.00	1210.00	1210.00	1195.00	1250.00	1250.00	1195.00	1250.00
PHHI	PSIA	483.00	420.00	401.00	395.00	373.00	458.00	446.00	369.00	451.00
PI	PSIA	306.00	325.00	310.00	325.00	301.00	326.00	334.00	302.00	335.00
P2	PSIA	291.00	309.00	300.00	316.00	292.00	270.00	299.00	293.00	295.00
PHHO	PSIA	210.00	224.00	210.00	220.00	201.00	186.00	204.00	201.00	200.00

HEAT BALANCE

QH	BTU/HR	78257.00	85287.20	75757.50	84766.50	81094.50	77679.00	83289.15	77679.00	86505.30
QHG	BTU/HR	70075.67	73866.90	72274.76	76974.59	72376.36	71281.68	75970.91	72964.78	73201.87
QH1	KW	2.34	1.88	1.02	2.28	2.92	1.87	2.14	1.38	3.90
QNET	LB/HR	1589.02	1628.46	1860.35	1879.72	1313.94	1885.76	1874.44	1930.29	1751.66

PREHEAT SECTION

DEPH	FT	0.0049	0.0049	0.0049	0.0049	0.0049	0.0049	0.0049	0.0049	0.0049
DLPHC	FT	1.25	1.25	1.25	1.25	1.25	1.25	1.25	1.25	1.00
DBPH	PSI	177.00	95.00	91.00	70.00	72.00	55.00	55.00	67.00	61.00
POC	PSIA	306.00	325.00	310.00	325.00	301.00	403.00	391.00	302.00	390.00
INCC	DEG-F	1112.00	1140.00	1108.00	1109.00	1103.00	1181.00	1163.00	1106.00	1155.00
TSCQ	DEG-F	1095.36	1106.00	1097.60	1176.00	1092.56	1149.44	1142.96	1093.12	1142.40
DLTAQ	DEG-F	16.64	34.00	10.40	3.00	10.44	31.56	20.04	12.88	12.60
QPHC	BTU/HR	9041.71	9655.81	9432.10	11393.52	10514.38	11145.26	11730.53	10608.59	11334.32
QPH-FLUX	BTU/HR-FT2	68997.27	73765.05	72055.94	86963.72	89324.05	118255.02	124464.94	81046.05	108234.84
UPH	BTU/HR-FT2-F	443.53	377.70	516.24	727.49	525.13	537.19	652.52	501.77	638.69
NUPH	FT	0.21	0.21	0.29	0.42	0.33	0.31	0.33	0.29	0.37
PELM	FT	0.0071	0.0071	0.0071	0.0073	0.0073	0.0073	0.0073	0.0073	0.0073
REPDM	FT	49692.90	52251.05	51324.59	52746.07	49549.34	49060.13	52282.67	49950.41	50295.11
PE	FT	151.57	368.59	363.29	384.23	362.93	357.30	379.56	365.85	365.51
FPH	FT	0.0109	0.0122	0.0121	0.0098	0.0101	0.0143	0.0107	0.0093	0.0131
ULI	FT/SEC	6.93	7.28	7.16	7.50	7.06	6.99	7.36	7.12	7.09

TFST RUN NO.
PLUG INSERT NO.

PLUG INSERT QUALITY SEC

PLUG	8-4C2	8-5C2	8-7C2	8-11C2	9-12C2	8-13C2	8-14C2	8-15C2	8-16C2	8-17C2
XPL	0.303	0.355	0.209	0.069	0.147	0.828	0.179	0.635	0.165	0.780
DLPL	3.000	3.000	3.000	3.000	3.000	3.350	3.000	3.350	3.000	3.250
DPPL	15.000	16.000	10.000	9.000	9.000	133.000	11.000	92.000	9.000	95.000
QX-FLUX	57274.	70475.	40847.	14058.	28408.	139490.	34918.	113969.	32074.	138944.
UMPL	1191.227	992.881	1352.543	1275.689	1135.417	1064.395	1365.054	1177.364	1133.341	1339.868
DTMPL	43.080	76.980	30.200	11.020	25.020	130.560	25.590	96.800	24.300	103.700
U2VPL	37.301	44.165	26.268	3.533	18.673	109.701	22.910	82.117	21.543	93.250
U2VT	13.216	15.441	9.184	3.020	6.535	34.353	8.010	28.700	7.357	34.349
REPL	48577.	50491.	49990.	51842.	49554.	47249.	47985.	50163.	49921.	48368.
PHIFG	0.2196	0.1629	0.2931	2.3245	0.5329	0.2622	0.4332	0.2712	0.4189	0.2096
LMPL	5.8554E 03	9.369E 03	3.366E 03	4.213E 02	1.753E 03	5.506E 04	2.544E 03	3.021E 04	2.179E 03	4.783E 04

UNPLUGGED TUBE QUAL. SEC

UNPLUGGED	8-4C2	8-5C2	8-7C2	8-11C2	9-12C2	8-13C2	8-14C2	8-15C2	8-16C2	8-17C2
DX	0.597	0.645	0.791	0.931	0.853	0.172	0.821	0.365	0.335	0.220
XMUPL	0.651	0.678	0.604	0.534	0.574	0.914	0.590	0.917	0.583	0.490
DMUPL	9.250	6.450	8.050	14.250	11.250	2.550	8.050	3.250	8.750	2.250
PMUPL	14.000	11.000	13.000	81.000	18.000	4.000	13.000	6.000	15.000	4.000
QUPL	42814.196	59556.543	57625.489	40062.983	43842.083	38040.035	59569.368	67596.632	55545.429	56710.364
UMUPL	290.226	351.293	493.876	330.716	385.459	152.907	540.459	329.933	494.810	263.722
DTMUPL	147.520	169.540	116.680	121.140	113.740	249.040	110.220	204.880	112.440	215.040
RE	75266.224	77934.686	77220.211	81854.545	75725.042	75683.016	77305.933	79388.388	77206.919	76320.131
PHIFG	0.161	0.161	0.192	0.748	0.211	0.081	0.199	0.115	0.217	0.100
LMUPL	3.371E 05	3.875E 05	2.602E 05	1.925E 05	2.233E 05	2.617E 06	2.434E 05	9.847E 05	2.343E 05	1.860E 06

TEST RUN NO.
PLUG INSERT NO.

MEAN QUALITY INCREMENT

	8-4C2	8-5C2	8-7C2	8-11C2	8-12C2	8-13C2	8-14C2	8-15C2	8-15C2	8-17C2
DX	0.1000	0.1000	0.1060	0.0345	0.0730	0.0700	0.0895	0.0219	0.0825	0.3217
DE	0.200	0.207	0.212	0.069	0.146	0.140	0.179	0.044	0.155	0.043
DLX	0.008	0.008	0.008	0.008	0.008	0.005	0.008	0.005	0.008	0.005
DPLX	2.450	2.450	3.700	3.000	0.000	0.350	3.000	0.350	3.000	0.250
DPX	12.000	14.000	10.000	9.000	9.000	77.000	11.000	57.000	9.000	55.000
PMX	300.000	313.000	305.000	320.500	295.500	364.500	294.500	362.500	297.500	362.500
QX-FLUX	4.636E 04	4.862E 04	4.144E 04	1.415E 04	2.815E 04	2.259E 05	3.486E 04	7.527E 04	3.211E 04	1.008E 05
UX	1219.379	869.411	1372.210	1279.550	1125.145	3561.971	1362.821	1905.652	1134.542	3194.216
DTM	33.000	55.920	30.200	11.000	25.020	63.380	25.580	39.500	28.300	31.500
DTCRX	36.721	38.317	42.026	14.076	27.747	375.537	34.033	124.927	31.439	123.124
DTCR2	245.421	255.087	267.508	94.975	185.445	2539.850	227.454	851.670	210.120	822.218
NUOX	0.489	0.406	0.532	0.265	0.401	0.404	0.499	0.327	0.429	0.422
CX2	1.637	1.770	1.458	0.286	1.334	0.447	1.395	0.723	1.429	0.750
BETAX	1.602	0.899	0.971	0.387	0.695	0.852	0.854	0.295	0.765	0.599
REX	4.852E 04	5.642E 04	4.996E 04	5.184E 04	4.955E 04	3.603E 05	4.998E 04	3.848E 05	4.992E 04	3.705E 05
NUX	344.974	597.005	944.190	877.585	781.058	1546.273	944.910	828.014	787.159	1390.106
KX	73.192	49.771	92.113	252.582	111.143	43.945	108.721	70.572	94.265	86.435
LAMX	3.034E 03	3.086E 03	3.504E 03	4.307E 02	1.741E 03	6.892E 03	2.565E 03	8.596E 02	2.200E 03	8.202E 02
PHIFG	0.490	0.542	0.291	2.273	0.537	0.031	0.430	0.207	0.415	0.307
FG	0.032	0.032	0.032	0.032	0.032	0.	0.032	0.	0.032	0.
PHI	15.311	16.943	8.790	71.029	16.781	0.	13.453	0.	12.967	0.

MEAN QUALITY INCREMENT

	8-4C2	8-5C2	8-7C2	8-11C2	8-12C2	8-13C2	8-14C2	8-15C2	8-15C2	8-17C2
DX	0.2500	0.2805	0.3060	0.1345	0.2730	0.1720	0.2895	0.1219	0.2825	0.1217
DE	0.100	0.161	0.184	0.131	0.254	0.060	0.221	0.155	0.235	0.156
DLX	0.008	0.008	0.008	0.033	0.033	0.008	0.033	0.008	0.033	0.008
DPLX	0.550	0.550	2.050	2.050	3.150	0.450	1.750	1.250	3.150	0.900
DPX	3.000	2.000	4.000	69.000	6.000	8.000	3.000	15.000	5.000	8.000
PMX	292.500	310.000	294.500	281.500	289.000	322.000	291.500	326.500	290.500	331.000
QX-FLUX	1.032E 05	1.745E 05	3.737E 04	2.814E 04	4.564E 04	7.525E 04	7.379E 04	7.516E 04	4.347E 04	1.007E 05
UX	1466.565	1878.949	562.495	543.801	753.280	736.471	1207.251	993.412	686.224	1534.292
DTM	70.400	92.900	66.440	51.820	61.920	102.180	61.120	75.660	63.340	65.040
DTCRX	84.034	96.420	22.218	11.483	20.071	59.082	21.234	46.377	20.789	44.475
DTCP2	561.631	644.409	148.492	70.742	134.142	394.867	141.917	309.955	134.940	297.243
NUOX	0.883	1.046	0.291	0.187	0.319	0.491	0.416	0.476	0.310	0.587
CX2	1.970	2.309	2.144	2.112	2.291	2.119	2.516	2.026	2.234	2.142
BETAX	2.184	3.020	0.779	0.492	0.909	1.301	1.309	1.206	0.865	1.573
REX	4.879E 04	5.065E 04	7.697E 04	8.149E 04	7.639E 04	4.763E 04	7.702E 04	5.068E 04	7.692E 04	4.868E 04
NUX	1020.616	1295.212	1710.703	1671.056	2303.870	504.748	3685.534	679.379	2096.810	1047.023
KX	39.492	29.950	41.857	53.621	44.892	27.242	45.486	36.797	43.389	42.421
LAMX	1.964E 04	2.517E 04	4.349E 04	8.608E 03	3.424E 04	8.236E 03	3.899E 04	4.455E 03	3.698E 04	4.259E 03
PHIFG	0.085	0.043	0.631	50.651	1.115	0.659	0.881	0.770	0.858	0.025
FG	0.032	0.032	0.	0.	0.	0.032	0.	0.032	0.	0.032
PHI	2.666	1.342	C.	0.	0.	20.593	0.	24.057	0.	19.537

8-16C2 8-17C2

3-15C2
6

8-14C2
6

9-13C2 6

8-1202⁶

8-11C2⁶

8-7C2
6

8-502⁶

3-4C2
6

TEST RUN NO.
PLUG INSERT NO.

[illegible]

TEST RUN NO.
PLUG INSERT NO.

		3-402	6	8-702	6	8-1102	6	8-1202	6	8-1302	6	8-1402	6	8-1502	6	8-1602	6	3-1702	6
MEAN QUALITY INCREMENT		7.7000		0.9200		0.7000		0.9000		0.7150		0.9000		0.7150		0.9000		0.6900	
DX		0.200		0.200		0.200		0.200		0.230		0.200		0.230		0.200		0.180	
DE		0.033		0.033		0.033		0.033		0.033		0.033		0.033		0.033		0.008	
DLX		1.750		2.000		2.000		3.200		0.900		2.900		0.250		2.900		0.400	
DPX		2.000		4.000		2.000		5.000		18.000		4.000		2.000		5.000		5.000	
PMX		287.000		289.000		241.000		275.500		279.000		282.000		293.000		240.500		297.500	
QX-FLUX		6.490E 04		5.331E 04		6.131E 04		3.615E 04		1.442E 05		4.030E 04		4.090E 05		4.222E 04		2.620E 05	
UX		423.430		320.343		354.418		212.141		683.155		251.125		2182.083		245.154		1457.639	
DTM		154.360		166.420		172.980		170.490		211.120		160.460		137.440		164.340		178.400	
DTGRX		58.260		42.345		61.129		41.071		251.876		42.296		58.075		42.238		253.463	
DTGR2		277.144		153.731		227.140		157.329		944.155		153.548		217.594		158.330		953.847	
AUX		0.443		0.925		0.434		0.434		1.218		0.469		1.015		0.455		1.683	
CX2		3.338		4.311		3.325		3.085		3.032		4.004		5.430		4.031		3.238	
B-TAX		1.849		2.832		1.805		2.156		4.619		2.350		6.889		2.342		6.815	
RTX		7.510E 04		7.748E 04		5.400E 04		7.709E 04		4.897E 04		7.756E 04		7.597E 04		7.749E 04		4.952E 04	
NOX		1247.481		973.752		1117.538		653.952		479.498		771.446		6636.311		753.813		1011.238	
KX		18.006		16.703		16.027		16.300		13.160		17.517		14.837		16.938		15.553	
LAX		4.477E 05		2.155E 05		5.461E 05		2.206E 06		3.538E 05		2.190E 06		4.981E 05		2.198E 05		2.964E 05	
PHIFG		0.105		0.095		0.067		0.081		0.037		0.071		0.043		0.089		0.025	
FG		0.		0.		0.		0.		0.032		0.		0.		0.		0.032	
PHI		0.		0.		0.		0.		1.160		0.		0.		0.		0.782	

		3-402	6	8-702	6	8-1102	6	8-1202	6	8-1302	6	8-1402	6	8-1502	6	8-1602	6	3-1702	6
MEAN QUALITY INCREMENT		0.9000		0.9000		0.9000		0.9000		0.9150		0.9000		0.9000		0.9000		0.8900	
DX		0.200		0.200		0.200		0.200		0.170		0.200		0.200		0.200		0.220	
DE		0.033		0.033		0.033		0.033		0.033		0.033		0.033		0.033		0.033	
DLX		5.850		4.900		4.900		0.033		2.550		0.033		3.000		0.033		2.250	
DPX		0.000		0.000		5.000		0.033		4.000		0.033		4.000		0.033		4.000	
PMX		241.500		237.500		237.500		268.000		268.000		295.000		295.000		295.000		295.000	
QX-FLUX		1.941E 04		2.502E 04		2.502E 04		3.763E 04		3.763E 04		4.010E 04		4.010E 04		5.663E 04		5.663E 04	
UX		100.164		120.305		120.305		151.085		151.085		183.435		183.435		253.345		253.345	
DTM		193.820		203.000		203.000		249.040		249.040		218.600		218.600		215.040		215.040	
DTGRX		41.114		45.430		45.430		38.534		38.534		43.349		43.349		43.324		43.324	
DTGR2		154.115		170.326		170.326		144.444		144.444		152.494		152.494		152.499		152.499	
AUX		0.297		0.346		0.346		0.384		0.384		0.394		0.394		0.404		0.404	
CX2		3.548		3.776		3.776		4.729		4.729		4.232		4.232		4.552		4.552	
DTAX		1.316		1.633		1.633		2.273		2.273		2.087		2.087		2.640		2.640	
WFX		7.540E 04		9.422E 04		9.422E 04		7.569E 04		7.569E 04		7.915E 04		7.915E 04		7.632E 04		7.632E 04	
NOX		307.796		380.235		380.235		468.259		468.259		558.924		558.924		803.413		803.413	
KX		14.336		13.326		13.326		11.149		11.149		12.720		12.720		12.929		12.929	
LAX		2.143E 06		2.601E 06		2.601E 06		2.686E 06		2.686E 06		2.165E 06		2.165E 06		1.881E 06		1.881E 06	
PHIFG		0.084		0.041		0.041		0.080		0.080		0.068		0.068		0.099		0.099	
FG		0.		0.		0.		0.		0.		0.		0.		0.		0.	
PHI		0.		0.		0.		0.		0.		0.		0.		0.		0.	

TEST RUN NO.
PLUG INSERT N.J.

TEST DATA		10-2C1	10-3	10-4C1	10-5	10-6	10-7	10-8	10-9
		7	7	7	7	7	7	7	7
KN	LB/HR	2040.00	2040.00	2040.00	2050.00	2040.00	2040.00	2040.00	2040.00
TNAT	DEG-F	1270.00	1320.00	1270.00	1315.00	1290.00	1330.00	1275.00	1325.00
TNAD	DEG-F	1110.00	1160.00	1090.00	1130.00	1110.00	1145.00	1090.00	1115.00
DELIN	DEG-F	160.00	160.00	180.00	185.00	180.00	185.00	185.00	210.00
WH	LB/HR	462.00	452.00	511.00	517.00	504.00	517.00	520.00	590.00
TH31	DEG-F	440.00	440.00	445.00	445.00	445.00	445.00	500.00	500.00
TH40	DEG-F	1200.00	1245.00	1200.00	1245.00	1220.00	1255.00	1210.00	1260.00
PH31	PSIA	346.00	359.00	343.00	347.00	362.00	391.00	344.00	393.00
P1	PSIA	304.00	305.00	302.00	315.00	299.00	314.00	299.00	339.00
P2	PSIA	297.00	237.00	291.00	315.00	289.00	291.00	292.00	342.00
PH50	PSIA	212.00	216.00	190.00	212.00	207.00	198.00	195.00	223.00

HEAT BALANCE		10-2C1	10-3	10-4C1	10-5	10-6	10-7	10-8	10-9
		7	7	7	7	7	7	7	7
QW	BTU/HR	58544.00	64544.00	77112.00	73642.50	77112.00	79254.00	79254.00	89964.00
QHG	BTU/HR	67940.35	66976.33	75070.50	76525.10	74289.57	76663.60	75596.30	86491.14
QHL1	KW	0.18	0.46	0.60	0.91	0.83	0.76	1.07	1.02
QWNET	LB/HR	2022.03	1993.34	1985.99	1969.78	1965.33	1973.32	1945.85	1961.25

PREHEAT SECTION		10-2C1	10-3	10-4C1	10-5	10-6	10-7	10-8	10-9
		7	7	7	7	7	7	7	7
DEPH	FT	0.0058	0.0058	0.0058	0.0053	0.0058	0.0058	0.0053	0.0058
DLPHC	FT	1.25	0.70	1.70	0.90	1.00	0.75	1.25	1.25
DLPPH	PSI	38.00	16.00	33.00	34.00	30.00	22.00	45.00	54.00
P2	PSIA	338.00	373.00	300.00	353.00	332.00	369.00	299.00	339.00
TH20	DEG-F	1133.00	1183.00	1115.00	1157.00	1136.00	1171.00	1114.00	1144.00
TS00	DEG-F	1000.48	1132.88	1092.00	1121.68	1109.92	1130.64	1091.28	1113.84
ELTA00	DEG-F	40.52	50.12	24.00	35.32	26.08	40.36	22.72	30.16
QPHC	BTU/HR	9357.05	13178.41	10745.05	11369.92	10891.39	11520.47	9992.63	11779.38
QPH-FLUX	3/HR-FT2	7532.36	138852.45	60357.52	120638.65	104005.20	146583.25	76338.15	89919.17
UPH	3/HR-FT2-F	345.95	552.37	319.83	550.56	527.19	634.47	438.27	463.57
NUPH		0.24	0.38	0.22	0.37	0.36	0.43	0.30	0.31
POLM		0.0073	0.0073	0.0073	0.0073	0.0073	0.0073	0.0071	0.0071
REPHM		34827.78	34006.33	38384.39	39333.05	37739.59	38724.99	39313.34	44807.92
PE		291.27	248.37	277.77	242.29	275.46	283.09	280.34	317.14
FBH		0.0257	0.0341	0.0234	0.0277	0.0289	0.0254	0.0237	0.0219
UL1	FT/SEC	4.15	4.06	4.59	4.65	4.53	4.65	4.67	5.31

TEST RUN NO. PLUG INSERT NO.		10-2C1	10-3	10-4C1	10-5	10-6	10-7	10-8	10-9
		7	7	7	7	7	7	7	7
PLUG INSERT QUALITY SEC									
XPL		0.215	0.805	0.088	2.315	0.308	0.661	0.176	0.218
DLPL	FT	2.000	2.550	1.550	2.350	2.250	2.500	2.000	2.000
DPPL	PSI	11.000	86.000	9.000	47.000	43.000	78.000	7.000	7.000
QA-FLUX	3/HR-FT2	58400	167802	33958	81317	81233	160517	53750	75532
UMPL	B/HR-FT2-F	1079.654	1314.029	1226.454	1121.928	1329.079	1418.875	1369.780	1477.540
DTMPL	DEG-F	54.100	127.700	33.740	72.480	51.120	113.200	39.240	51.120
U2VPL	FT/SEC	24.754	93.413	11.355	39.479	39.651	86.046	23.121	29.003
U2VT	FT/SEC	8.430	33.304	4.048	14.375	14.139	30.890	8.243	10.361
REFPL	FT/SEC	46349	44653	51505	51089	50335	51075	52412	58109
PHIFG		0.5603	0.2769	2.8567	0.8208	0.8147	0.2906	0.4128	0.2331
LMP		3.359E 03	4.969E 04	0.836E 02	7.234E 03	7.139E 03	3.459E 04	2.565E 03	3.84CE 03
UNPLUGGED TUBE QUAL. SEC									
DX		0.785	0.195	0.912	0.585	0.692	0.339	0.824	0.782
XMIPL		0.608	0.903	0.544	0.657	0.654	0.830	0.588	0.609
DLUPL	FT	6.250	3.750	11.250	6.250	5.850	2.650	9.250	8.750
DPUP	PSI	9.000	5.000	19.000	7.000	9.000	5.000	17.000	17.000
QUPL	A/HR-FT2	68102.839	27598.249	48727.931	66611.359	70059.309	77787.144	54472.249	61874.747
UMUPL	B/HR-FT2-F	533.173	124.227	438.390	405.919	457.426	361.339	431.020	424.265
DTMUPL	DEG-F	127.900	222.160	119.320	164.100	153.160	215.280	126.380	145.840
RF		71547.194	70409.620	79775.939	79516.559	78509.842	80299.119	81061.723	89682.676
PHIFG		0.197	0.084	0.228	0.108	0.149	0.109	0.206	0.177
LAMUP		2.495E 05	2.058E 06	1.961E 05	3.512E 05	3.541E 05	1.120E 06	2.520E 05	2.830E 05

TEST RUN NO.
PLUG INSERT NO.

	10-2C1	10-3	10-4C1	10-5	10-6	10-7	10-8	10-9
	7	7	7	7	7	7	7	7
MEAN QUALITY INCREMENT								
DX	0.1000	0.0630	0.0865	0.0135	0.0135	0.0485	0.0880	0.1100
DE	0.200	0.126	0.173	0.027	0.027	0.097	0.176	0.220
DLX	0.308	0.006	0.008	0.006	0.006	0.006	0.008	0.008
DPX	2.009	0.550	1.550	0.350	0.250	0.500	2.000	2.000
PMX	11.000	68.000	9.000	37.000	33.000	55.000	7.000	7.000
QX-FLUX	302.500	339.000	295.500	334.500	315.500	341.500	295.500	335.500
UX	5.430E 04	1.217E 05	6.714E 04	4.585E 04	6.400E 04	1.179E 05	5.380E 04	7.617E 04
DTM	1022.644	1567.551	1668.419	982.757	1714.933	1863.585	1371.061	1490.051
OTCRX	53.100	77.660	40.240	47.680	37.320	63.260	39.240	51.120
DEG-F	35.158	192.445	33.267	48.515	47.817	170.540	35.135	48.370
DEG-F	234.977	1286.179	227.012	324.242	319.579	1139.785	234.824	323.273
NUDX	0.452	0.489	0.540	0.179	0.242	0.466	0.494	0.552
CX2	1.900	1.022	1.839	0.964	0.999	0.956	1.708	1.757
RETAX	1.074	0.626	1.242	0.216	0.303	0.557	1.055	1.213
FEX	4.635E 04	2.541E 05	5.151E 04	2.913E 05	2.970E 05	2.902E 05	5.241E 04	5.811E 04
MUX	721.447	811.893	1141.766	510.999	898.297	964.074	971.143	1034.660
KX	57.363	35.866	69.102	58.408	74.569	44.034	77.863	54.479
LAMX	2.962E 03	4.498E 03	2.478E 03	3.006E 02	3.096E 02	3.061E 03	2.596E 03	3.996E 03
PHIFG	0.541	0.093	0.725	1.314	1.633	0.108	0.408	0.226
FG	0.032	0.	0.032	0.	0.	0.	0.032	0.032
PHI	20.042	0.	22.668	0.	0.	0.	12.749	7.067

	10-2C1	10-3	10-4C1	10-5	10-6	10-7	10-8	10-9
	7	7	7	7	7	7	7	7
MEAN QUALITY INCREMENT								
DX	0.3000	0.1630	0.2865	0.1135	0.1135	0.1485	0.2880	0.3100
DE	0.200	0.074	0.227	0.173	0.173	0.103	0.224	0.180
DLX	0.033	0.008	0.033	0.008	0.008	0.008	0.033	0.033
DPX	0.750	0.350	1.550	1.450	1.250	0.650	1.500	1.250
PMX	1.000	3.000	2.000	7.000	6.000	3.000	3.000	3.000
QX-FLUX	296.500	303.500	295.000	312.500	296.000	310.000	290.500	330.500
UX	1.448E 05	1.124E 05	8.791E 04	7.247E 04	8.202E 04	9.629E 04	9.130E 04	9.972E 04
DTM	1723.475	1011.802	1134.826	966.282	1283.952	994.904	1223.110	1121.406
OTCRX	84.020	111.040	74.200	75.000	63.880	96.400	74.340	88.920
DEG-F	20.902	54.055	22.345	44.206	43.296	55.719	22.829	26.992
DEG-F	139.695	361.272	149.340	295.643	289.364	379.077	152.575	180.396
NUDX	0.514	0.580	0.419	0.465	0.545	0.545	0.427	0.407
CX2	3.307	2.511	2.713	2.042	2.062	2.215	2.714	2.663
RETAX	2.128	1.823	1.421	1.187	1.405	1.511	1.451	1.355
FEX	7.134E 04	4.532E 04	7.928E 04	5.158E 04	5.078E 04	5.165E 04	8.065E 04	8.933E 04
MUX	5246.470	713.453	3621.450	678.401	909.158	702.150	3752.583	3356.621
KX	33.097	25.051	37.465	37.102	43.531	28.863	37.395	31.314
LAMX	3.927E 04	7.525E 03	3.912E 04	4.051E 03	4.112E 03	6.375E 03	4.007E 04	4.744E 04
PHIFG	0.750	0.394	0.538	0.357	0.359	0.529	0.946	0.850
FG	0.	0.032	0.	0.032	0.032	0.032	0.	0.
PHI	0.	12.310	0.	11.159	11.206	16.525	0.	0.

TEST RUN NO.
PLUG INSERT NO.

	10-201	10-3	10-4C1	10-5	10-6	10-7	10-8	10-9
	7	7	7	7	7	7	7	7
MEAN QUALITY INCREMENT	0.5000	0.3000	0.5000	0.2550	0.2550	0.3000	0.5000	0.5000
DX	0.200	0.200	0.200	0.110	0.110	0.200	0.200	0.200
DE	0.033	0.008	0.033	0.008	0.008	0.008	0.033	0.033
DLX	0.700	0.900	1.700	0.550	0.750	0.600	1.250	1.400
DPX	1.200	8.000	3.000	3.000	4.000	8.000	2.000	2.000
PMX	295.500	298.000	287.500	307.500	291.000	302.000	283.500	328.000
QX-FLUX	1.551E 05	1.181E 05	7.569E 04	1.215E 05	8.692E 04	2.025E 05	9.782E 04	9.892E 04
UX	1398.488	891.619	654.432	1217.268	982.345	1628.565	896.271	798.934
DTM	111.740	132.440	108.000	99.800	88.480	124.380	109.140	123.820
OTCRX	50.109	91.133	55.594	91.160	89.341	104.108	56.562	63.139
OTCR2	187.833	609.077	209.395	609.259	597.096	695.794	212.023	236.676
NUDX	0.631	0.766	0.438	0.809	0.740	1.030	0.512	0.462
CX2	3.959	2.426	2.767	2.164	1.969	2.552	2.982	2.855
BETAX	2.309	2.324	1.515	2.189	1.822	3.289	1.909	1.648
REFX	7.139E 04	4.543E 04	7.943E 04	5.172E 04	5.097E 04	5.188E 04	8.079E 04	8.946E 04
NUX	4220.371	630.562	2063.619	855.676	697.772	1149.187	2742.922	2394.250
KX	24.985	20.998	25.736	27.877	31.420	22.363	25.468	22.486
LAMX	1.383E 05	2.731E 04	1.531E 05	2.009E 04	2.129E 04	3.013E 04	1.551E 05	1.558E 05
PHIFG	0.289	0.119	0.284	0.079	0.078	0.138	0.249	0.193
FG	0.	0.032	0.	0.032	0.032	0.032	0.	0.
PHI	0.	3.716	0.	2.469	2.429	4.306	0.	0.

MEAN QUALITY INCREMENT

DX	0.7000	0.5000	0.7000	0.4550	0.4550	0.5300	0.7000	0.7000
DE	0.200	0.200	0.200	0.290	0.290	0.260	0.200	0.200
DLX	0.033	0.008	0.033	0.033	0.033	0.008	0.033	0.033
DPX	0.800	0.500	2.200	1.000	1.150	0.750	1.700	1.800
PMX	2.200	4.000	4.000	2.000	2.000	7.000	5.000	4.000
QX-FLUX	294.000	292.000	284.000	305.000	283.000	294.500	284.500	325.000
UX	1.458E 05	2.126E 05	5.462E 04	1.762E 05	1.494E 05	2.107E 05	7.193E 04	7.694E 04
DTM	974.418	1301.941	383.702	1332.457	1234.758	1277.058	502.415	479.383
OTCRX	139.320	163.260	140.520	132.200	120.640	167.900	143.160	160.500
OTCR2	54.370	218.894	60.374	53.117	52.084	257.055	61.425	63.587
NUDX	203.307	920.485	225.313	199.110	195.238	963.570	230.252	257.100
CX2	0.682	1.273	0.437	0.575	0.566	1.307	0.496	0.452
PE TAX	3.968	2.924	3.025	3.500	3.435	2.748	3.226	3.121
REFX	3.386	4.654	1.651	2.584	2.431	4.493	2.001	1.905
NUX	7.147E 04	4.567E 04	7.963E 04	7.940E 04	7.831E 04	5.215E 04	8.100E 04	9.961E 04
KX	2970.989	924.206	1192.567	4037.529	3791.061	905.124	1540.964	1438.680
LAMX	19.957	17.029	19.777	21.043	23.040	16.856	19.412	17.345
PHIFG	4.246E 05	9.743E 04	4.722E 05	1.146E 05	1.171E 05	1.273E 05	4.782E 05	4.795E 05
FG	0.256	0.038	0.148	0.359	0.343	0.030	0.231	0.152
PHI	0.	0.032	0.	0.	0.	0.032	0.	0.
	0.	1.182	0.	0.	0.	0.945	0.	0.

TEST RUN NO.
PLUG INSERT NO.

MEAN QUALITY INCREMENT

	10-2C1	10-3	10-4C1	10-5	10-6	10-7	10-8	10-9
DX	0.9000	0.7000	0.9000	0.7000	0.7000	0.7300	0.9000	0.9000
DE	0.200	0.200	0.200	0.200	0.200	0.140	0.200	0.200
DLX	0.033	0.008	0.033	0.033	0.033	0.033	0.033	0.033
DPX	4.000	0.300	5.000	0.950	1.000	0.550	4.800	4.300
DMX	5.000	3.000	10.000	1.000	2.000	2.000	7.000	8.000
OX-FLUX	290.500	288.500	277.000	303.500	286.000	290.000	273.500	319.000
UX	2.715E 04	3.543E 05	2.072E 04	1.279E 05	1.185E 05	1.547E 05	2.547E 04	3.221E 04
UTM	161.288	1842.403	117.676	749.837	745.062	778.475	142.327	161.556
OTCRX	158.340	192.280	176.062	170.540	159.090	194.730	179.980	199.363
OTCR2	43.413	237.639	44.951	60.653	59.403	60.286	45.713	51.093
NUOX	151.489	890.975	164.501	227.359	223.030	225.984	171.355	191.523
NUOX	0.380	1.960	0.330	0.592	0.603	0.637	0.362	0.363
NUOX	3.774	3.778	3.412	3.872	3.809	4.348	3.574	3.597
NUOX	1.792	9.257	1.409	2.867	2.872	3.464	1.619	1.657
NUOX	7.165E 04	4.579E 04	8.004E 04	7.947E 04	7.842E 04	8.021E 04	8.136E 04	8.991E 04
NUOX	492.827	1310.740	362.638	2273.759	2283.033	2379.434	438.198	486.245
NUOX	16.514	14.456	15.779	16.311	17.471	13.990	15.522	13.961
NUOX	2.018E 06	3.004E 05	2.271E 06	4.534E 05	4.644E 05	5.618E 05	2.293E 06	2.297E 06
NUOX	0.077	0.024	0.093	0.089	0.168	0.270	0.068	0.076
NUOX	0.000	0.032	0.000	0.000	0.000	0.000	0.000	0.000
NUOX	0.000	0.032	0.000	0.000	0.000	0.000	0.000	0.000
NUOX	0.000	0.746	0.000	0.000	0.000	0.000	0.000	0.000

MEAN QUALITY INCREMENT

	10-2C1	10-3	10-4C1	10-5	10-6	10-7	10-8	10-9
DX	0.9000	0.9000	0.9000	0.9000	0.9000	0.9000	0.9000	0.9000
DE	0.200	0.200	0.200	0.200	0.200	0.200	0.200	0.200
DLX	0.033	0.033	0.033	0.033	0.033	0.033	0.033	0.033
DPX	3.700	3.700	3.700	3.700	3.700	3.700	3.700	3.700
PMX	5.000	5.000	5.000	5.000	5.000	5.000	5.000	5.000
OX-FLUX	284.500	284.500	284.500	284.500	284.500	284.500	284.500	284.500
UX	2.872E 04	2.872E 04	2.872E 04	2.872E 04	2.872E 04	2.872E 04	2.872E 04	2.872E 04
UTM	129.584	129.584	129.584	129.584	129.584	129.584	129.584	129.584
OTCRX	221.660	221.660	221.660	221.660	221.660	221.660	221.660	221.660
OTCR2	39.634	39.634	39.634	39.634	39.634	39.634	39.634	39.634
NUOX	148.567	148.567	148.567	148.567	148.567	148.567	148.567	148.567
NUOX	0.343	0.343	0.343	0.343	0.343	0.343	0.343	0.343
NUOX	4.156	4.156	4.156	4.156	4.156	4.156	4.156	4.156
NUOX	1.783	1.783	1.783	1.783	1.783	1.783	1.783	1.783
NUOX	7.041E 04	7.041E 04	7.041E 04	7.041E 04	7.041E 04	7.041E 04	7.041E 04	7.041E 04
NUOX	397.450	397.450	397.450	397.450	397.450	397.450	397.450	397.450
NUOX	12.538	12.538	12.538	12.538	12.538	12.538	12.538	12.538
NUOX	2.016E 06	2.016E 06	2.016E 06	2.016E 06	2.016E 06	2.016E 06	2.016E 06	2.016E 06
NUOX	0.085	0.085	0.085	0.085	0.085	0.085	0.085	0.085
NUOX	0.000	0.000	0.000	0.000	0.000	0.000	0.000	0.000
NUOX	0.000	0.000	0.000	0.000	0.000	0.000	0.000	0.000
NUOX	0.000	0.000	0.000	0.000	0.000	0.000	0.000	0.000

APPENDIX B

CL-4 BOILER TEST DATA REDUCTION PROGRAM

APPENDIX B

CL-4 BOILER TEST DATA REDUCTION PROGRAM

The test data representation as provided on the NaK temperature profile recording sheets (Figure B-1) was utilized to reduce these data and establish the boiler thermal and dynamic operating parameters in dimensional and non-dimensional form for each data point set. The test data reduction program as utilized with the IBM-7094 Mod. 2 computer consists of two steps. The first computer input step provides the heat balance and the boiler overall thermal and dynamic operating parameters. These results in conjunction with NaK temperature profile representations are then used to generate the second computer input set (Figure B-2), which comes into the program just prior to equation 75. This results in the determination of the thermal and dynamic operating parameters in dimensional and non-dimensional form for the boiler preheat and vapor quality sections. The vapor quality section analysis was performed on a local boiling heat transfer basis by dividing the section into 20% quality increments. The mean boiling heat transfer parameters in the plug insert section and the unplugged tube section were determined as well.

FIRST INPUT SET

D , in. - Boiler tube ID
 w_i , in. - Machined plug insert thread width
 h_i , in. - Machined plug insert thread height
 δ_0 , in. - Wire diameter
 p_1 , in. - Plug insert wire or thread pitch in preheat section
 p_2 , in. - Plug insert wire pitch in vapor quality section
 p_3 , in. - Unplugged tube wire pitch
 ΔL_{p_1} , in. - Preheat section plug insert length
 ΔL_{p_2} , in. - Vapor quality section plug insert length
 g_c , $\frac{\text{lbf-ft}}{\text{lbf-sec}^2}$ - Gravitational constant

w_N , lbf/hr - NaK flow rate
 T_{Nbi} , °F - NaK inlet temperature
 T_{Nbo} , °F - NaK exit temperature
 ΔT_N , °F - NaK temperature drop
 w , lbf/hr - Mercury flow rate
 T_{Hbi} , °F - Mercury inlet temperature
 T_{Hbo} , °F - Mercury vapor exit temperature
 P_{Hbi} , psia - Mercury inlet pressure
 P_1 , psia - Mercury pressure at preheat section end point
 P_2 , psia - Mercury pressure at plug insert end point
 P_{Hbo} , psia - Mercury pressure at boiler exit
 ΔP_{PH} , psi - Preheat section pressure drop
 ΔP_x , psi - Plug insert vapor section pressure drop
 T_{N-2} , °F - NaK temperature at plug insert end point
 f_{g-PL} , - Frictional pressure drop coefficient for all vapor flow in the plug insert vapor quality section

HEAT BALANCE

1. $q_N = .21 w_N \Delta T_N$ Btu/hr
2. $T_S = f(P_{Hbo})$ °F Fig. B-4 Re: 1
3. $\Delta T_{PH} = T_2 - T_{Hbi}$ °F
4. $\Delta T_{SH} = T_{Hbo} - T_2$ °F
5. $q_{PH} = .0325 w \Delta T_3$ Btu/hr
6. $h_{fv} = f(T_2)$ Btu/lbm Fig. B-13 Re: 1
7. $q_B = w h_6$ Btu/hr
8. $q_{SH} = .025 w \Delta T_4$ Btu/hr
9. $q_{Hg} = q_5 + q_7 + q_8$ Btu/hr
10. $q_{HL} = \frac{q_1 - q_9}{3413}$ kw
11. $w_{N-HL} = \frac{3413 q_{10}}{.21 \Delta T_N}$ lbm/hr
12. $w_{N-Net} = w_N - w_{11}$ lbm/hr

PREHEAT SECTION

13. $\tan \alpha_1 = \frac{\pi D}{P_1}$
14. $\sin \alpha_1 = f(\tan \alpha)_{13}$
15. $\cos \alpha_1 = f(\tan \alpha)_{13}$
16. $\ell_1 = p_1 \sin \alpha_{14} - w_i$ in.
17. $A_{C-PH} = \frac{\ell_{16} h_i}{144}$ ft²

18. $P_{W-PH} = \frac{2(\ell_{16} - h_i)}{12}$ ft
19. $De_{PH} = \frac{4 A_{17}}{P_{18}}$ ft
20. $\Delta L'_{PH} = \frac{\Delta L_{p1}}{12 \cos \alpha_{15}}$ ft
21. $G_{PH-1} = \frac{w}{A_{17}}$ lbm/hr-ft²
22. $G_{PH-2} = \frac{G_{21}}{3600}$ lbm/sec-ft²
23. $T_{S-1} = f(P_1)$ °F Fig. B-4 Re: 1
24. $\rho_{L-1} = f(T_{23})$ lbm/ft³ Fig. B-1 Re: 1
25. $u_{L-1} = \frac{G_{22}}{\rho_{24}}$ ft/sec
26. $T_{L-M} = \frac{T_{Hbi} + T_{23}}{2}$ °F
27. $\mu_{L-M} = f(T_{26})$ lbm/hr-ft Fig. B-6 Re: 1
28. $Re_{L-M} = \frac{G_{21} De_{19}}{\mu_{27}}$
29. $\rho_{L-M} = f(T_{26})$ lbm/hr-ft Fig. B-1 Re: 1
30. $f_L = \frac{144 \times 2g_c De_{19}}{\Delta L'_{20}} \frac{\rho_{29} \Delta P_{PH}}{G_{22}^2}$
31. $c_{p-IM} = f(T_{26})$ Btu/lbm-°F Fig. B-5 Re: 1
32. $q_{PH} = w c_{p31} (T_{23} - T_{Hbi})$ Btu/hr

$$\begin{aligned}
33. \quad \Delta T_{N-PH} &= \frac{q_{32}}{.21 w_{12}} & ^\circ F \\
34. \quad T_{NOO} &= T_{Nbo} + \Delta T_{33} & ^\circ F \\
35. \quad k_{L-M} &= f(T_{26}) & \text{Btu/hr-ft-}^\circ F \\
36. \quad Pr &= \frac{c_{p31} \mu_{27}}{k_{35}}
\end{aligned}$$

PLUG INSERT VAPOR QUALITY SECTION

$$\begin{aligned}
37. \quad \tan \alpha_2 &= \frac{\pi D}{p_2} \\
38. \quad \sin \alpha_2 &= f(\tan \alpha)_{37} \\
39. \quad \cos \alpha_2 &= f(\tan \alpha)_{37} \\
40. \quad \ell_2 &= p_2 \sin \alpha_{38} - \delta & \text{in.} \\
41. \quad A_{C-x} &= \frac{\ell_{40} \delta}{144} & \text{ft}^2 \\
42. \quad P_{W-x} &= \frac{2(\ell_{40} + \delta)}{12} & \text{ft} \\
43. \quad De_x &= \frac{4 A_{41}}{P_{42}} & \text{ft} \\
44. \quad \Delta L'_x &= \frac{\Delta L p_2}{12 \cos \alpha_{39}} & \text{ft} \\
45. \quad G_{x-1} &= \frac{w}{A_{41}} & \text{lbm/hr-ft}^2 \\
46. \quad G_{x-2} &= \frac{G_{45}}{3600} & \text{lbm/sec-ft}^2 \\
47. \quad \Delta T_{N-x} &= T_{N-2} - T_{34} & ^\circ F \\
48. \quad q_{N-x} &= .21 w_{12} \Delta T_{47} & \text{Btu/hr}
\end{aligned}$$

$$49. \quad T_{S-2} = f(P_2) \quad ^\circ\text{F} \quad \text{Fig. B-4} \quad \text{Re: 1}$$

$$50. \quad T_{x-SM} = \frac{T_{23} + T_{49}}{2} \quad ^\circ\text{F}$$

$$51. \quad h_{x-fv-M} = f(T_{50}) \quad \text{Btu/lbm} \quad \text{Fig. B-13} \quad \text{Re: 1}$$

$$52. \quad x_{PL} = \frac{q_{48}}{w h_{51}}$$

$$53. \quad \rho_{v-2} = 18.7 \frac{P_2}{T_{49} + 460} \quad \text{lbm/ft}^3$$

$$54. \quad u_{v-PL-2} = \frac{x_{52} G_{46}}{\rho_{53}} \quad \text{ft/sec}$$

UNPLUGGED TUBE VAPOR QUALITY SECTION

$$55. \quad A_{C-xx} = \frac{\pi}{4 \times 144} D^2 \quad \text{ft}^2$$

$$56. \quad \tan \alpha_3 = \frac{\pi D}{P_3}$$

$$57. \quad G_{xx-1} = \frac{w}{A_{55}} \quad \text{lbm/hr-ft}^2$$

$$58. \quad G_{xx-2} = \frac{G_{57}}{3600} \quad \text{lbm/sec-ft}^2$$

$$59. \quad u_{v-T-2} = \frac{x_{52} T_{58}}{\rho_{53}} \quad \text{ft/sec}$$

$$60. \quad h_{fv-2} = f(T_{49}) \quad \text{Btu/lbm}$$

$$61. \quad q_{N-xx} = (1 - x_{52}) w h_{60} \quad \text{Btu/hr}$$

$$62. \quad \Delta T_{N-xx} = \frac{q_{61}}{.21 w_{12}} \quad ^\circ\text{F}$$

$$63. \quad \Delta T_{N-B} = \Delta T_{47} + \Delta T_{62} \quad ^\circ\text{F}$$

$$64. \quad T_{N100} = T_{34} + \Delta T_{63} \quad ^\circ\text{F}$$

$$65. \quad \Delta T_{N\Delta x} = \frac{\Delta T_{63}}{5} \quad ^\circ\text{F}$$

$$66. \quad q_B = q_{48} + q_{61} \quad \text{Btu/hr}$$

$$67. \quad q_{B\Delta x} = \frac{q_{66}}{5} \quad \text{Btu/hr}$$

$$68. \quad T_{N00} = T_{Nbo} + \Delta T_{33} \quad ^\circ\text{F}$$

$$69. \quad T_{N20} = T_{68} + \Delta T_{65} \quad ^\circ\text{F}$$

$$70. \quad T_{N40} = T_{68} + 2\Delta T_{65} \quad ^\circ\text{F}$$

$$71. \quad T_{N60} = T_{68} + 3\Delta T_{65} \quad ^\circ\text{F}$$

$$72. \quad T_{N80} = T_{68} + 4\Delta T_{65} \quad ^\circ\text{F}$$

$$73. \quad T_{N100} = T_{68} + 5\Delta T_{65} \quad ^\circ\text{F}$$

$$74. \quad C = \frac{\pi D}{12} \quad \text{ft}$$

PREHEAT SECTION

$$75. \quad \Delta L_{PHc} = L_{00} - .5 \quad \text{ft}$$

$$76. \quad A_{PH} = C_{74} \Delta L_{75} \quad \text{ft}^2$$

$$77. \quad T_{S00} = f(P_{00}) \quad ^\circ\text{F}$$

Fig. B-4 Re: 1

$$78. \quad q_{PHc} = .0325 w (T_{77} - T_{Hbi}) \quad \text{Btu/hr}$$

$$79. \quad q''_{PH} = \frac{q_{78}}{A_{76}} \quad \text{Btu/hr-ft}^2$$

$$80. \quad \Delta T_{PHi} = T_{Nbo} - T_{Hbi} \quad ^\circ F$$

$$81. \quad \Delta T_{PHo} = T_{NOO} - T_{77} \quad ^\circ F$$

$$82. \quad \Delta T_{PH-M} = \frac{\Delta T_{80} - \Delta T_{81}}{\ln \frac{\Delta T_{80}}{\Delta T_{81}}} \quad ^\circ F$$

$$83. \quad h_{PH} = \frac{q''_{79}}{\Delta T_{82}} \quad \text{Btu/hr-ft}^2\text{-}^\circ F$$

$$84. \quad Nu_{PH} = \frac{De \, h_{83}}{k_{35}}$$

$$85. \quad T_{PH-M} = \frac{T_{Hbi} + T_{77}}{2} \quad ^\circ F$$

$$86. \quad \rho_{PH-M} = f(T_{85}) \quad \text{lbm/ft}^3 \quad \text{Fig. B-1 Re: 1}$$

$$87. \quad \mu_{PH-M} = f(T_{85}) \quad \text{lbm/hr-ft} \quad \text{Fig. B-6 Re: 1}$$

$$88. \quad Re_{PH} = \frac{G_1 \, De}{\mu_{87}}$$

$$89. \quad \Delta P_{PHc} = P_{Hbi} - P_{00}$$

$$90. \quad f_{PH} = f_{30} \frac{\rho_{86}}{\rho_{29}} \frac{\Delta P_{89}}{\Delta P_{PH}} \frac{\Delta L_{20}}{\Delta L_{75}} \cos \alpha$$

$$91. \quad Pe_{PH} = Re_{88} \, Pr_{36}$$

$$92. \quad \Delta T_{00} = T_{NOO} - T_{77} \quad ^\circ F$$

MEAN QUALITY INCREMENT

$$93. \quad \bar{x} = \frac{x_n + x_{n+1}}{2}$$

$$94. \quad \Delta x = x_{n+1} - x_n$$

$$95. \quad \Delta L = L_{x_{n+1}} - L_{x_n} \quad \text{ft}$$

$$96. \quad \Delta P = P_n - P_{n+1} \quad \text{psi}$$

$$97. \quad P_M = \frac{P_n + P_{n+1}}{2} \quad \text{psia}$$

$$98. \quad T_{N-M} = \frac{T_{Nx_n} + T_{Nx_{n+1}}}{2} \quad ^\circ\text{F}$$

$$99. \quad A_{\bar{x}} = C_{74} \Delta L_{95} \quad \text{ft}^2$$

$$100. \quad q''_{\bar{x}} = \frac{Z_{\bar{x}} q_{67}}{A_{99}} \quad \text{Btu/hr-ft}^2$$

$$101. \quad T_{S-M} = f(P_{97}) \quad ^\circ\text{F} \quad \text{Fig. B-4 Re: 1}$$

$$102. \quad \Delta T_M = T_{98} - T_{101} \quad ^\circ\text{F}$$

$$103. \quad h = \frac{q''_{100}}{\Delta T_{102}} \quad \text{Btu/hr-ft}^2\text{-}^\circ\text{F}$$

$$104. \quad \rho_L = f(T_{101}) \quad \text{lbm/ft}^3 \quad \text{Fig. B-1 Re: 1}$$

$$105. \quad \rho_v = f(T_{101}) \quad \text{lbm/ft}^3 \quad \text{Fig. B-8 Re: 1}$$

$$106. \quad \mu_L = f(T_{101}) \quad \text{lbm/hr-ft} \quad \text{Fig. B-6 Re: 1}$$

$$107. \quad \mu_v = f(T_{101}) \quad \text{lbm/hr-ft} \quad \text{Fig. B-11 Re: 1}$$

$$108. \quad k_L = f(T_{101}) \quad \text{Btu/hr-ft-}^\circ\text{F} \quad \text{Fig. B-7} \quad \text{Re: 1}$$

$$109. \quad k_v = f(T_{101}) \quad \text{Btu/hr-ft-}^\circ\text{F} \quad \text{Fig. B-12} \quad \text{Re: 1}$$

$$110. \quad \Delta L' = \frac{\Delta L_{95}}{\cos \alpha} \quad \text{ft}$$

$$111. \quad \phi f_g = 144 \frac{2g_c \text{ De } \Delta P_{96} \rho_{105}}{\Delta L'_{110} (\bar{x}_{93} G_2)^2}$$

$$112. \quad \text{Re} = \frac{G_1 \text{ De}}{\mu_{107}}$$

$$113. \quad \phi = \frac{(\phi f_g)_{111}}{f_g}$$

$$114. \quad \lambda = \text{Re}_{112}^{.8} \frac{\mu_{107}}{\mu_{106}} \frac{\rho_{104}}{\rho_{105}} \frac{\bar{x}_{93}^{1.8}}{1 - \bar{x}_{93}}$$

$$115. \quad \text{Nu} = \frac{\text{De } h_{103}}{k_{109}}$$

$$116. \quad h_{fv} = f(T_{101}) \quad \text{Btu/lbm} \quad \text{Fig. B-17} \quad \text{Re: 1}$$

$$117. \quad K = \frac{h_{116} \mu_{107}}{k_{109} \Delta T_{102}}$$

$$118. \quad \Delta T_{\text{cr-1}} = \frac{h_{116} \mu_{107} C_{\bar{x}}^2 (7488)^{\frac{1}{2}} (k_{109}/k_{108})^3 \text{Re}_{112} E_{\bar{x}} (1 - \bar{x}_{93})^{\frac{1}{2}} \bar{x}_{93}}{k_{109} \left(\frac{12 \text{ De}}{\delta}\right)^{3/2} \left(\frac{\rho_{105}}{\rho_{104}}\right)^{1/2}}$$

Note: If $\Delta T_{118} > \Delta T_{102}$ use Eq. 119

If $\Delta T_{118} < \Delta T_{102}$ use Eq. 120

$$119. \quad Nu_{\delta} = \left[\frac{32 Nu_{115}}{(k_{108}/k_{109})^2 \left(\frac{12 De}{\delta}\right)^2 (\rho_{105}/\rho_{104}) \frac{(1-\bar{x}_{93})^{1/3}}{\bar{x}_{93}}} \right]^{1/2}$$

$$120. \quad \Delta T_{cr-2} = C_{\bar{x}}^3 K_{117} \Delta T_{102} \frac{(936)^{3/4} (k_{109}/k_{108})^3 Re_{112} E_{\bar{x}} (1-\bar{x}_{93})^{1/2} \bar{x}_{93}}{6^{1/4} \left(\frac{12 De}{\delta}\right)^{3/2} (\rho_{105}/\rho_{104})^{1/2} \beta_{\bar{x}}}$$

Note: If $\Delta T_{120} > \Delta T_{102}$ use Eq. 121.

If $\Delta T_{120} < \Delta T_{102}$ use Eq. 122.

$$121. \quad C_{\bar{x}} = \left[\frac{Nu_{115}}{234 \left(\frac{k_{109}}{k_{108}}\right)^4 \left(\frac{\delta}{12 De}\right) E_{\bar{x}}^2 Re_{112}^2 K_{117}^2 (1-\bar{x}_{93})^{4/3} \bar{x}_{93}} \right]^{1/4}$$

$$122. \quad \beta_{\bar{x}} = \frac{4 Nu_{115}}{6^{1/3} \left(\frac{12 De}{\delta}\right) (Re_{112} E_{\bar{x}} \frac{\rho_{105}}{\rho_{104}} K_{117})^{2/3} \frac{(1-\bar{x}_{93})^{2/3}}{\bar{x}_{93}}}$$

PLUG INSERT VAPOR QUALITY SECTION

$$123. \quad \Delta L_{PL-x} = L_{PL} - L_{00} \quad \text{ft.}$$

$$124. \quad A_x = C_{74} \Delta L_{123} \quad \text{ft}^2$$

$$125. \quad q'' = \frac{q_{48}}{A_{124}} \quad \text{Btu/hr-ft}^2$$

$$126. \quad T_{S-MPL} = f(P_M) \quad ^\circ\text{F} \quad \text{Fig. B-4 Re: 1}$$

$$127. \quad \rho_{v-MPL} = 18.7 \frac{P_M}{T_{126} + 460} \quad \text{lbm/ft}^3$$

$$128. \quad \mu_{v-MPL} = f(T_{126}) \quad \text{lbm/hr-ft} \quad \text{Fig. B-11 Re: 1}$$

$$129. \quad \Delta L'_{PL-x} = \frac{\Delta L_{123}}{\cos \alpha_{39}} \quad \text{ft}$$

$$130. \quad \bar{x}_{PL} = \frac{1}{2} x_{52}$$

$$131. \quad (\phi f_g)_{PL} = 144 \frac{2g_c De_{43} \Delta P_{PL-x} \rho_{127}}{\Delta L_{129} (\bar{x}_{130} G_{46})^2}$$

$$132. \quad Re_{PL-x} = \frac{G_{45} De_{43}}{\mu_{128}}$$

$$133. \quad \rho_{L-MPL-x} = f(T_{126}) \quad \text{lbm/ft}^3 \quad \text{Fig. B-1 Re: 1}$$

$$134. \quad \mu_{L-MPL-x} = f(T_{126}) \quad \text{lbm/hr-ft}$$

$$135. \quad \lambda_{MPL} = Re_{132}^{.8} \frac{\mu_{128} \rho_{133} \bar{x}_{130}^{-1.8}}{\mu_{134} \rho_{127} 1 - \bar{x}_{130}}$$

$$136. \quad \Delta T_{MPL-x} = T_{NMx} - T_{126} \quad ^\circ F$$

$$137. \quad h_{MPL-x} = \frac{q_{125}''}{\Delta T_{136}} \quad \text{Btu/hr-ft}^2\text{-}^\circ F$$

UNPLUGGED TUBE VAPOR QUALITY SECTION

$$138. \quad \Delta L_{UPL-x} = L_{100} - L_{xPL} \quad \text{ft}$$

$$139. \quad A_{UPL-x} = C_{74} \Delta L_{138} \quad \text{ft}^2$$

$$140. \quad q_{UPL-x}'' = \frac{q_{61}}{A_{139}} \quad \text{Btu/hr-ft}^2$$

$$141. \quad T_{S-MUPL} = f(P_{M-UPL}) \quad ^\circ F$$

$$142. \quad \rho_{v-MUPL} = 18.7 \frac{P_{M-UPL}}{T_{141} + 460} \quad \text{lbm/ft}^3$$

$$143. \quad \rho_{L-MUPL} = f(T_{141}) \quad \text{lbm/ft}^3 \quad \text{Fig. B-1 Re: 1}$$

$$144. \quad \mu_{V-MUPL} = f(T_{141}) \quad \text{lbm/hr-ft} \quad \text{Fig. B-11 Re: 1}$$

$$145. \quad \mu_{L-MUPL} = f(T_{141}) \quad \text{lbm/hr-ft} \quad \text{Fig. B-6 Re: 1}$$

$$146. \quad (\phi f_g)_{UPL} = 144 \frac{2 g_c D \Delta P_{UPL} \rho_{142}}{12 \Delta L_{UPL} (\bar{x}_{UPL} G_{58})^2}$$

$$147. \quad Re = \frac{G_{57} D}{12 \mu_{144}}$$

$$148. \quad \lambda = Re_{147}^{.8} \frac{\mu_{144}}{\mu_{145}} \frac{\rho_{143}}{\rho_{142}} \frac{\bar{x}_{UPLM}^{1.8}}{1 - \bar{x}_{UPLM}}$$

$$149. \quad \Delta T_{M-UPL} = T_{NMx} - T_{141} \quad ^\circ F$$

$$150. \quad h_{MUPL} = \frac{q_{140}''}{\Delta T_{149}} \quad \text{Btu/hr-ft}^2\text{-}^\circ F$$

Reference

1. Properties of SNAP-8 Fluids, NaK and Mercury, ET-378, March 1964, Aerojet-General Corporation.

NOMENCLATURE

A	-	Area
C	-	Circumference, also a constant
c_p	-	Specific heat at constant pressure
D_e	-	Equivalent tube diameter
E	-	Geometric constant
f	-	Friction factor
f()	-	Function of ()
G	-	Specific mass flow
h	-	Heat transfer coefficient
h_{fv}	-	Latent heat
K	-	$\left(\frac{\mu_v h_{fv}}{k_v \Delta T_m} \right)$
k	-	Thermal conductivity
ℓ_1	-	Helical flow passage width in preheat section
ℓ_2	-	Helical flow passage width in plug insert vapor section
ΔL	-	Axial tube length
$\Delta L'$	-	Flow passage helical length
Nu	-	Nusselt number
Nu_δ	-	Droplet Nusselt number
P	-	Pressure
ΔP	-	Pressure drop
P_w	-	Wetted perimeter
Pe	-	Peclet number
Pr	-	Prandtl number

NOMENCLATURE (Cont.)

q	-	Heat transfer rate
q''	-	Heat flux
Re	-	Reynolds number
u	-	Velocity
w	-	Mass flow rate
x	-	Vapor quality
Δx	-	Vapor quality increment
\bar{x}	-	Mean vapor quality
$z_{\bar{x}}$	-	$\frac{\Delta x}{.20}$

GREEK SYMBOLS

- α - Swirl wire angle
- β - $\frac{Nu \text{ (actual)}}{Nu_{\delta} \text{ (film-sphere)}}$
- λ - Martinelli correlating parameter
- δ - Droplet diameter, Swirl wire diameter
- ρ - Density
- μ - Viscosity
- ϕ - Two-phase flow ration $\Delta P_{TP}/\Delta P_V$

SUBSCRIPTS

B	-	Boiling
C	-	Flow cross-section
Hg	-	Mercury
HL	-	Heat loss
L	-	Liquid
M	-	Mean
N	-	NaK
PH	-	Preheat section
PL	-	Plugged section
S	-	Saturation
SH	-	Superheat section
SM	-	Saturation-Mean
T	-	Tube
UPL	-	Unplugged section
c	-	Corrected
cr	-	Critical
f	-	Liquid at saturation temperature
g	-	Gas, vapor
i	-	Inlet
o	-	Outlet, exit
v	-	Vapor
x	-	Plug insert vapor quality section
xx	-	Vapor quality section in unplugged tube

SUBSCRIPTS (cont.)

Unless otherwise indicated, numerical subscripts refer to numbered equations.

Exceptions:

- 1 - Refers to the point at which P_1 is measured
- 2 - Refers to the point at which P_2 is measured
- 00 - Liquid-vapor interface location
- 20 - 20% quality location
- 40 - 40% quality location
- 60 - 60% quality location
- 80 - 80% quality location
- 100 - 100% quality location

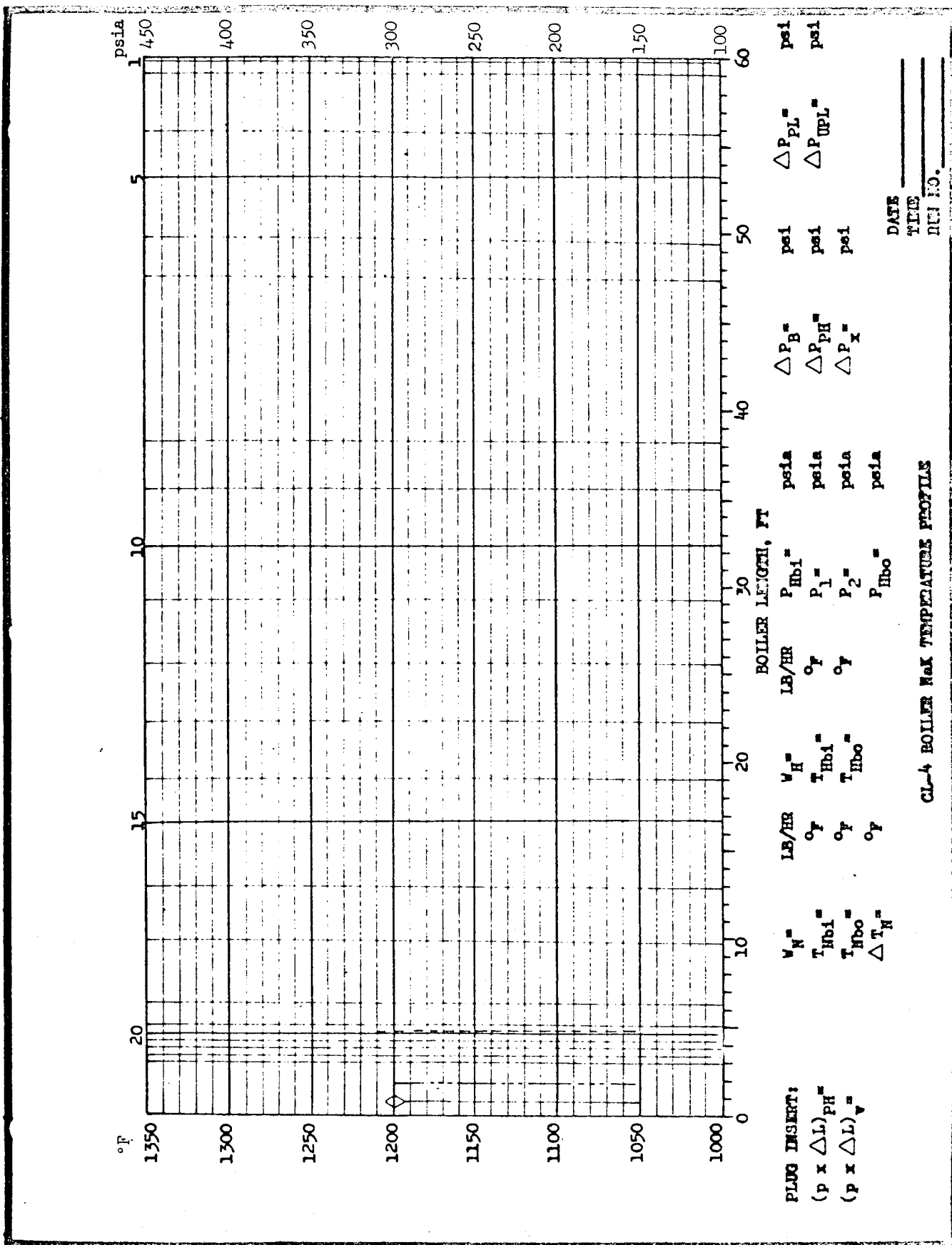


Fig. B-1

BOILER TEST DATA REDUCTION - Second Input Set

	PREHEAT SECT.	VAPOR QUALITY SECTIONS										FLUE INS. QUAL. SECT.	UPL. TUBE QUAL. SECT.
		0	∞	x ₁	x ₂	x ₃	x ₄	x ₅	x ₆				
T _N	0										x _{PL-EX}		
x			∞								T _{N2}		
L	.5										x _{PL}		
P	PHBI										P ₂		
Δx			x ₁	x ₂ - x ₁ $\frac{x_1 + x_2}{2}$	x ₃ - x ₂ $\frac{x_2 + x_3}{2}$	x ₄ - x ₃ $\frac{x_3 + x_4}{2}$	x ₅ - x ₄ $\frac{x_4 + x_5}{2}$	x ₆ - x ₅ $\frac{x_5 + x_6}{2}$			x _{PL}	x ₁₀₀ - x _{PL}	
\bar{x}	PREHEAT SECT.		$\frac{x_1}{2}$								x _{PL} /2	$\frac{x_{100} + x_{PL}}{2}$	
D _o	DEFI												
G ₁	GPIL												
G ₂													
cos α	COSAL												
E _x													
C _x													
R _x													
Z _x													
ΔL	L ₀₀ - .5		L _{x1} - L ₀₀	L _{x2} - L _{x1} $\frac{P_{x1} - P_{x2}}{2}$	L _{x3} - L _{x2} $\frac{P_{x2} - P_{x3}}{2}$	L _{x4} - L _{x3} $\frac{P_{x3} - P_{x4}}{2}$	L _{x5} - L _{x4} $\frac{P_{x4} - P_{x5}}{2}$	L _{x6} - L _{x5} $\frac{P_{x5} - P_{x6}}{2}$			L _{xPL} - L ₀₀	L ₁₀₀ - L _{xPL}	
ΔP	P _{Hbi} - P ₀₀		P ₀₀ - P _{x1} $\frac{P_{00} + P_{x1}}{2}$	P _{x1} - P _{x2} $\frac{P_{x1} + P_{x2}}{2}$	P _{x2} - P _{x3} $\frac{P_{x2} + P_{x3}}{2}$	P _{x3} - P _{x4} $\frac{P_{x3} + P_{x4}}{2}$	P _{x4} - P _{x5} $\frac{P_{x4} + P_{x5}}{2}$	P _{x5} - P _{x6} $\frac{P_{x5} + P_{x6}}{2}$			P ₀₀ - P ₂ $\frac{P_{00} + P_2}{2}$	P ₂ - P ₁₀₀ $\frac{P_2 + P_{100}}{2}$	
P _M												$\frac{T_{N00} + T_{N2}}{2}$	
T _{NHx}												$\frac{T_{N2} + T_{100}}{2}$	

2nd Input Set #

To be used with 1st Input #

Final Output Notation

APPENDIX C

NaK TEMPERATURE PROFILES AND ASSOCIATED TEST DATA

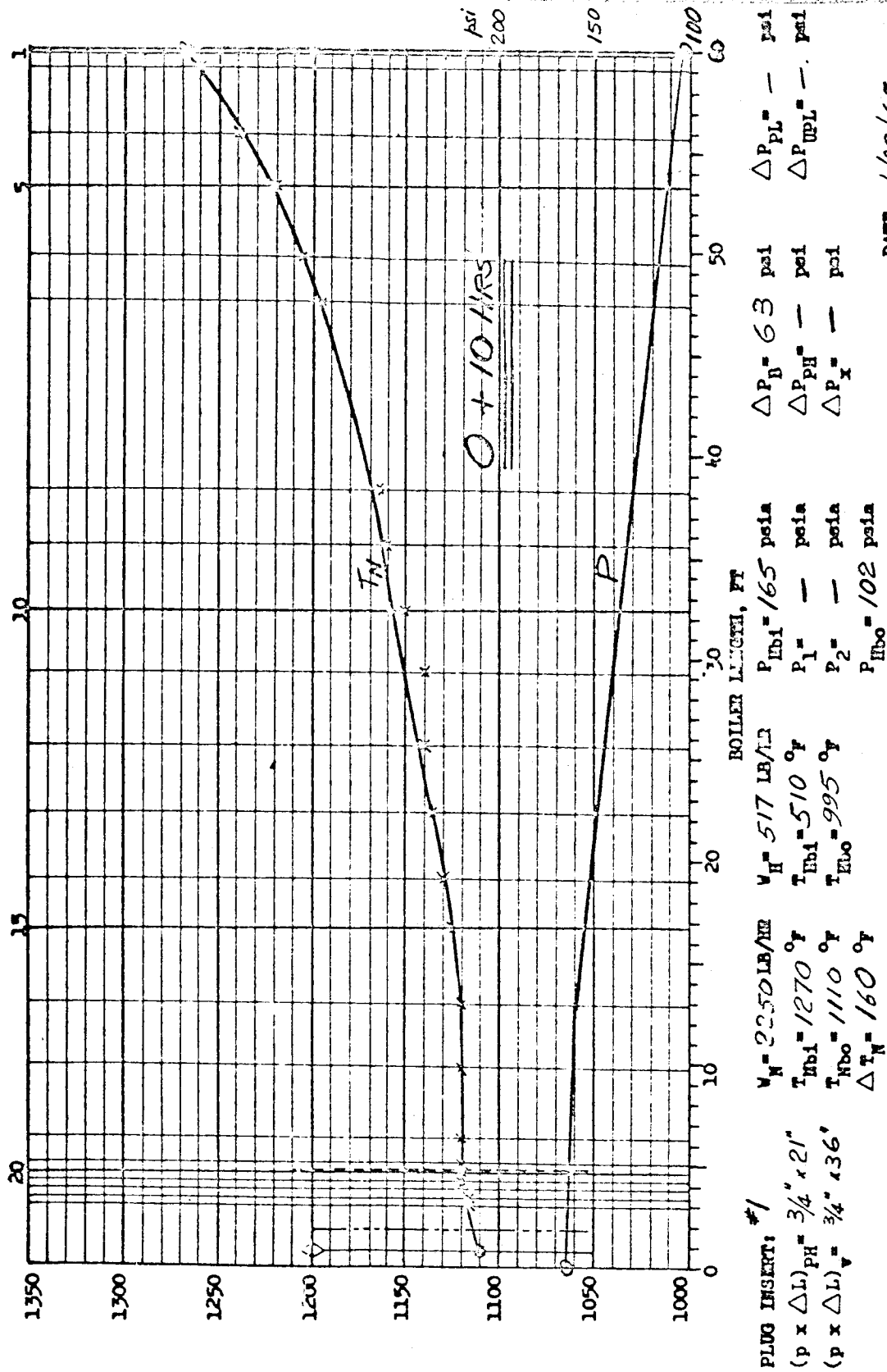


Fig. C-1

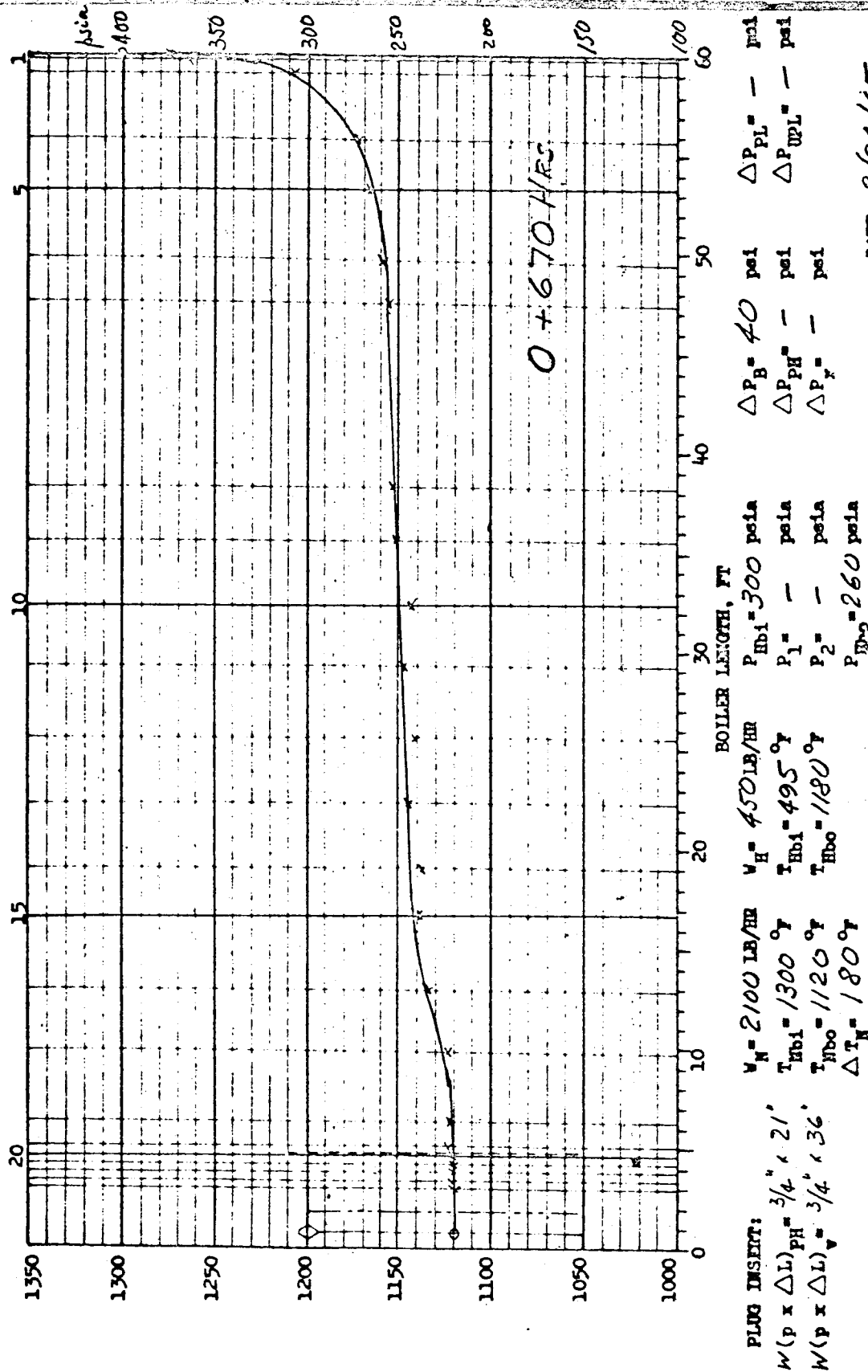


Fig. C-2

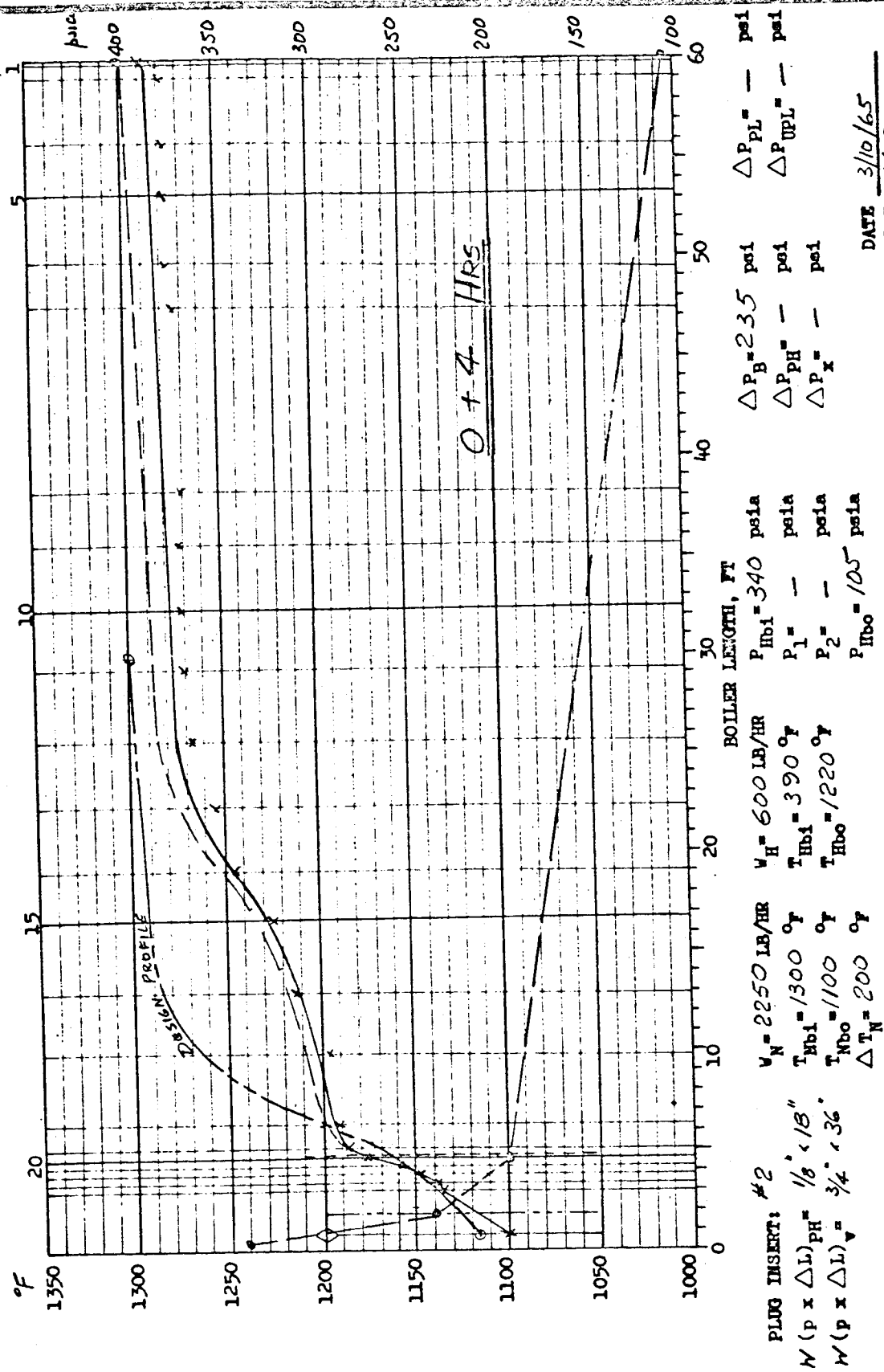


Fig. C-3

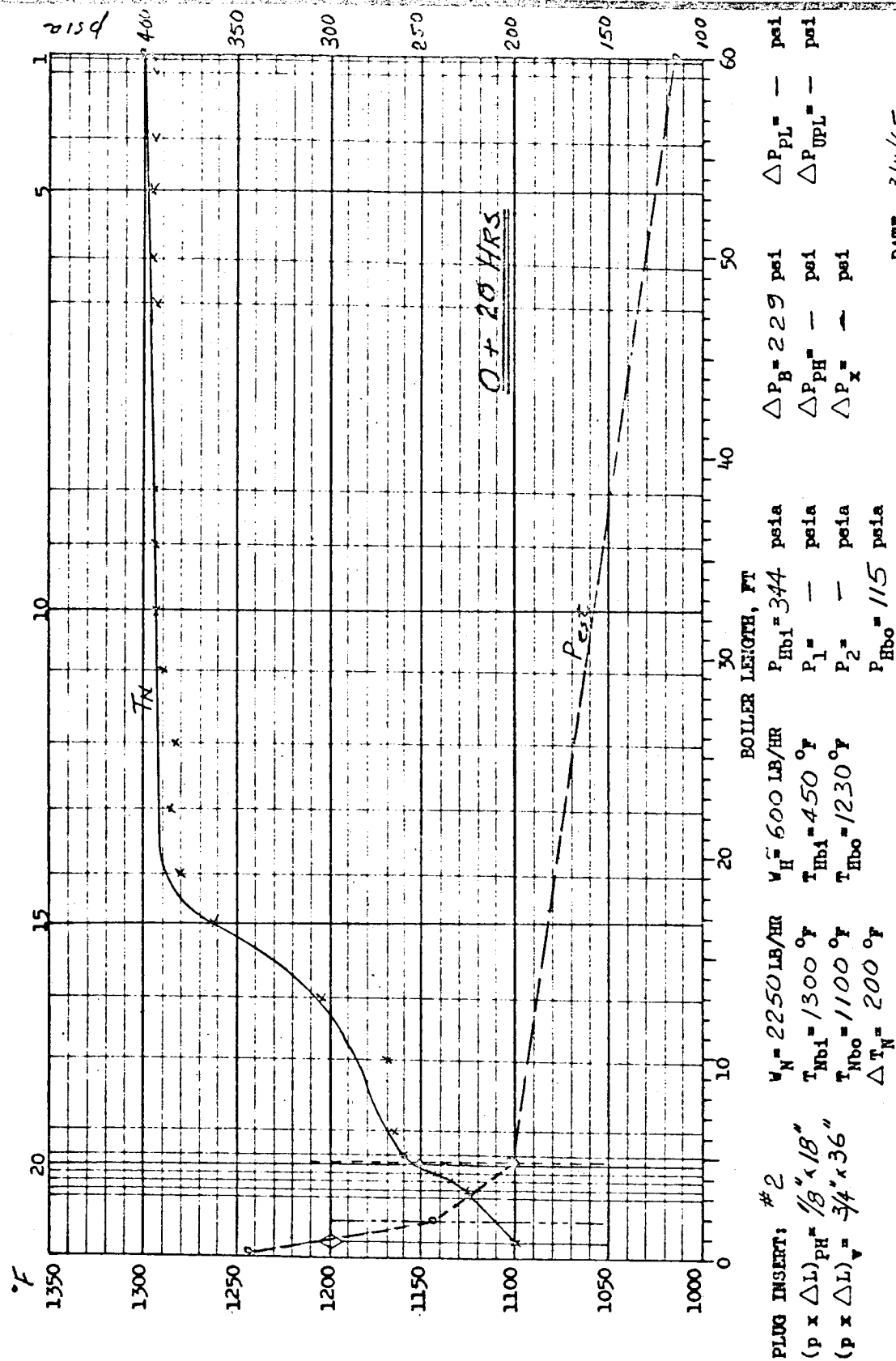


Fig. C-4

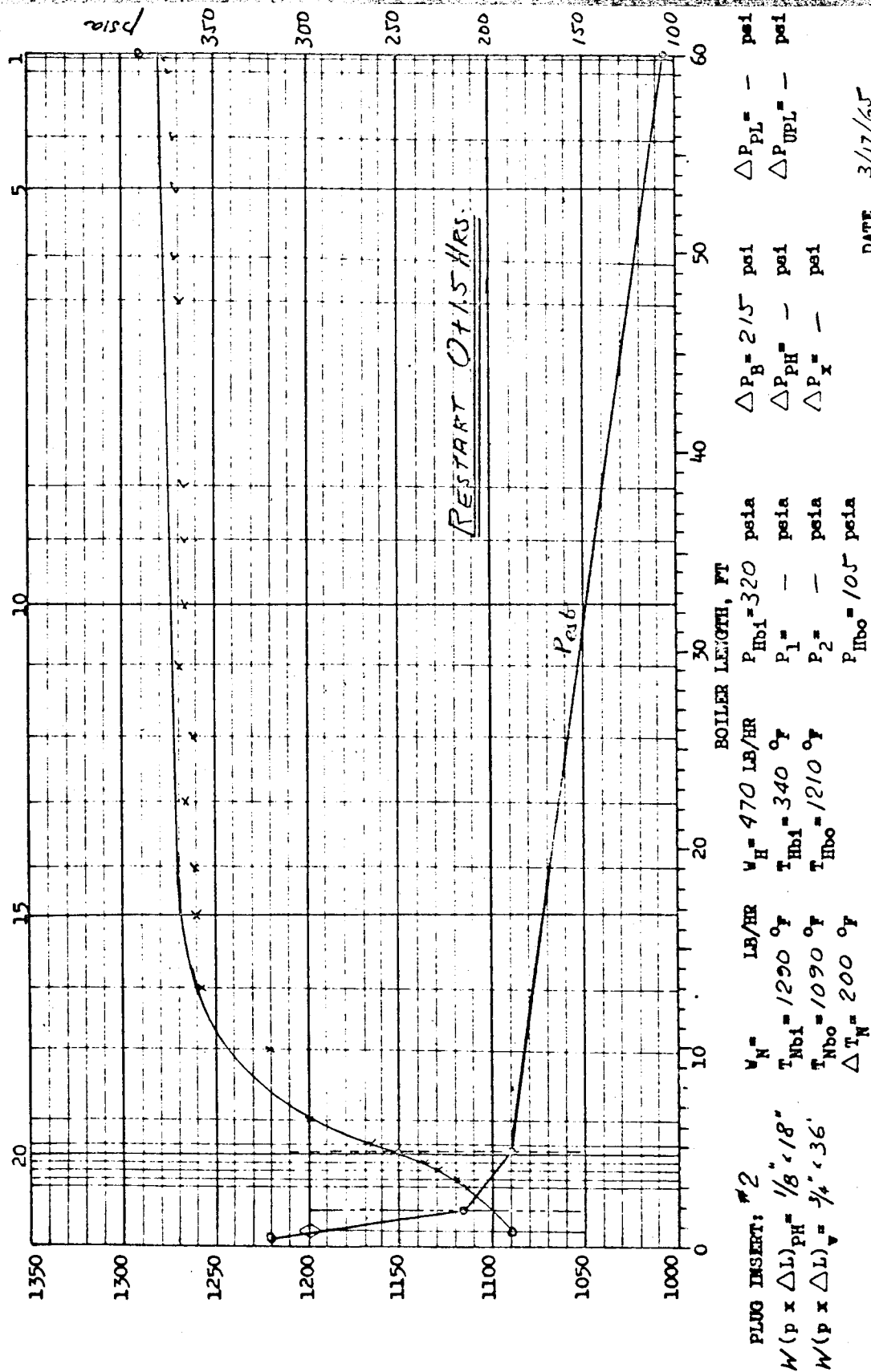
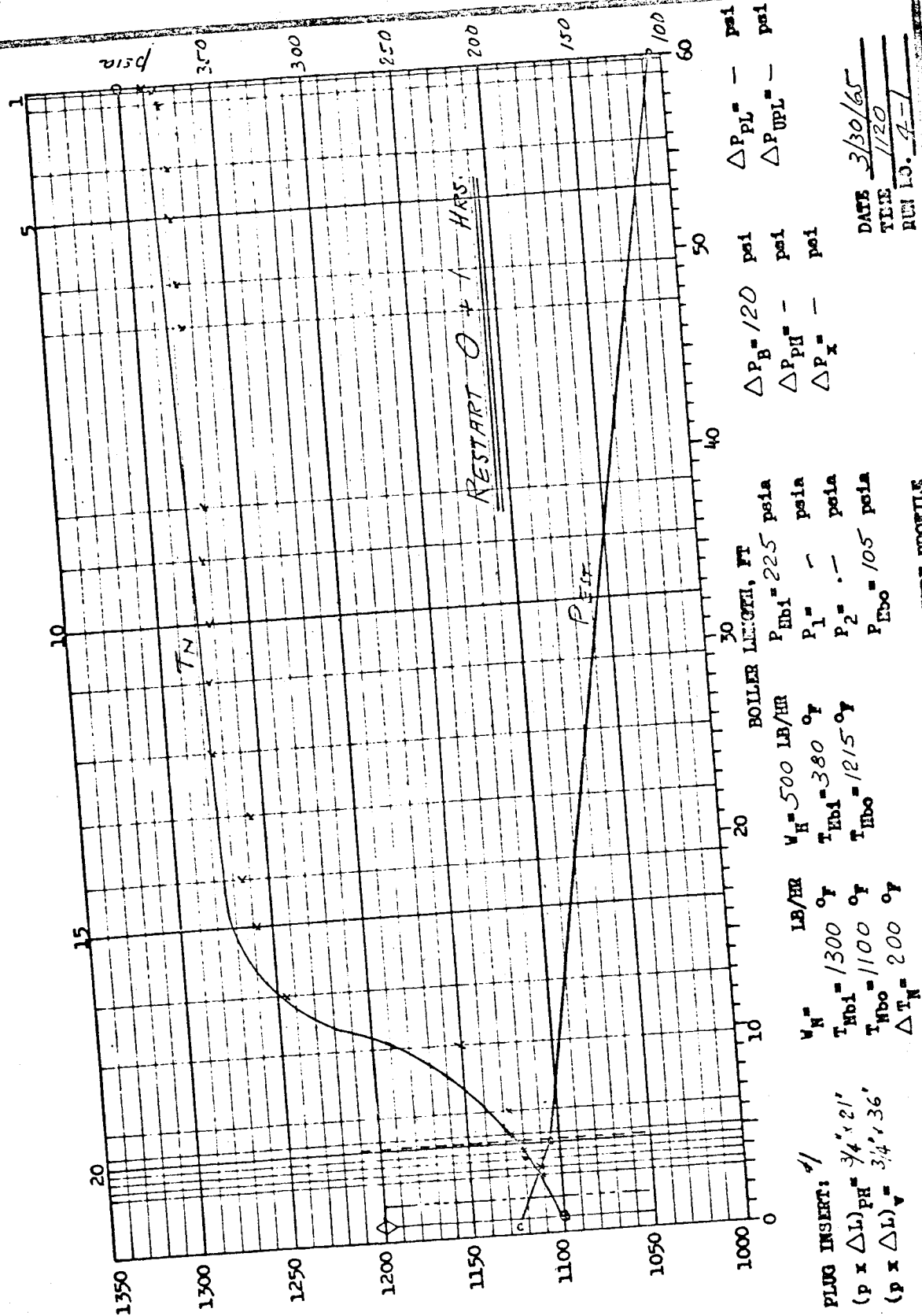
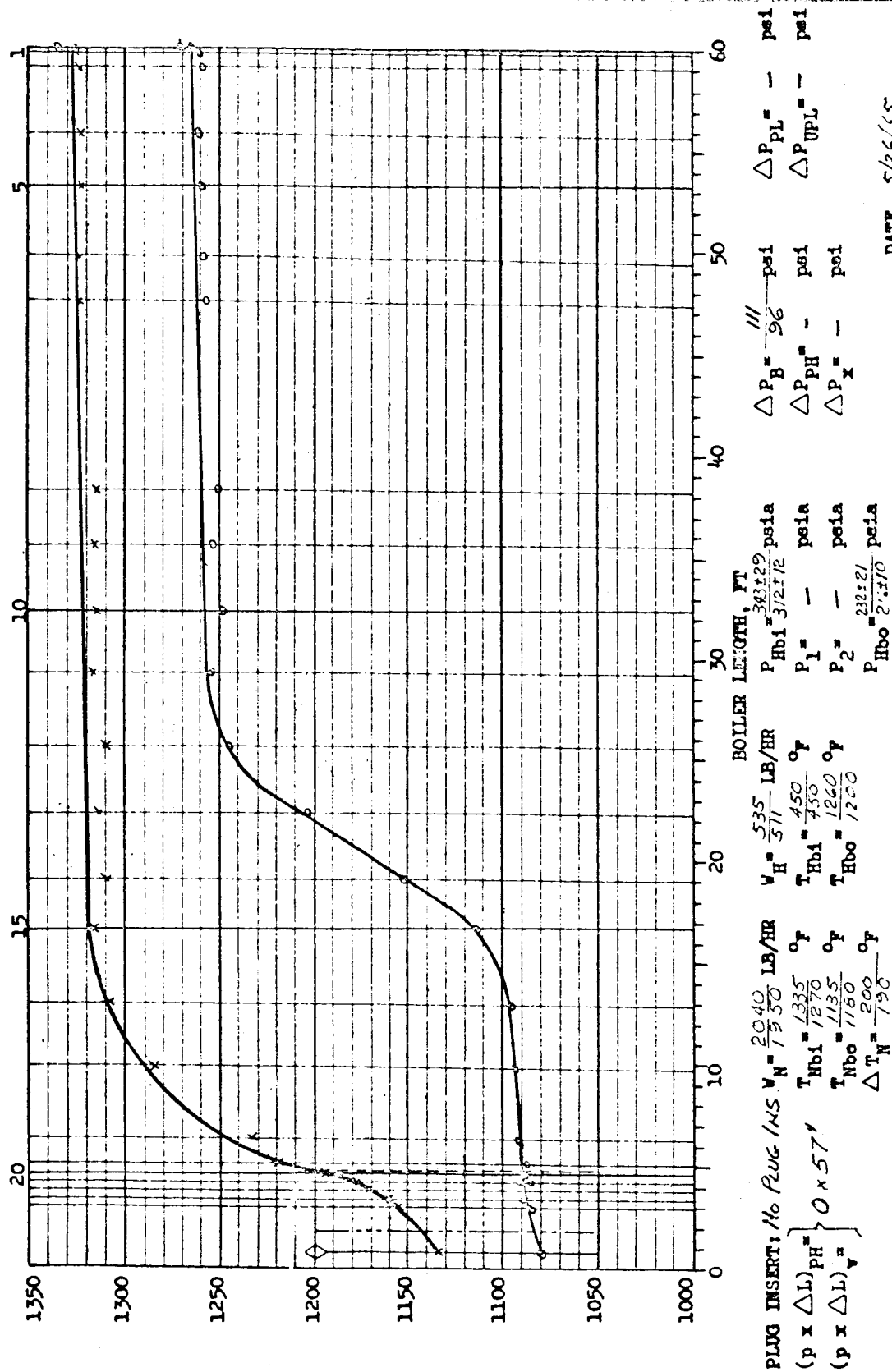


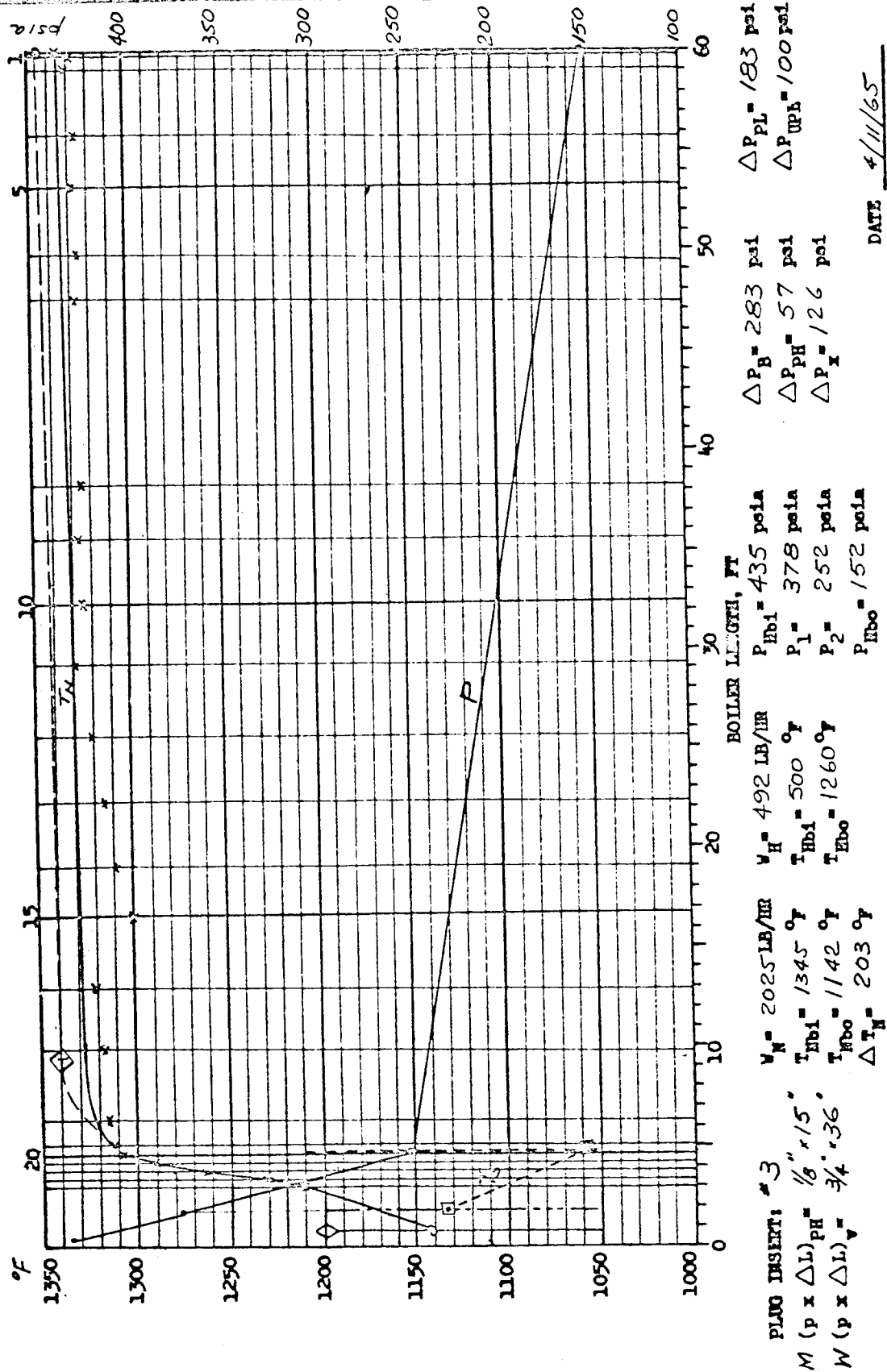
Fig. C-5



CL-4 BOILER MAX TEMPERATURE PROFILE



CL-4 BOILER MAX TEMPERATURE PROFILE



DATE 4/11/65
 TIME 1820
 RUN NO. 5-16

Fig. C-8

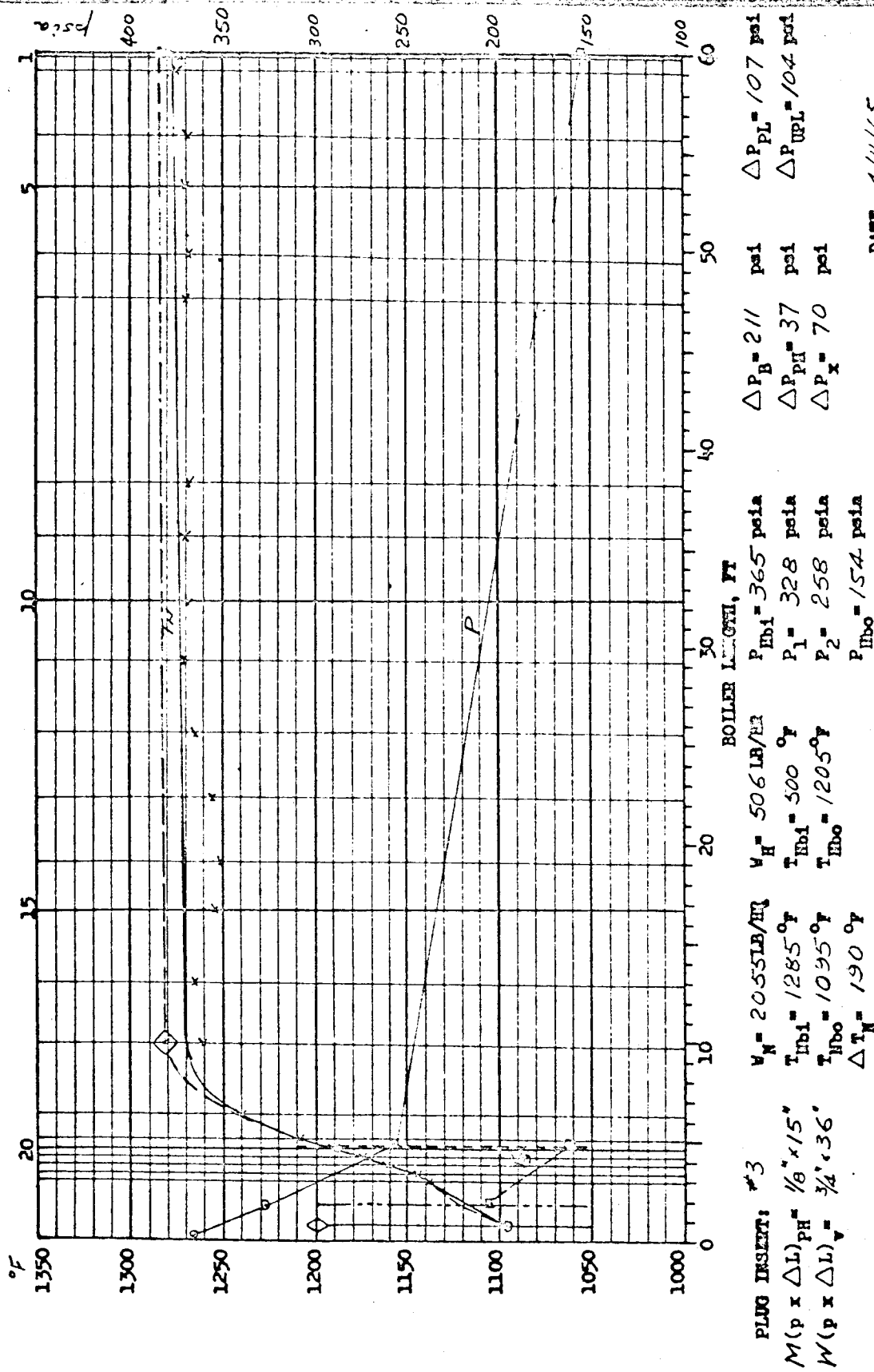


Fig. C-9

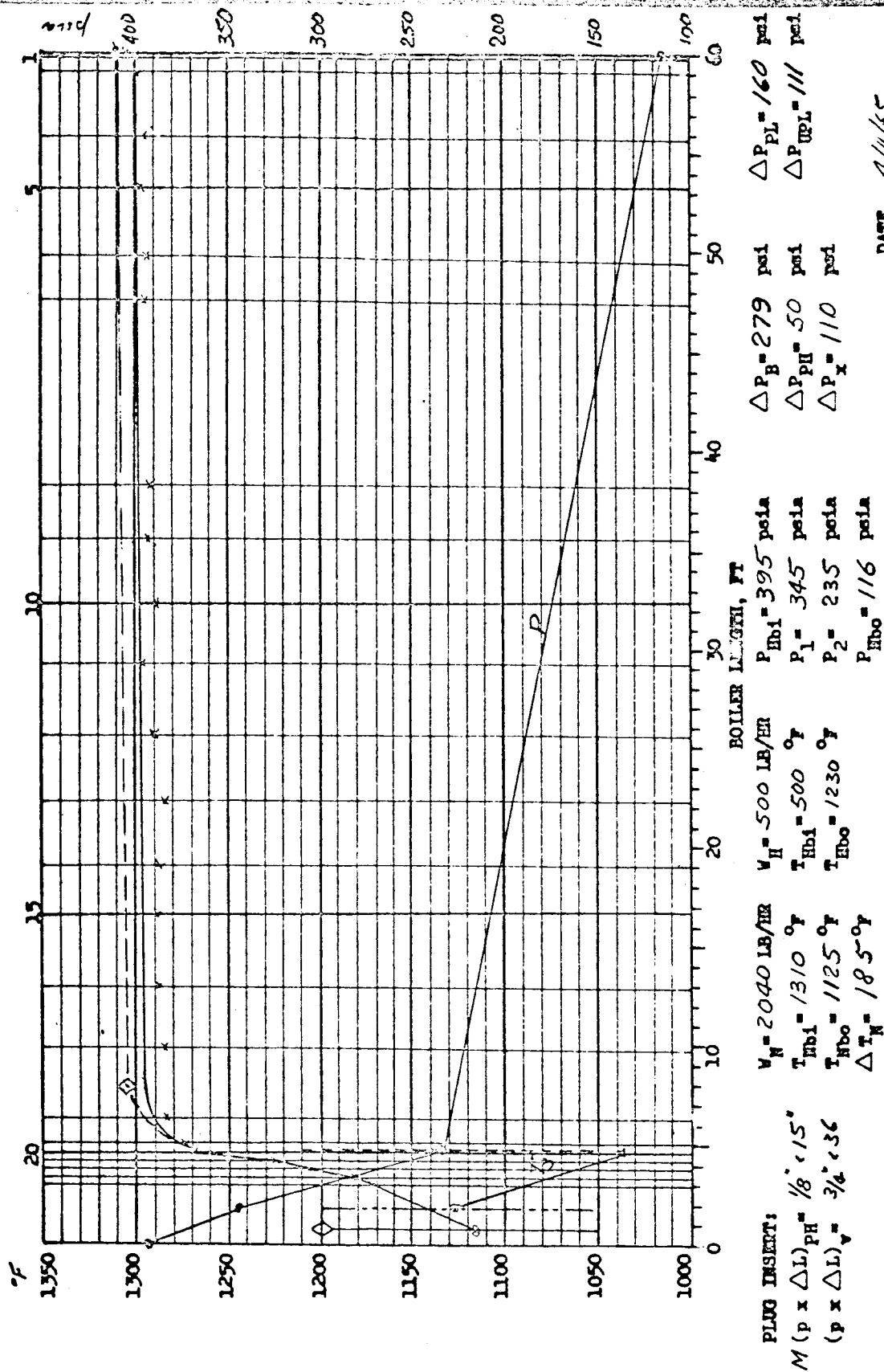
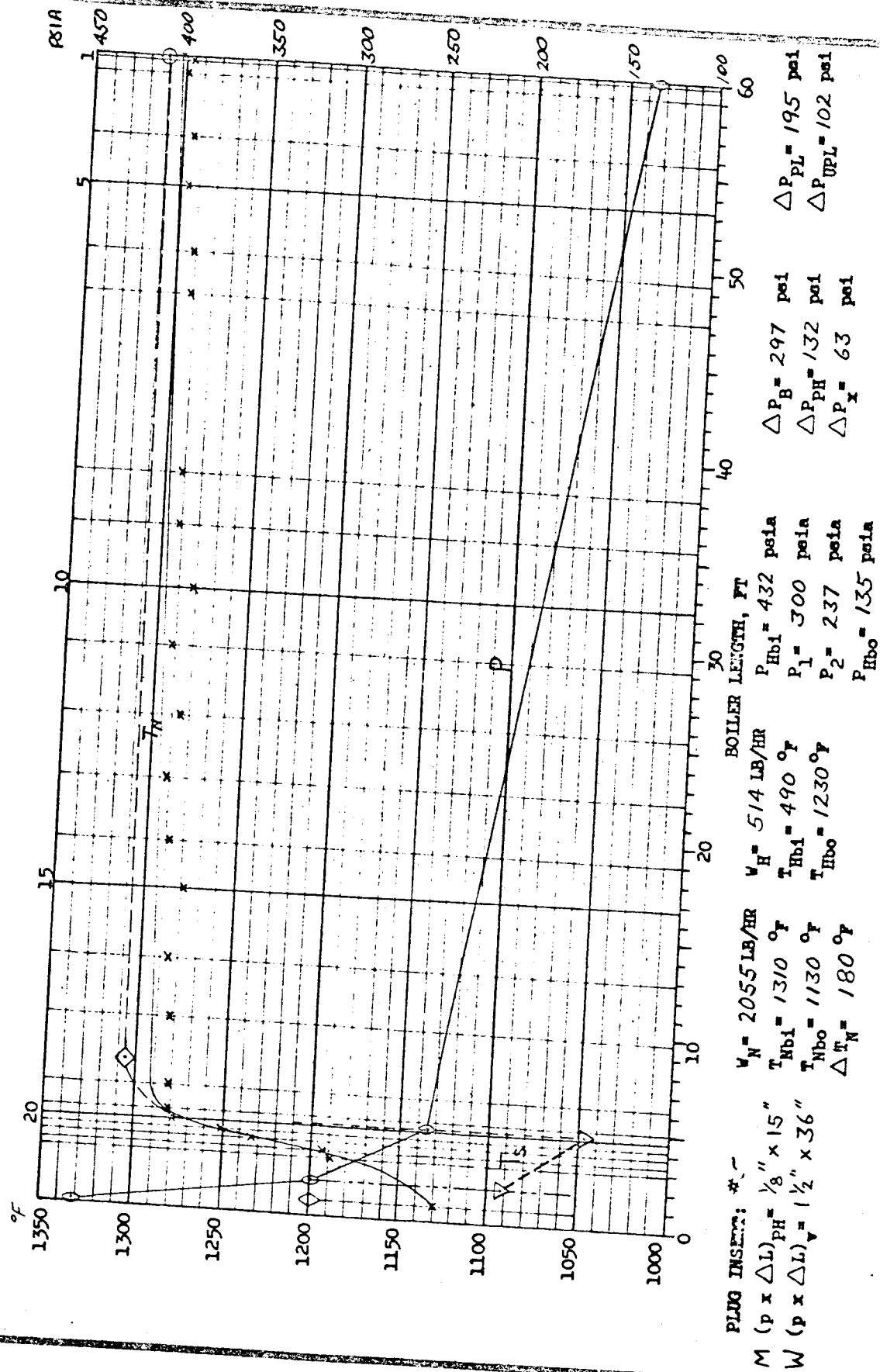


Fig. C-10



DATE 5-6-65
 TIME 1558
 RUN NO. 7-1

Fig. C-11

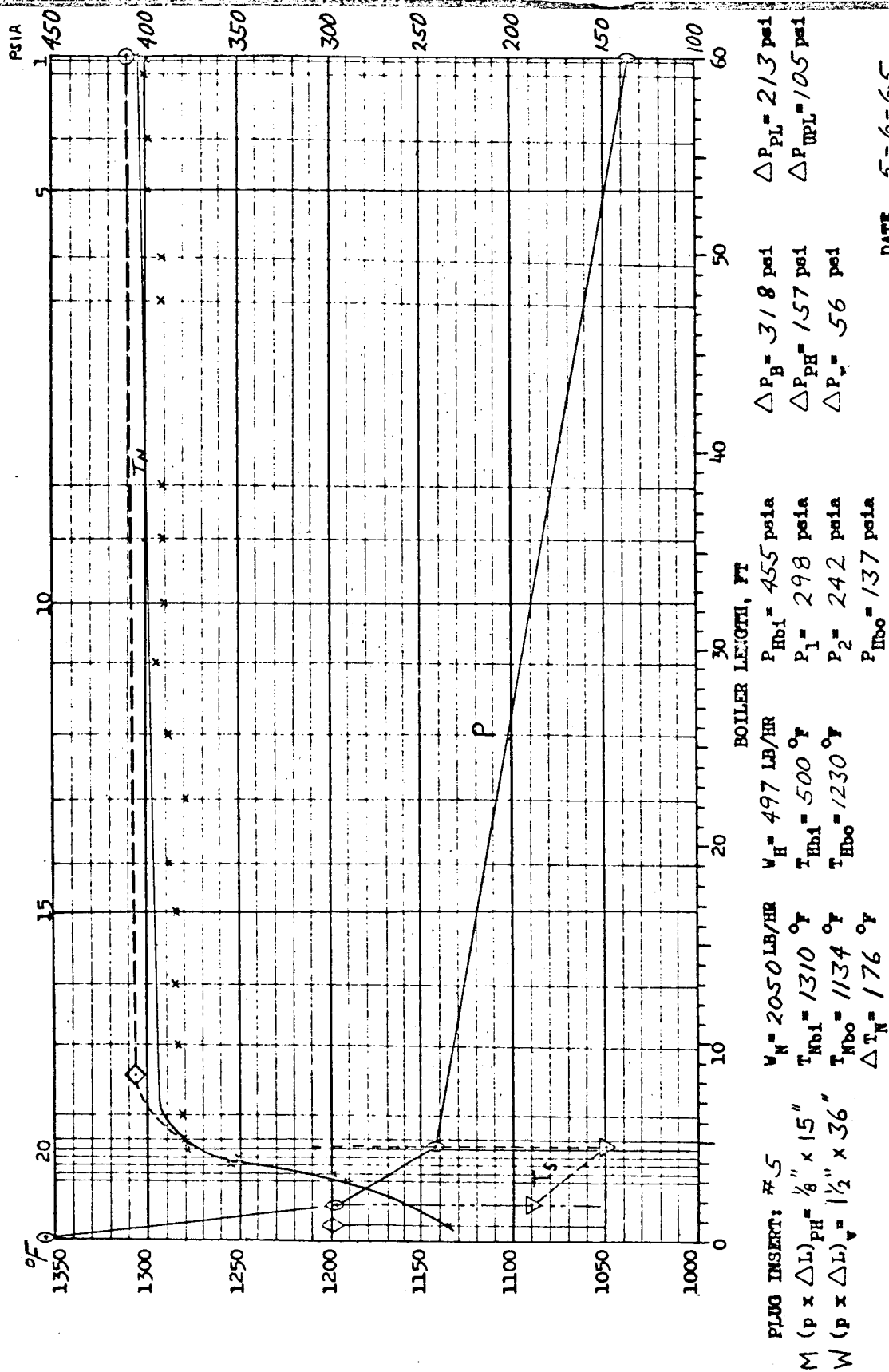


Fig. C-12

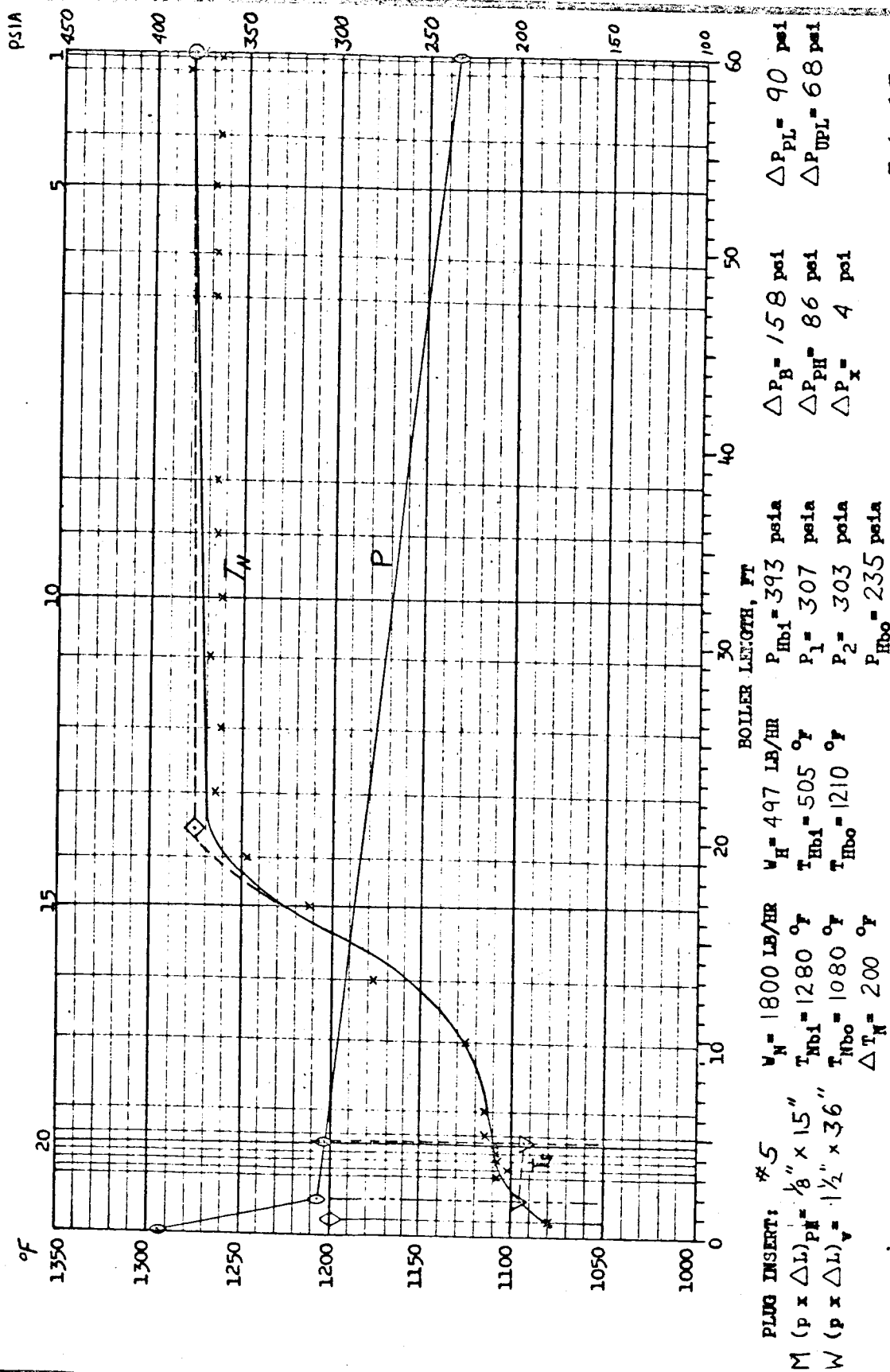
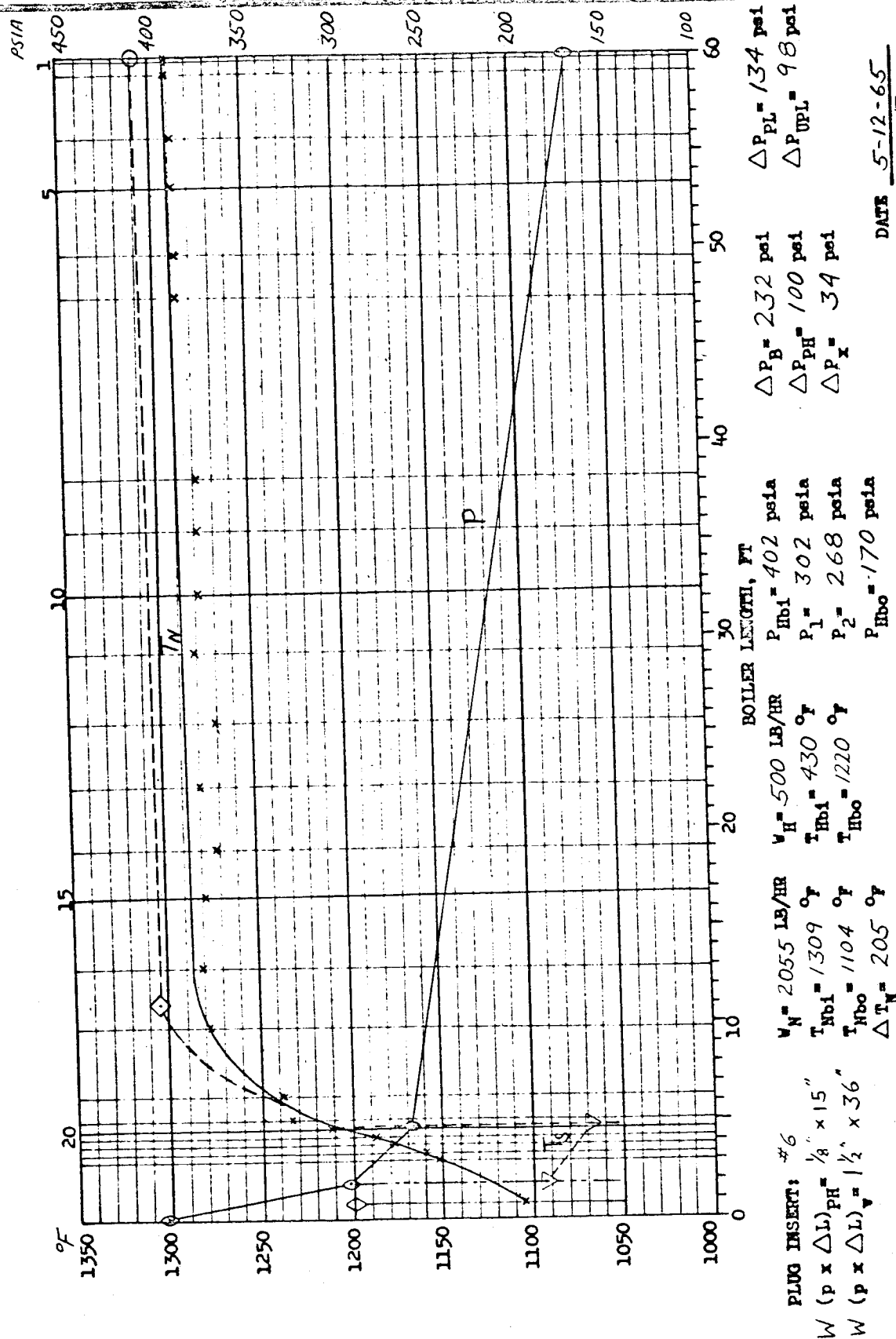


Fig. C-14



CL-4 BOILER MAX TEMPERATURE PROFILE

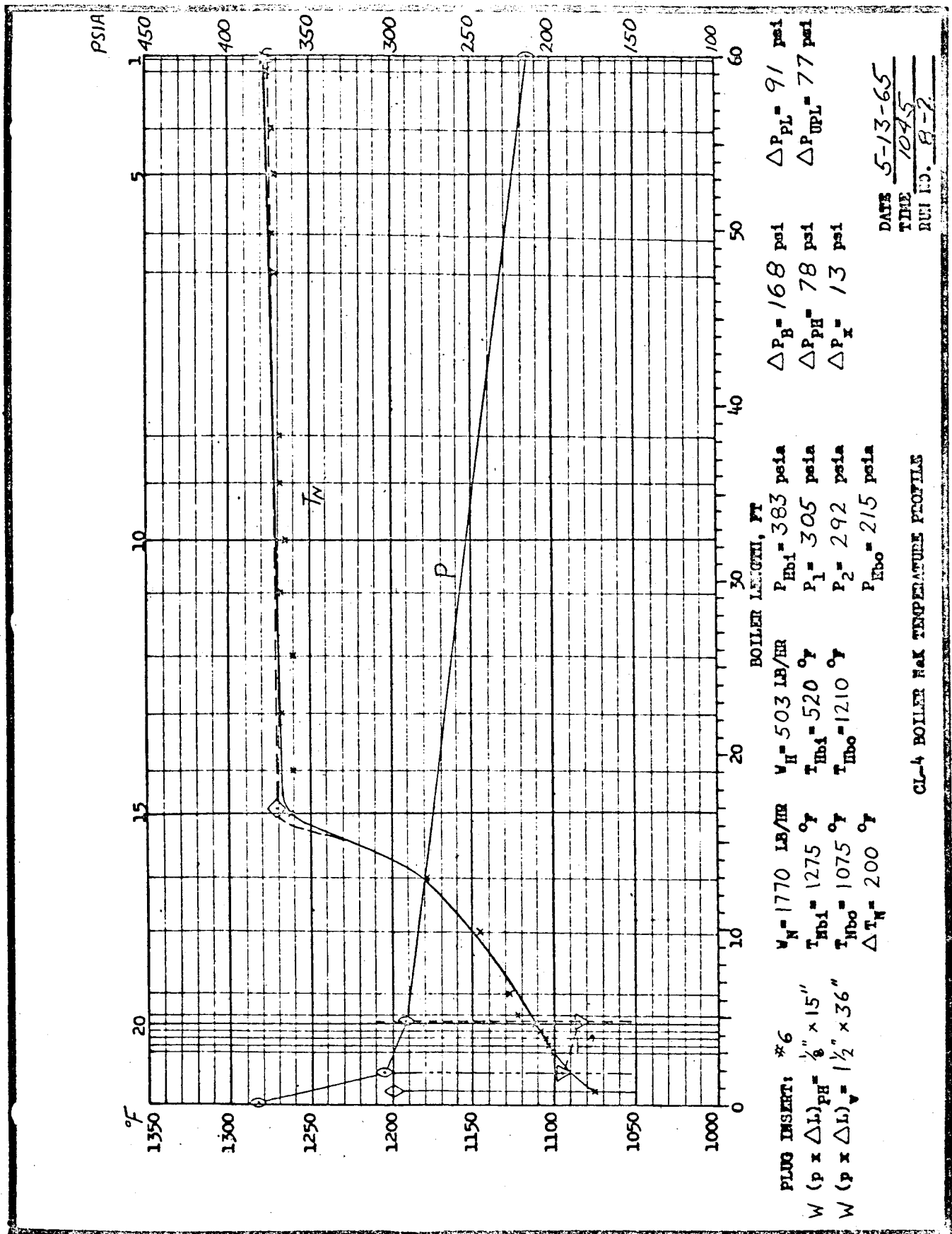


Fig. C-16

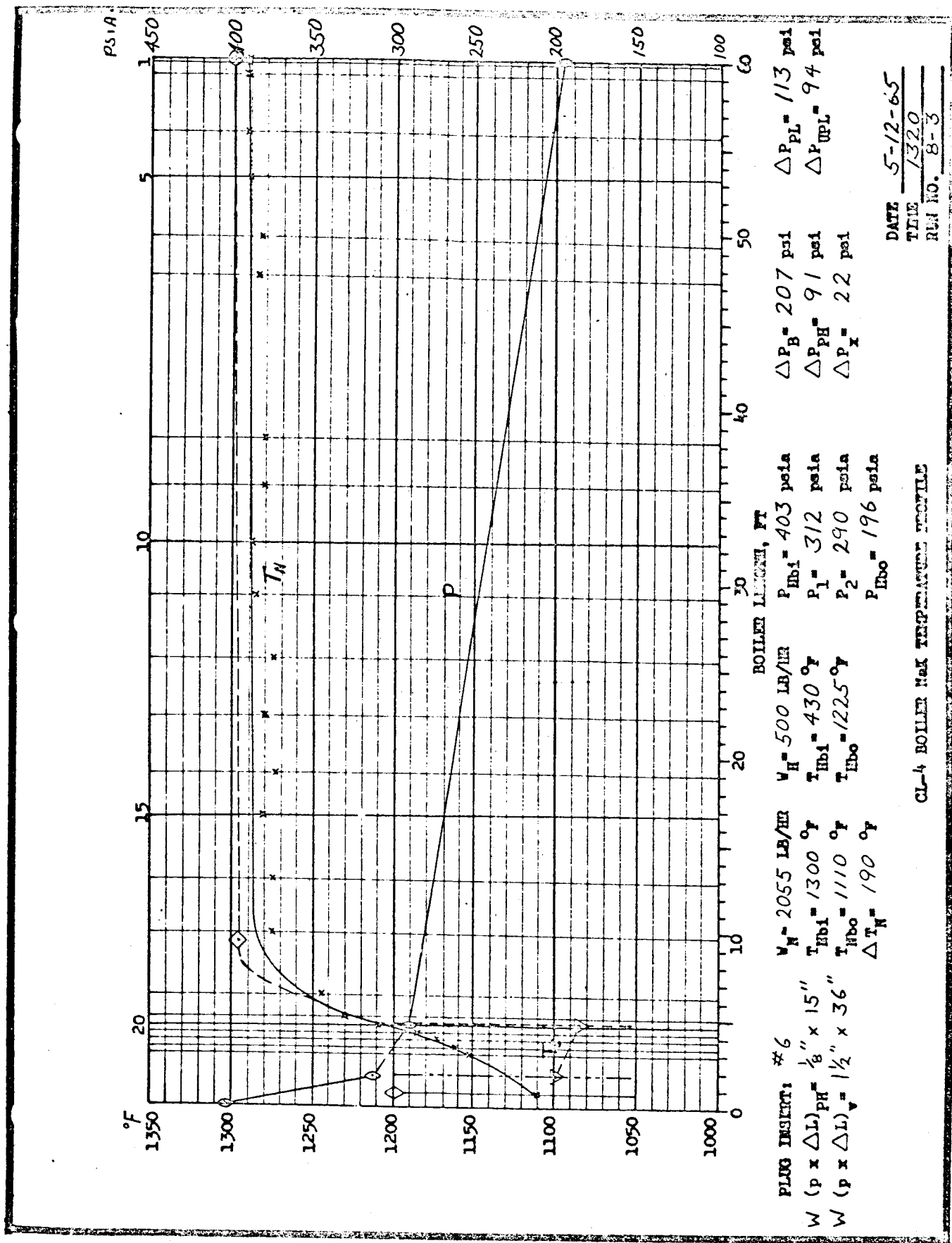


Fig. C-17

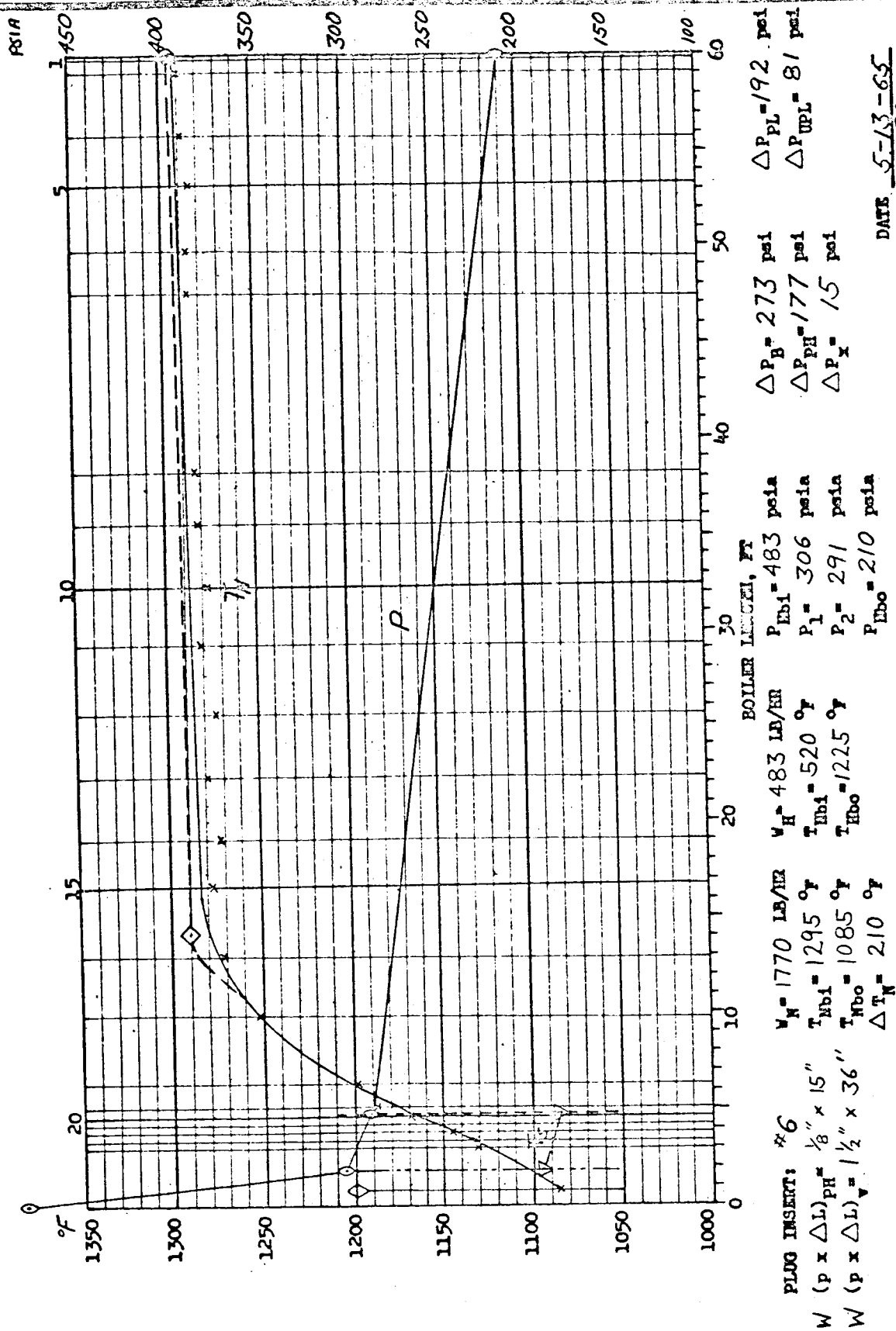
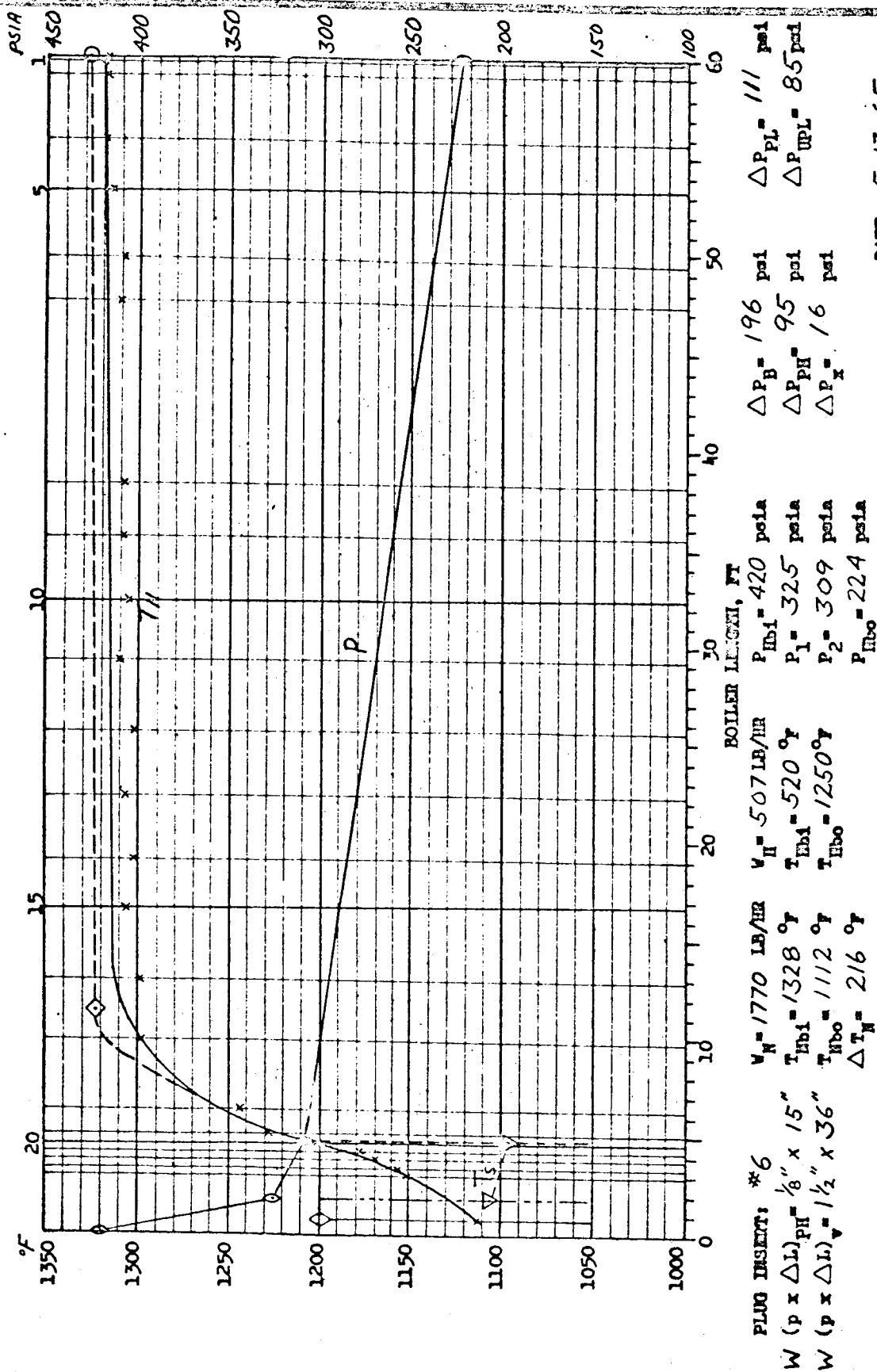


Fig. C-18



DATE 5-13-65
 TIME 1330
 RUN NO. 8-5

CL-4 BOILER MAX TEMPERATURE PROFILE

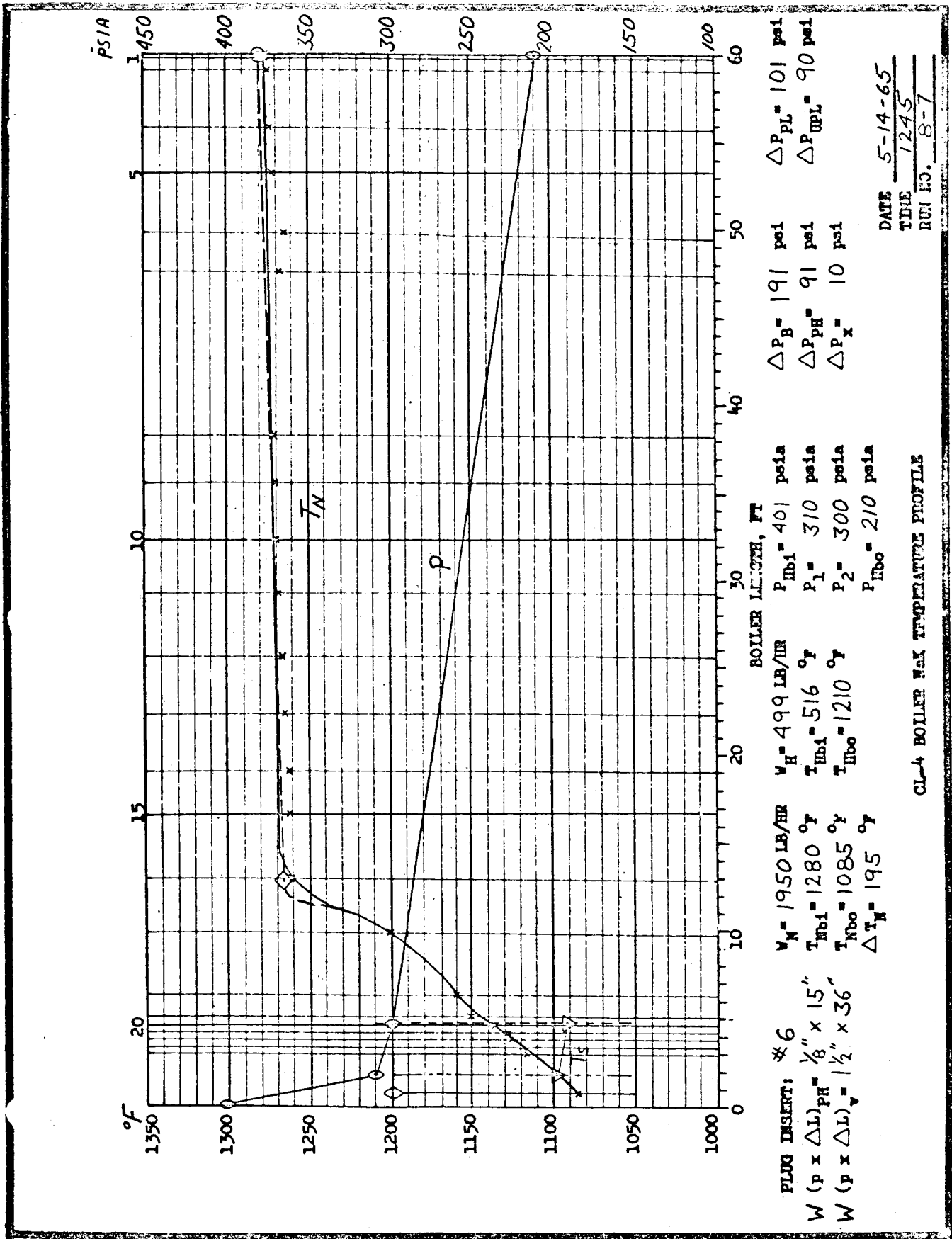


Fig. C-20

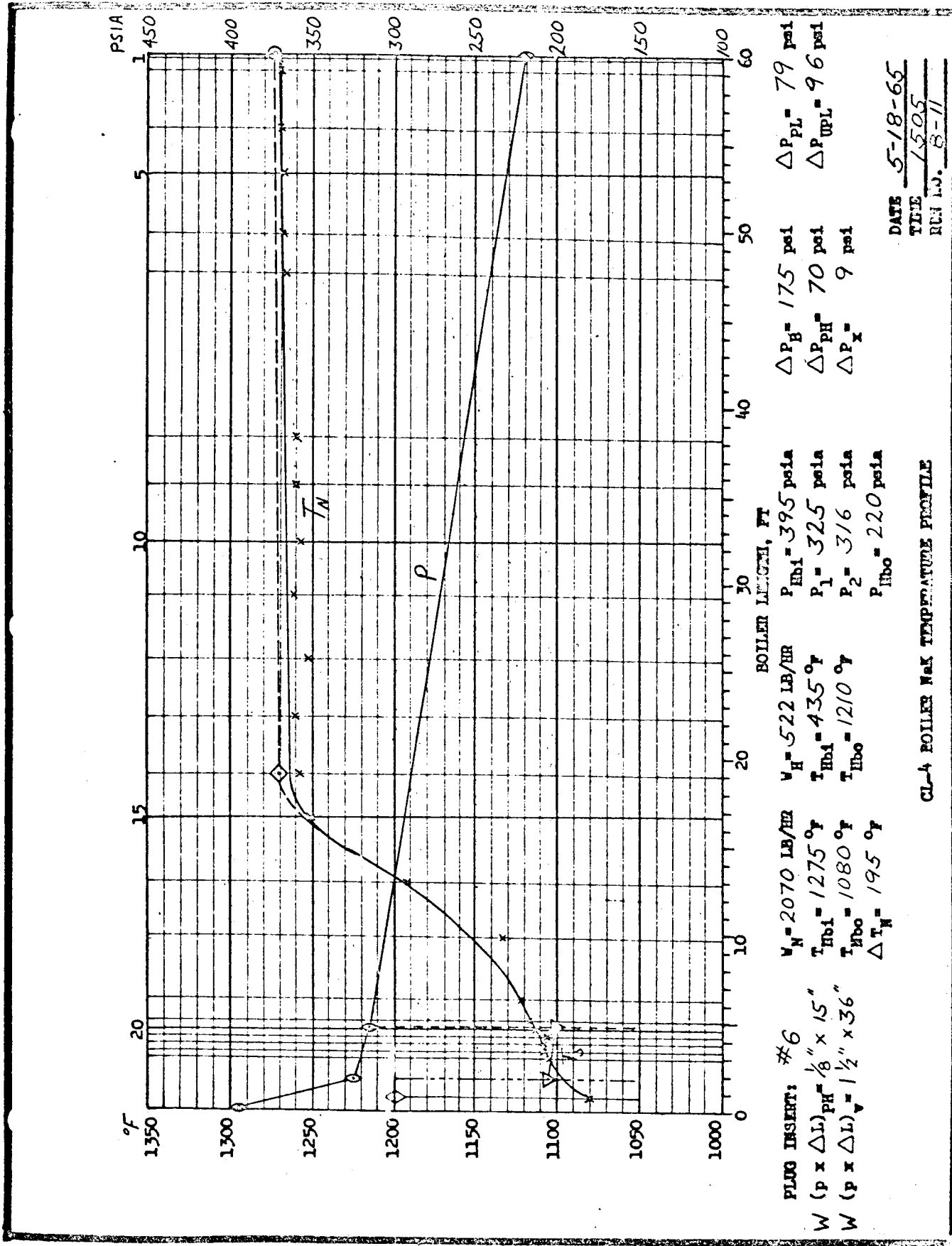


Fig. C-21

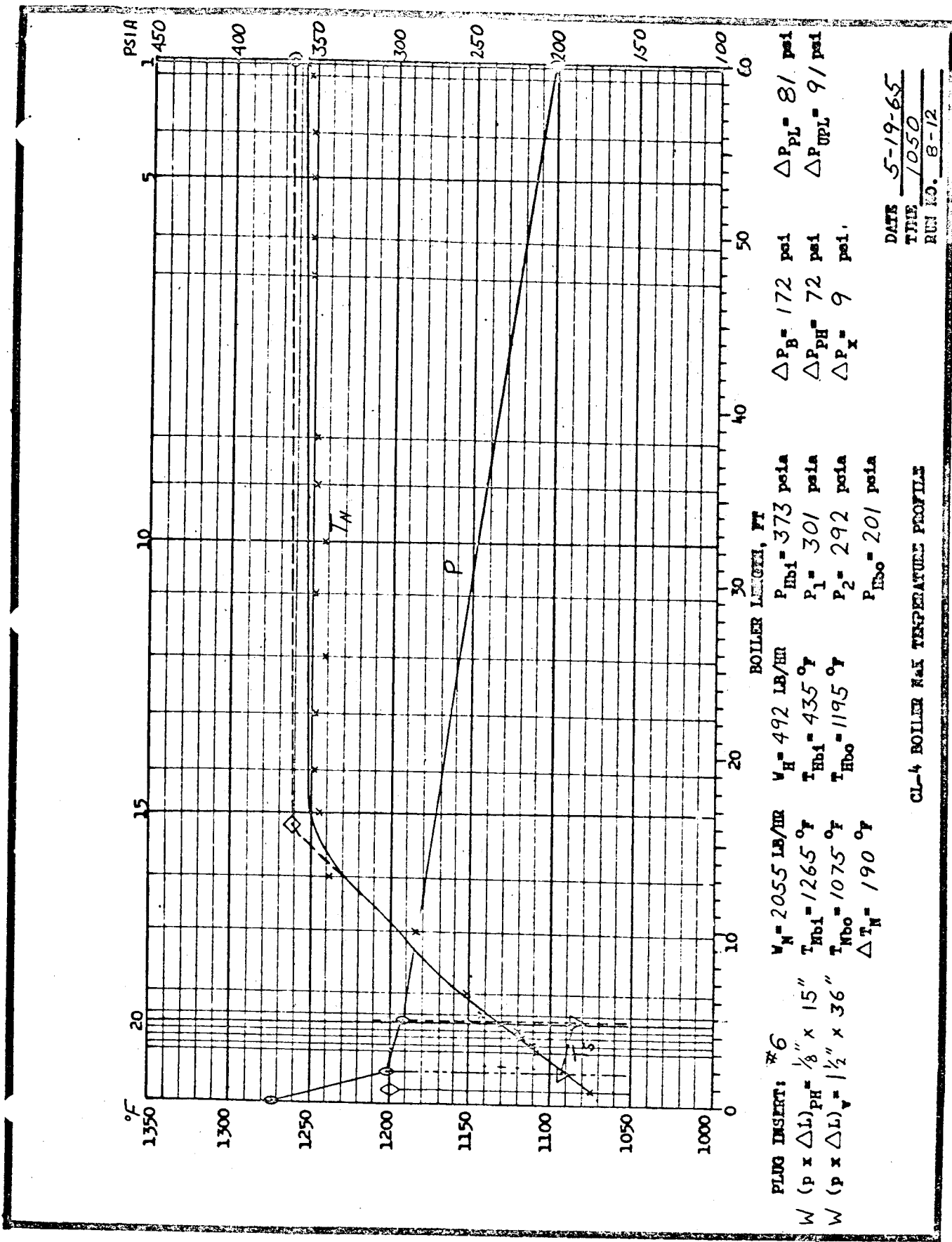


Fig. C-22

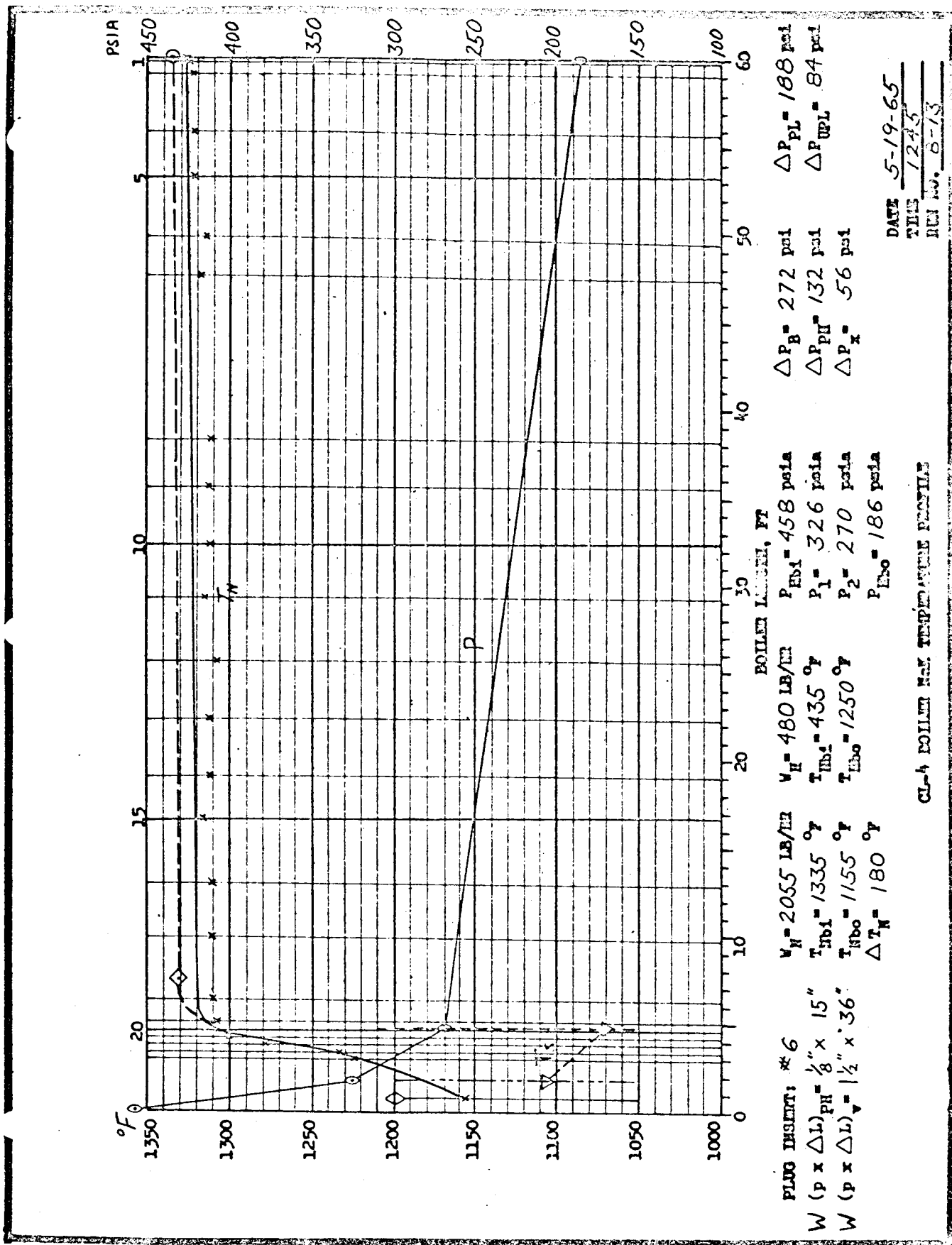


Fig. C-23

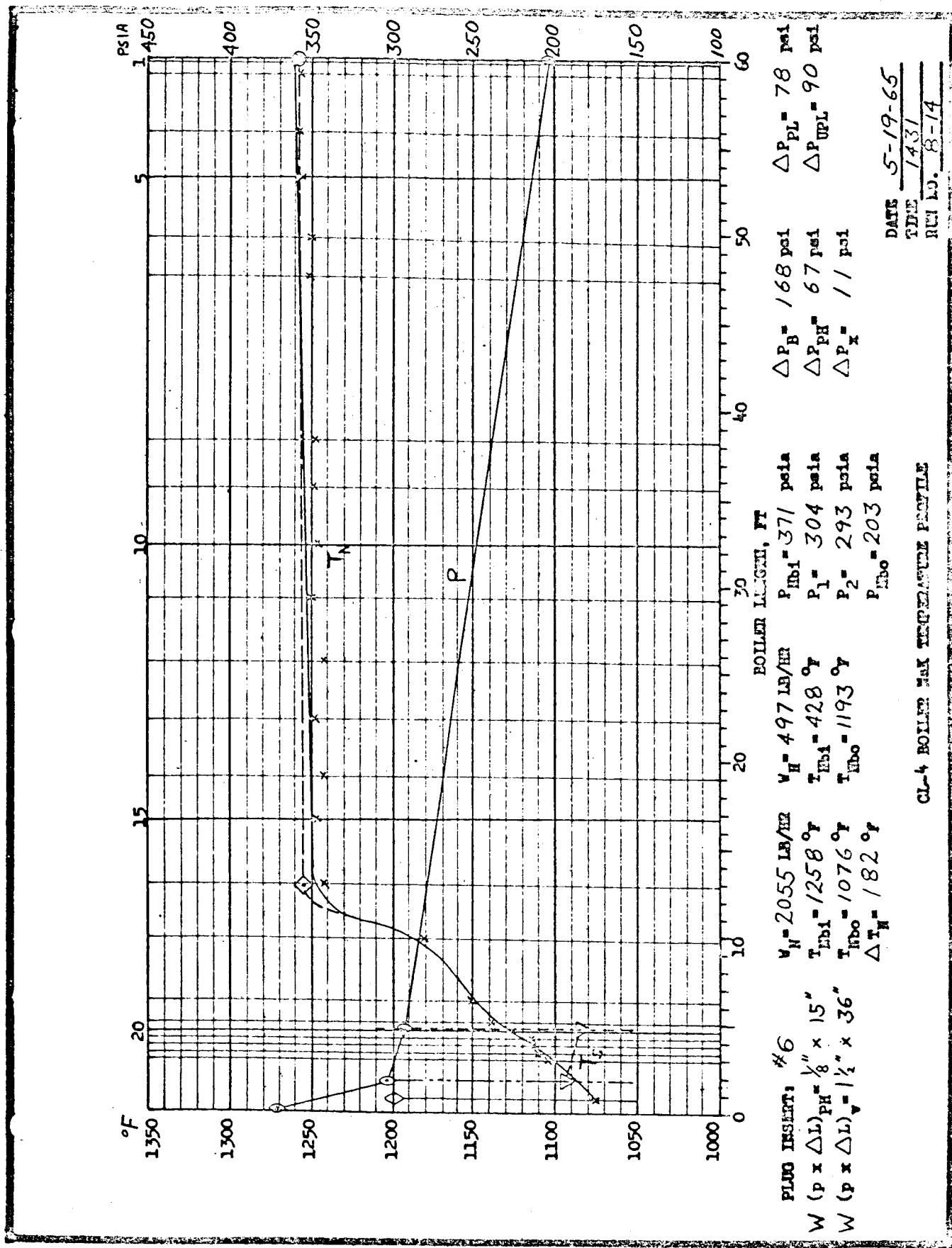
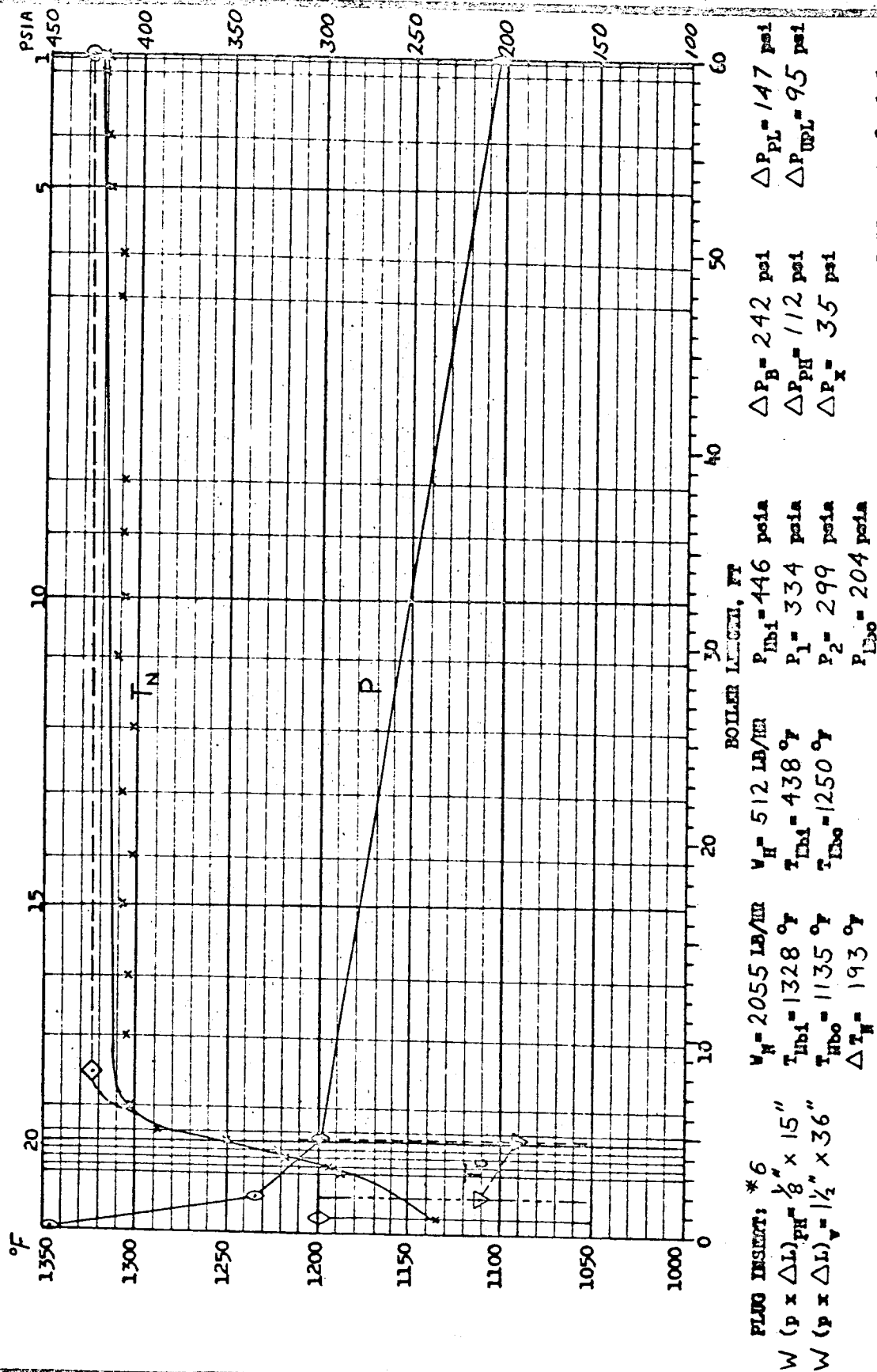


Fig. C-24



DATE 5-19-65
 TIME 1610
 RUN LO. 8-15

CL-4 BOILER MAX TEMPERATURE PROFILE

Fig. C-25

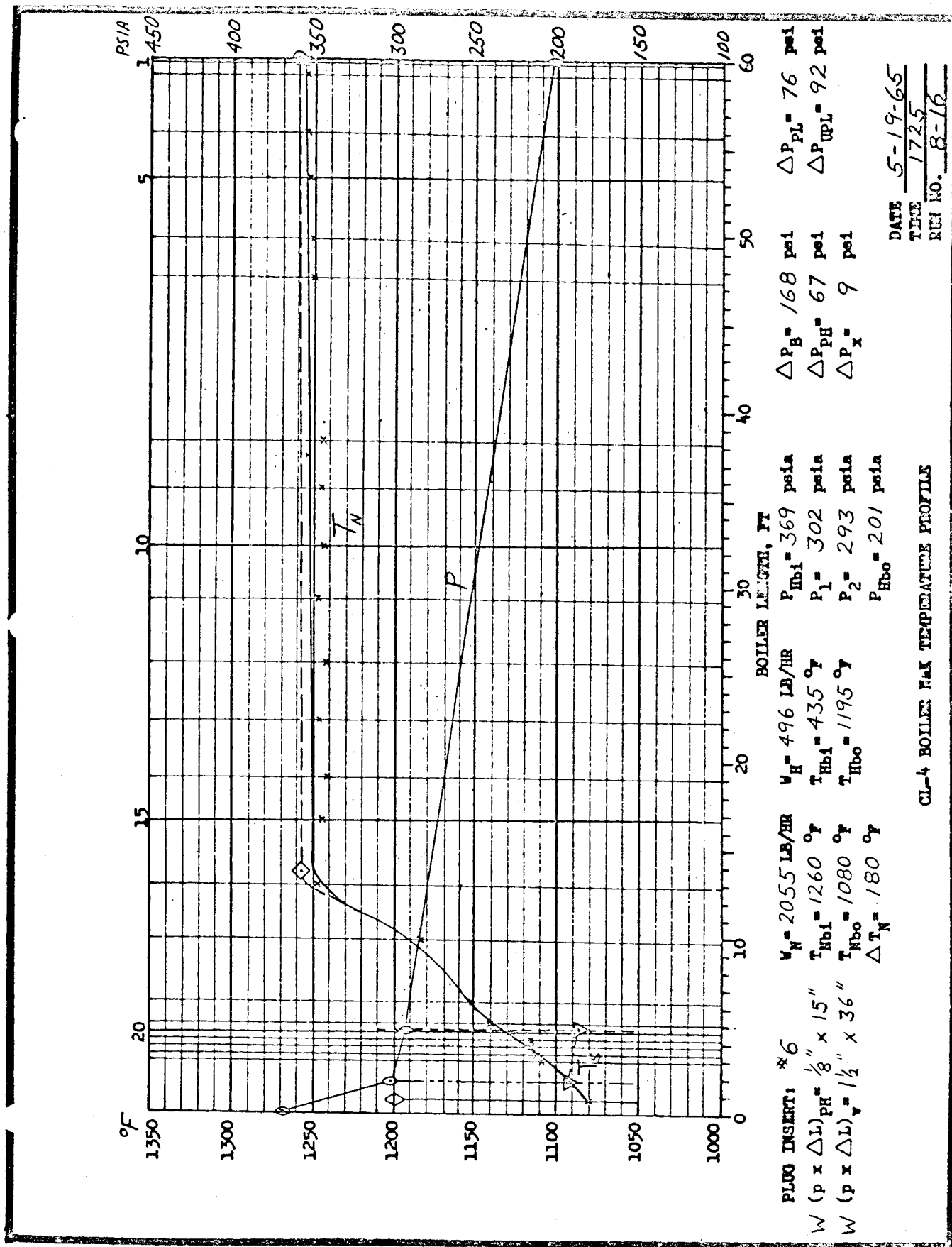


Fig. C-26

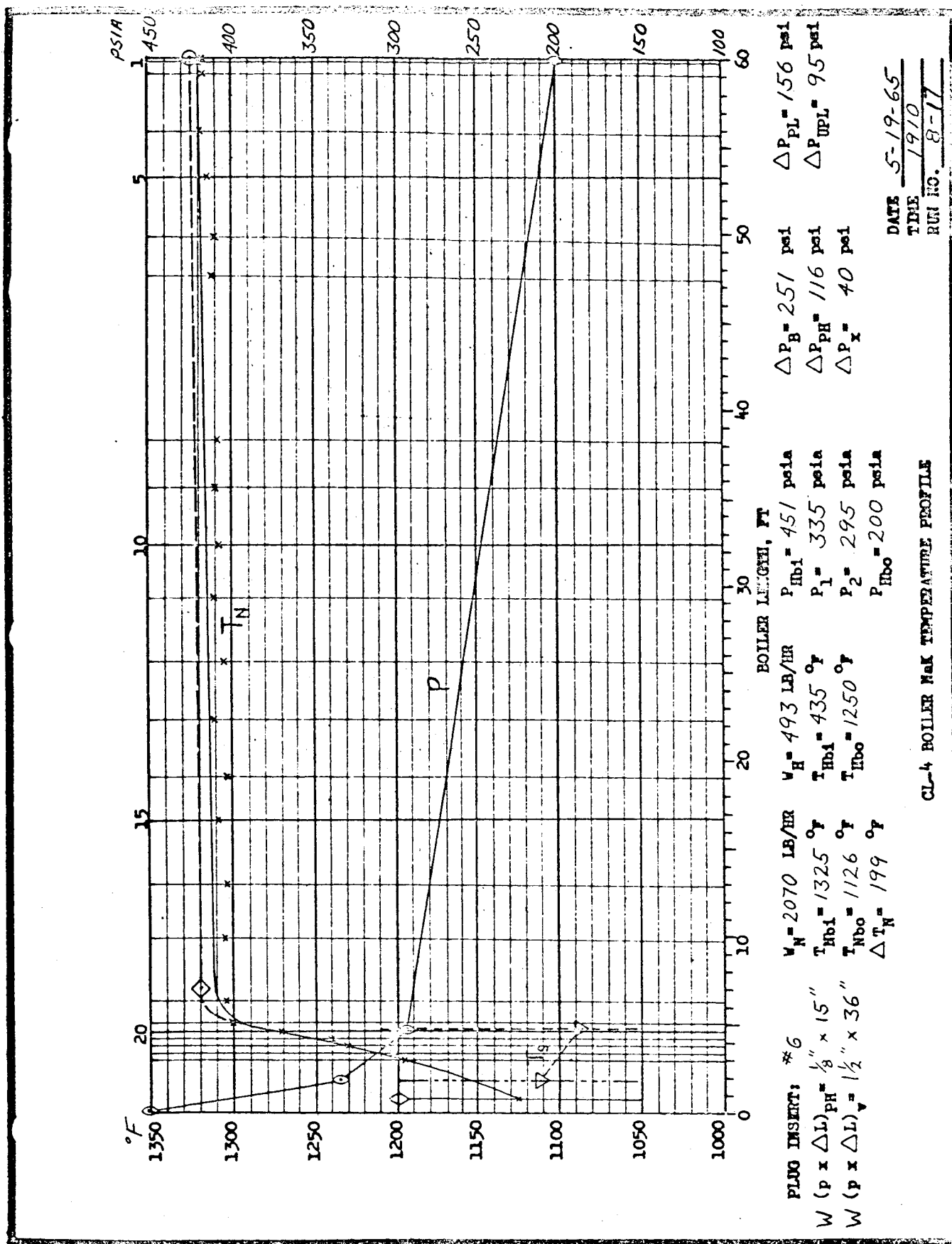
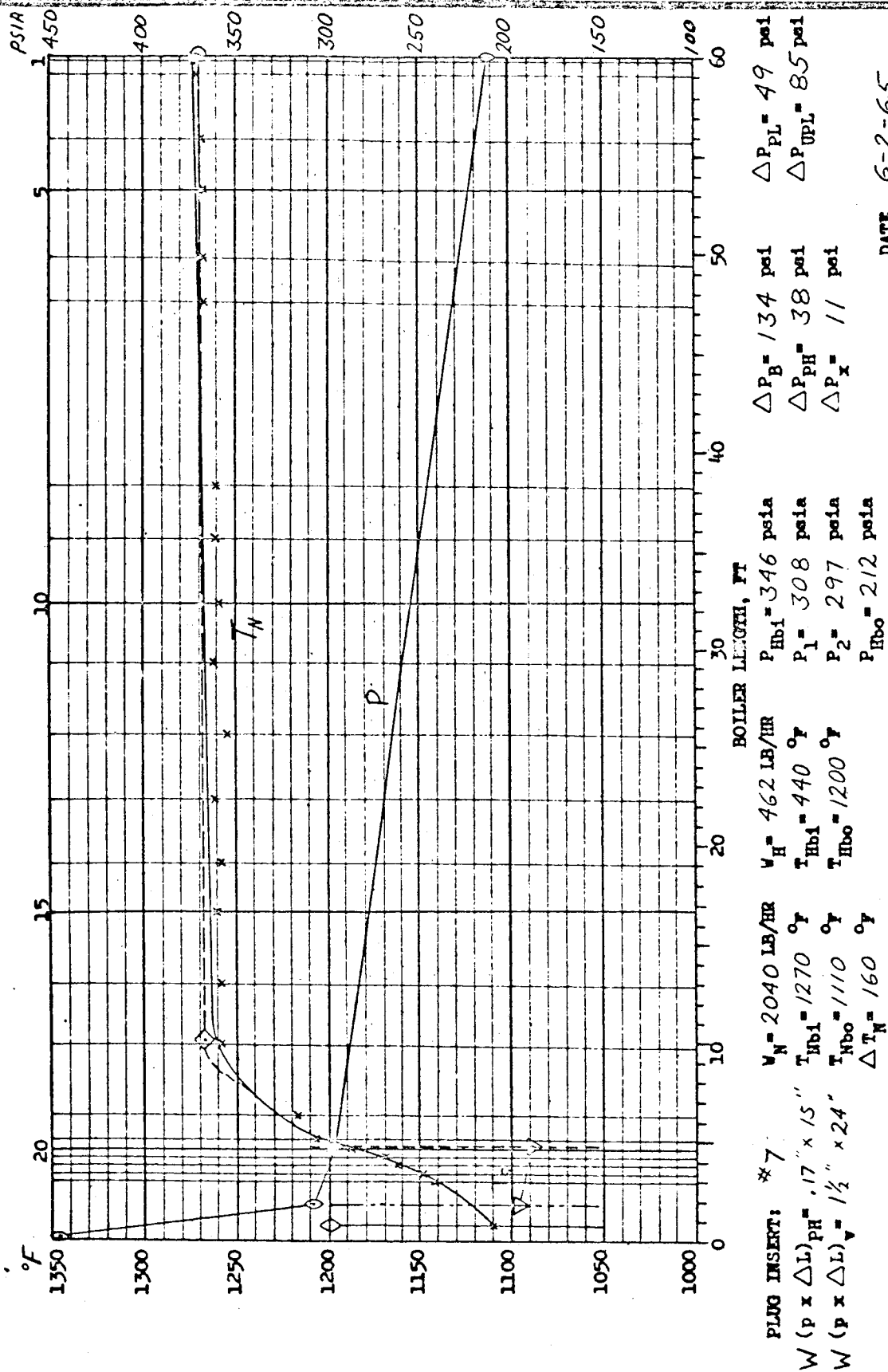


Fig. C-27



CL-4 BOILER MAX TEMPERATURE PROFILE

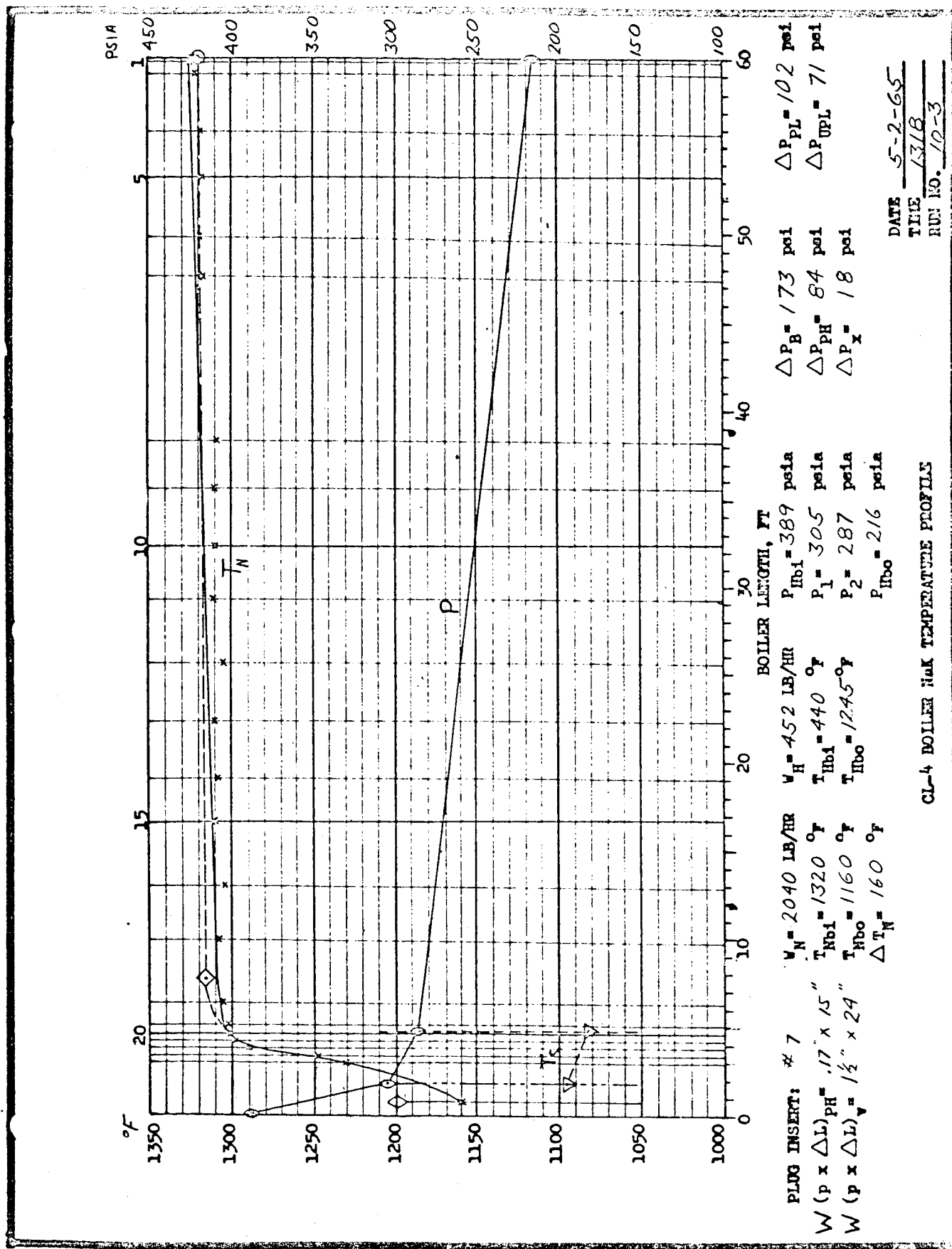


Fig. C-29

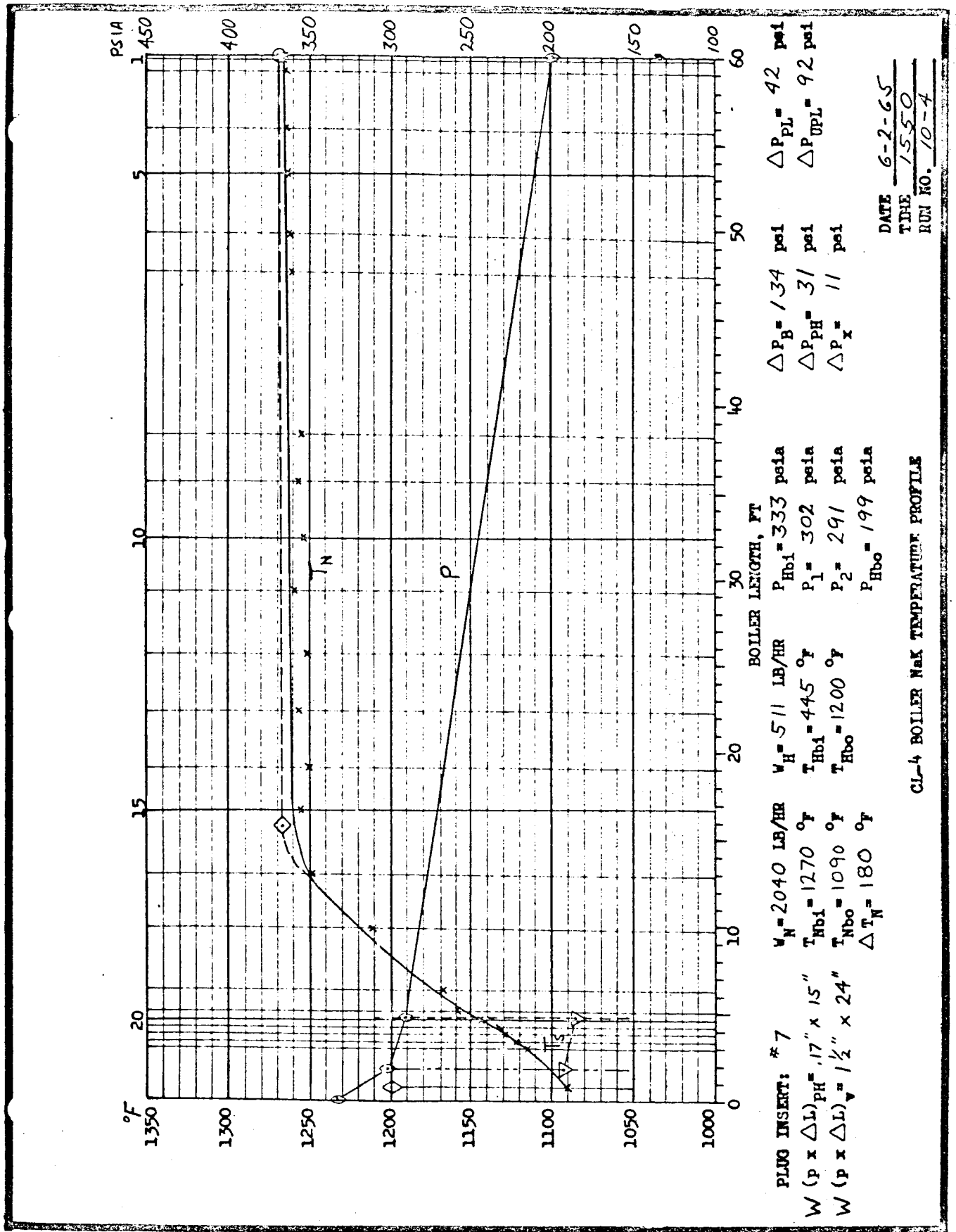


Fig. C-30

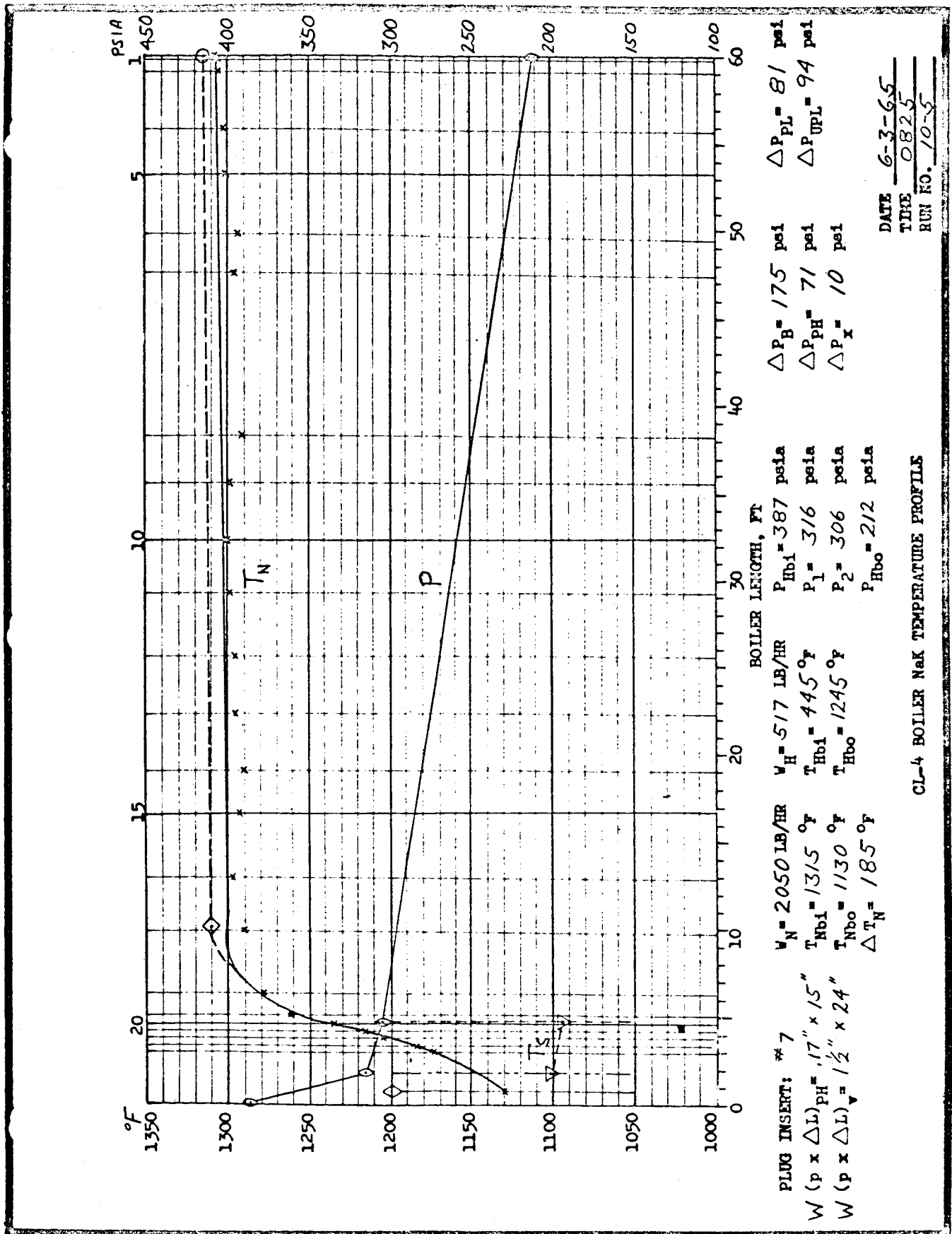


Fig. C-31

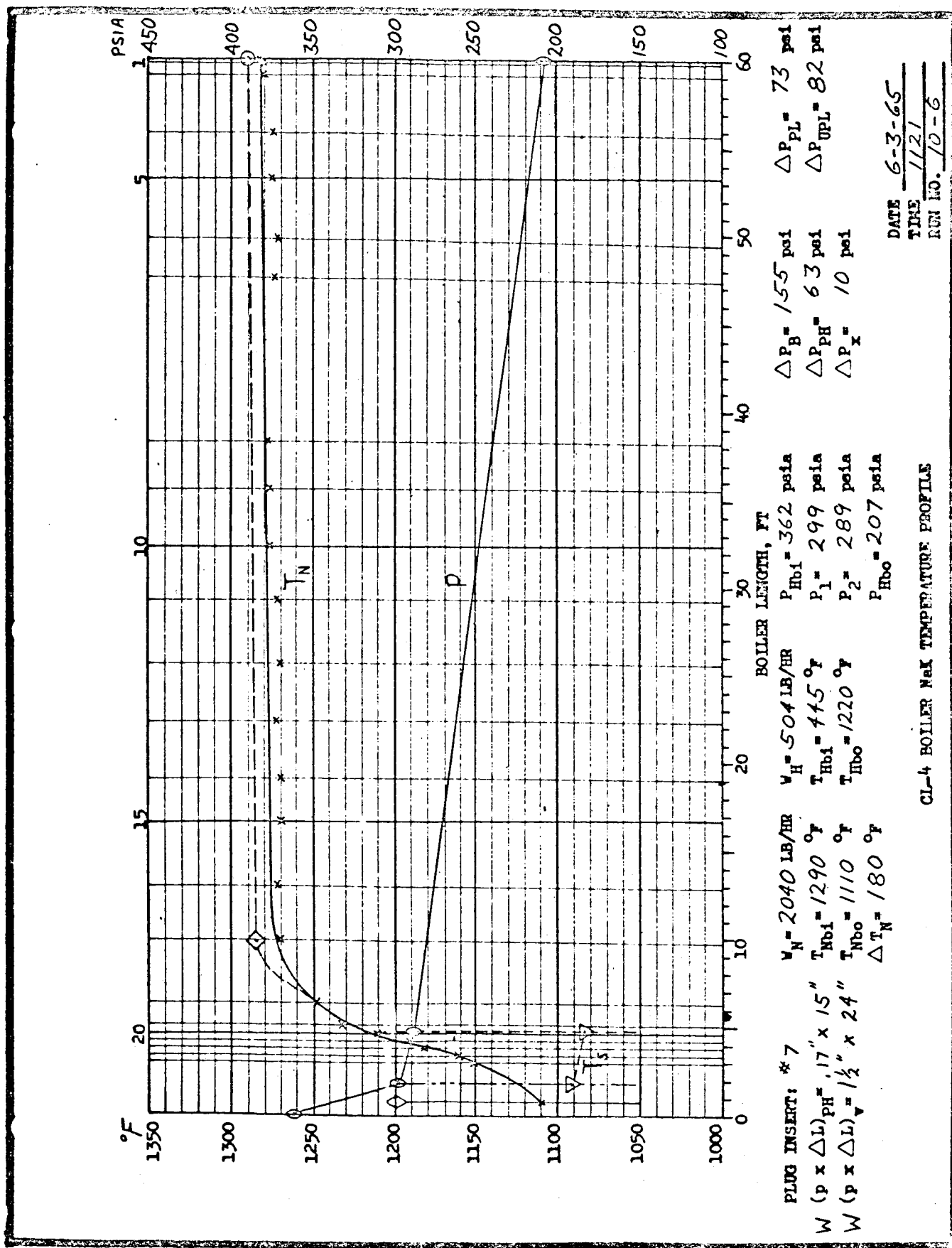
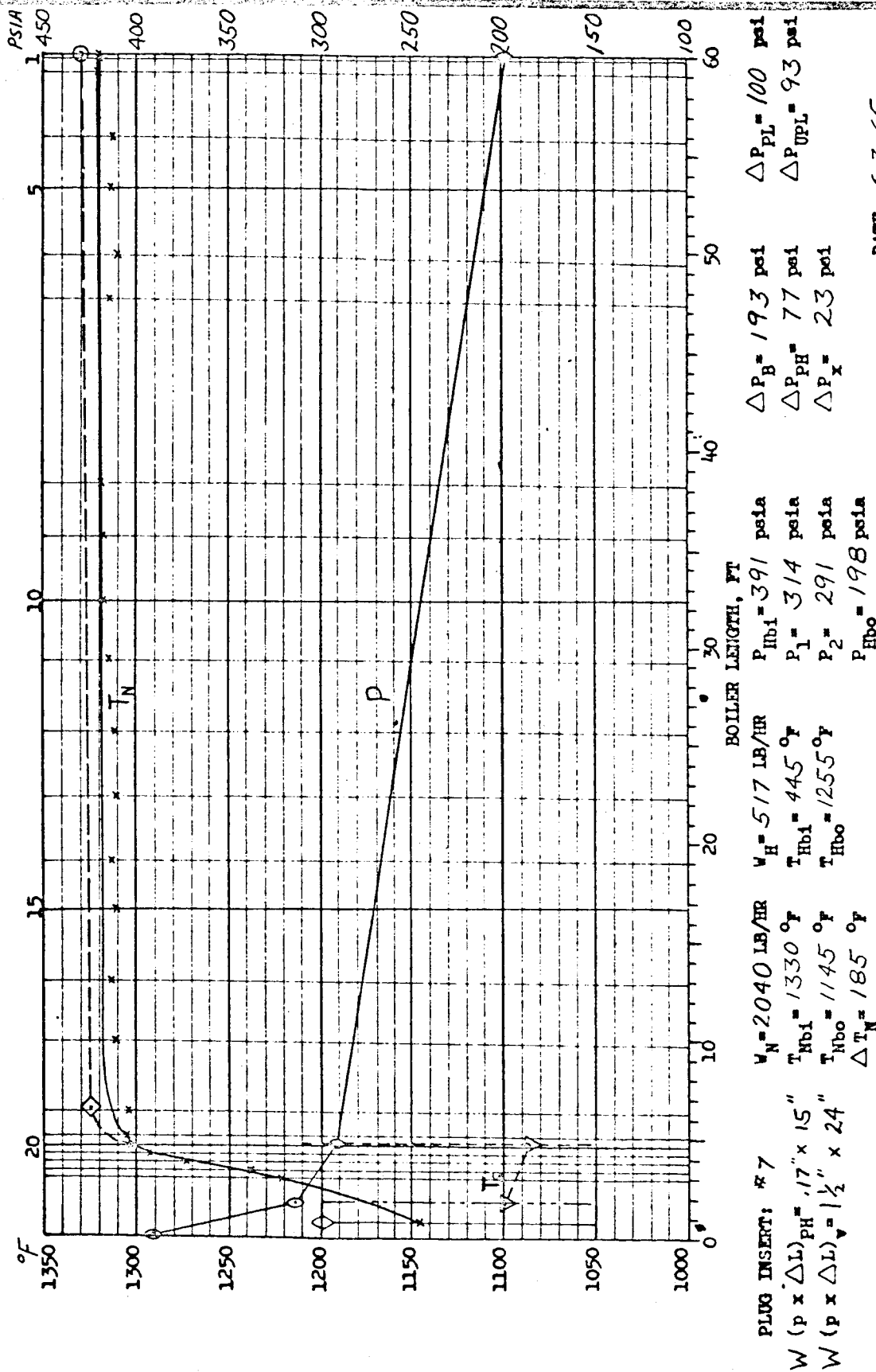


Fig. C-32



CL-4 BOILER NAK TEMPERATURE PROFILE

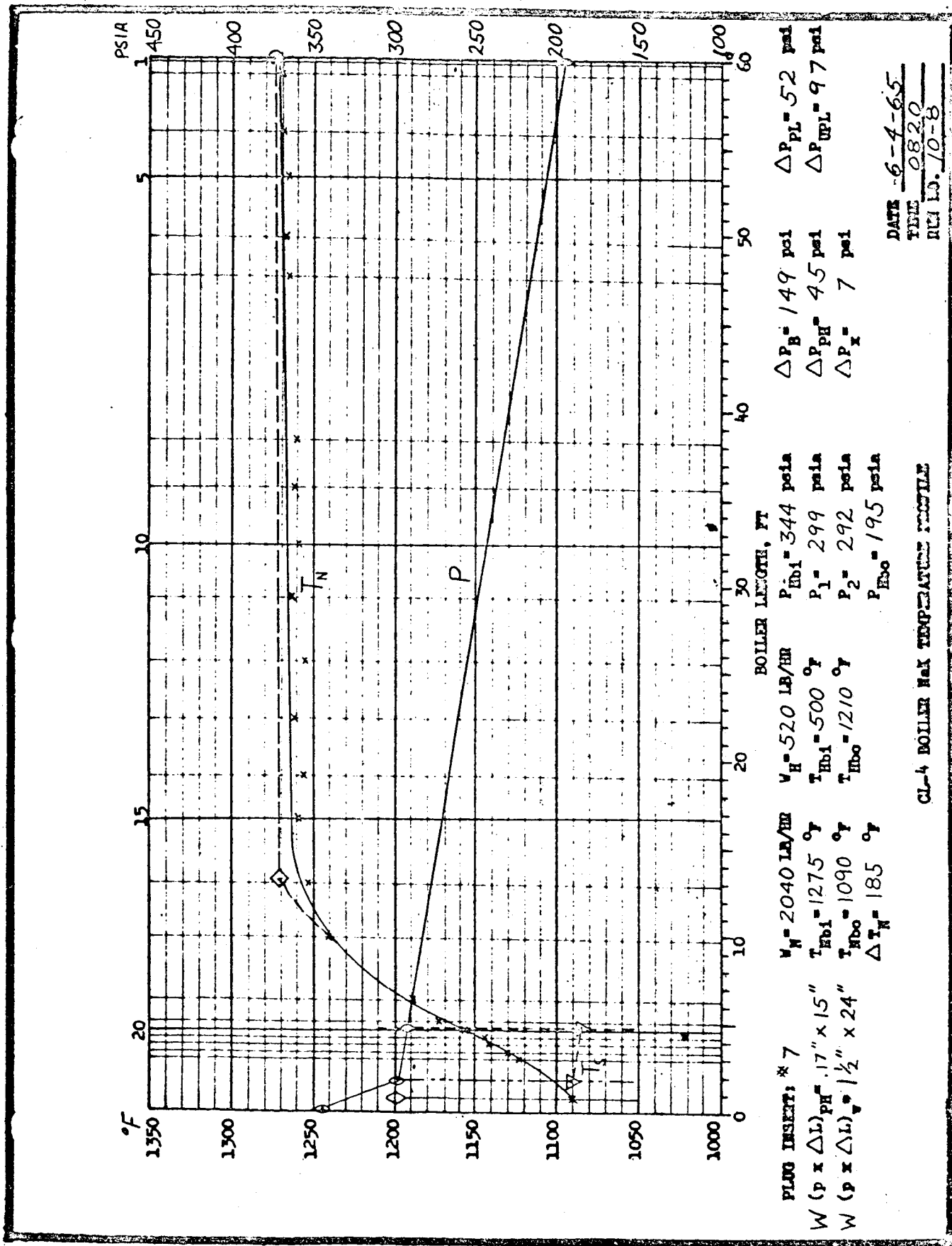


Fig. C-34

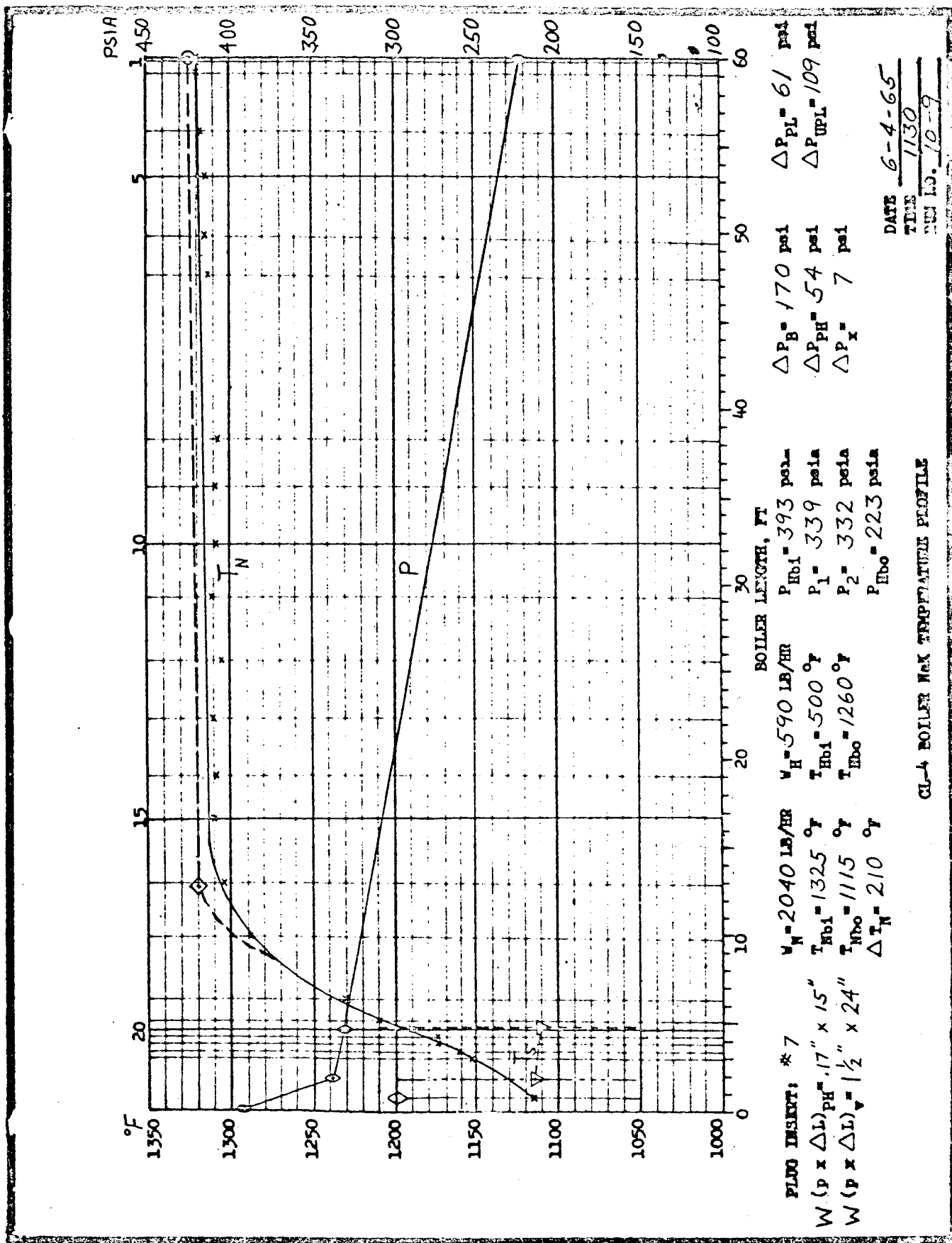


Fig. C-35